



**University of
Sunderland**

Mannan Baig, Abdul (2020) Identification of chemotherapeutic agents for the treatment of Acanthamoeba infections: rationale for repurposing drugs via the discovery of novel cellular targets. Doctoral thesis, University of Sunderland.

Downloaded from: <http://sure.sunderland.ac.uk/id/eprint/12948/>

Usage guidelines

Please refer to the usage guidelines at <http://sure.sunderland.ac.uk/policies.html> or alternatively contact sure@sunderland.ac.uk.



**Identification of chemotherapeutic agents for the treatment
of *Acanthamoeba* infections: rationale for repurposing
drugs via the discovery of novel cellular targets**

ABDUL MANNAN BAIG

A thesis submitted in partial fulfillment of the requirements of the
University of Sunderland for the degree of Doctor of Philosophy

Doctor of Philosophy

December 2020

Contents Page:

Part 1: Commentary	vii
List of tables:	viii
List of figures:	viii
List of abbreviations	ix-x
Acknowledgments and remarks:	xi
Abstract:	xii
1 Introduction - Background	1
1.1 Global burden of parasitic diseases	1
1.1.1 Challenges in antiparasitic drug discovery	3
1.1.2 Mounting interests in orphan drugs for orphan diseases	3
1.2 <i>Acanthamoeba</i> species: Biology, pathogenesis, and infections	4
1.2.1 Genotypes of <i>Acanthamoeba</i>	5
1.2.2 Classification of <i>Acanthamoeba</i> species	7
1.2.3 Free-living amoebae	7
1.2.4 First report of <i>Acanthamoeba</i> spp. as an FLA	9
1.3 Life cycle	9
1.3.1 Cyst stage	9
1.3.2 Trophozoite Stage	9
1.3.3 Cell biology of <i>Acanthamoeba</i> spp.	10
1.3.4 Feeding in <i>Acanthamoeba</i> spp.	10
1.3.5 Interaction between <i>Acanthamoeba</i> and other Microbial Pathogens	11
1.4 Epidemiology of <i>Acanthamoeba</i> Infections	12
1.4.1 <i>Acanthamoeba</i> Keratitis (AK)	12
1.4.2 Granulomatous Amoebic Encephalitis (GAE) Caused by <i>Acanthamoeba</i> spp.	14
1.4.3 Cutaneous and respiratory infections	15
1.4.4 Pathogenesis of <i>Acanthamoeba</i> Keratitis	15
1.4.5 Pathogenesis of GAE	16
1.5 Clinical Features of <i>Acanthamoeba</i> infections	16
1.5.1 <i>Acanthamoeba</i> Keratitis	16
1.5.2 Skin and Wound infection	17
1.5.3 Sign and symptoms in GAE:	18
1.6 Diagnosis of <i>Acanthamoeba</i> Infections	19
1.7 Treatment of AK and GAE	20
1.7.1 Main reasons behind the failure of treatment in AK	20
1.7.2 <i>Acanthamoeba</i> Infections as Orphan Diseases	21
1.7.3 Orphan drug development in <i>Acanthamoeba</i> infections	22
1.7.4 Key reasons behind the failure of treatment in GAE caused by <i>Acanthamoeba</i> spp.	22
1.7.5 Lack of drug development for the treatment of GAE	23
1.8 Drugs with the potential to be orphan drugs in infections caused by <i>Acanthamoeba</i> spp. .	23
1.9 Use of Bioinformatics computational tools in anti-parasitic drug target discovery	23
1.9.1 In silico screening in the discovery of Antiparasitic drugs	24
1.9.2 Identification of Protein Targets in Parasites:	25
1.9.3 Molecular Docking:	28
1.9.4 The rationale of the study presented in published work	28
1.9.5 Aims of the study:	30
2 Material and Methods	32
Section 1	32
2.1 Experimental Assays	32
2.1.1 List of the Drugs used in experiments:	32

2.1.2	<i>A. castellanii</i> cultures, amoebistatic, amoebicidal, encystation, and cysticidal assays ...	34
2.1.3	<i>A. castellanii</i> cultures	34
2.1.4	Amoebistatic and amoebicidal assays.....	34
2.1.5	Cysticidal assays.	35
2.2	Drug combination assays in <i>A. castellanii</i> spp. and <i>Balamuthia mandrillaris</i>	36
2.2.1	Materials and methods	36
2.2.2	Human brain microvascular endothelial cell culture	36
2.2.3	Cultures of <i>B. mandrillaris</i>	36
2.3	Amoebicidal assays	36
2.4	Determination of Intracellular Calcium.	37
2.4.1	Material:	37
2.4.2	Fura 2-AM staining Method:	37
2.5	Immunostaining for Muscarinic Cholinergic Receptor in <i>A. castellanii</i>	38
2.5.1	Materials and Methods	38
2.5.2	Immunostaining.....	38
2.6	ACh Detection in <i>A. castellanii</i> trophozoites	39
2.6.1	Materials and Methods	39
2.6.2	Colorimetric Acetylcholine Assay for ACh Detection in <i>Acanthamoeba</i>	39
2.7	Apoptosis in <i>A. castellanii</i> belonging to the T4 Genotype.....	40
2.7.1	Material and Methods:	40
2.7.2	Immunofluorescence: Imaging Apoptosis at different intervals:	40
2.7.3	FACS Analysis	41
2.8	Detection of phosphatidylserine (PS) externalization in <i>Acanthamoeba</i>	41
2.8.1	Cytotoxicity Assay - LDH release experiments.....	42
2.9	Genome databases and bioinformatic computational tools in the identification of drug targets in <i>A. castellanii</i> spp.	43
2.9.1	Transcriptomics of <i>A. castellanii</i>	43
2.10	Reverse transcription-polymerase chain reaction (RT-PCR) with Real-time polymerase chain reaction (qPCR).....	43
2.10.1	Processing of <i>Acanthamoeba</i> trophozoites:	43
2.10.2	Processing and Treatment of PC3/DU145 with trifluoperazine:	44
2.10.3	Extraction of WBCs:.....	44
2.10.4	mRNA Extraction from <i>Acanthamoeba</i> trophozoites, PC3, and DU145 cells: Preparation of lysis buffer:.....	44
2.10.5	Detection of RNA concentration:	45
2.10.6	cDNA synthesis:.....	45
2.10.7	Real-Time PCR:.....	45
2.10.8	qPCR Analysis:	45
	Section 2.....	46
2.11	Genomic, transcriptomic, and Bioinformatics Computational Tools in drug target discovery ...	46
2.11.1	General sequence identification and similarity searches	46
2.11.2	BLASTp: Scores and E-values	46
2.11.3	PSI-BLAST.....	47
2.11.4	Multiple Sequence analysis (MSA) and alignment with functional annotations	47
2.11.5	Evolutionary analysis of <i>A. castellanii</i> protein.....	48
2.11.6	Homology Modeling: Automated Protein Homology Modeling Servers.....	48
2.11.7	Annotation of ligands in SWISS-MODEL template library (SMTL).....	49
2.11.8	Template search and selection.....	49
2.11.9	Modeling of the Ligands:.....	50
2.12	Drug and Ligand docking predictions:.....	50
2.12.1	PatchDock: Molecular Docking Algorithms:.....	51
2.12.2	The PatchDock web server: Input, Output, and results.	51
3	Experimental Assays, immunostaining, ELISA, colorimetric analysis,	52
	FACS analysis and DNA staining	52

3.1	Introduction:	52
3.1.1	Materials and Methods overview	54
3.2	Amoebistatic, Amoebicidal, and cysticidal drug assays.....	55
3.3	Reproducibility and the effects of drug combinations in <i>A. castellanii</i> and related FLA.	58
3.4	Drugs targeting Ca ²⁺ signaling adapter proteins:.....	60
3.4.1	VGCC blocker exert apoptotic and amoebicidal effects	62
3.5	Fura-2 AM staining of trophozoites treated with VGCC blockers	64
3.5.1	Ca ²⁺ depletion caused by Ca ²⁺ ion chelators EDTA and pirenixine in <i>A. castellanii</i>	67
3.6	Effects of Drugs targeting human-like ion channels and proteins	67
3.7	The first evidence of a cholinergic ligand and druggable human-like muscarinic receptor (mAChR) like protein in <i>Acanthamoeba</i> spp.	70
3.7.1	Anti-human mAChR1 Antibody showed Immunostaining in <i>A. castellanii</i> trophozoites..	70
3.7.2	Validation of the presence of ligand Acetylcholine in <i>Acanthamoeba castellanii</i> trophozoites.	71
3.7.3	mAChR antagonists exert amoebicidal effects in <i>Acanthamoeba castellanii</i> trophozoites.	72
3.7.4	Agonist effects clue towards human-like receptors and VGCC in <i>A. castellanii</i>	73
3.8	Elucidation of cell death mechanisms in <i>Acanthamoeba</i> trophozoites and cysts.....	76
3.8.1	Cytotoxic death in <i>Acanthamoeba</i> trophozoites	76
3.8.2	Programmed cell death: Apoptosis like features induced by drugs in <i>A. castellanii</i>	77
3.9	Discussion.....	81
3.9.1	Discussion.....	82
3.9.2	Summary of findings.....	86
3.9.3	Aims achieved.....	86
4	Identification of drug targets: Bioinformatic computational tools and drug docking predictions	86
4.1	Introduction:	86
4.2	Materials and Methods.....	89
4.3	The Transcriptome of <i>Acanthamoeba castellanii</i> trophozoites.	90
4.3.1	Evidence of mRNA encoding drug target proteins in <i>Acanthamoeba</i> spp.	90
4.4	Induction of CaM gene expression in <i>A. castellanii</i>	92
4.5	mRNA encoding human-like cholinergic enzymes and mAChR like proteins	94
4.6	mRNA encoding K-channels, Na-K ATPase, and cytochrome -C	94
4.7	BLASTp results and phylogenetics of human-like drug targets in <i>A. castellanii</i>	95
4.7.1	Identification of Human-like VGCC and CaM in <i>Acanthamoeba castellanii</i>	95
4.7.2	Identification of cholinergic ligand-receptor organizations in <i>Acanthamoeba castellanii</i>	103
4.7.3	Identification of human-like individual drug targets in <i>Acanthamoeba castellanii</i>	106
4.8	Homology Modeling:	111
4.8.1	Human-like VGCC and CaM in <i>Acanthamoeba castellanii</i>	111
4.8.2	Evidence of human-like muscarinic receptor and cholinergic enzymes in <i>A. castellanii</i>	115
4.8.3	Human-like K-Channels in <i>Acanthamoeba castellanii</i>	119
4.8.4	Human-like Na-K ATPase in <i>Acanthamoeba castellanii</i>	120
4.8.5	Human-like Carbonic anhydrase and Aquaporins in <i>Acanthamoeba castellanii</i>	122
4.8.6	Human-like Cytochrome-c in <i>Acanthamoeba castellanii</i>	123
4.9	Results of Drug Docking Predictions:	124
4.9.1	Molecular Docking of Loperamide on templates generated for <i>A. castellanii</i> proteins..	124
4.9.2	Molecular docking of Amlodipine on templates generated for <i>Acanthamoeba</i> proteins.	126
4.9.3	Docking prediction of Atropine on templates generated for ACA1_153000	128
4.9.4	Molecular docking prediction for Amiodarone on templates generated for <i>Acanthamoeba</i> proteins.	129

4.9.5	Discussion.....	130
4.9.6	Summary.....	136
4.9.7	Aims Achieved:	133
5	Evaluation of my contribution to the biology and drug target discovery in <i>Acanthamoeba</i>	
spp.	134
5.1	Contribution to the knowledge of drug targets in trophozoites and cysts of <i>A. castellanii</i> .	134
5.1.1	Providing explanations to the cure of retrospective cases of <i>Acanthamoeba</i> keratitis.	134
5.2	The first evidence of the role of Ca ²⁺ ion in the biology of <i>Acanthamoeba</i> trophozoites ...	135
5.3	Potential of the re-purposing drugs tested in my assays in AK.	135
5.4	Potential of the possible use of the experimented drugs in clinical trials and treatment of	
GAE	136
5.5	Possibility to extend the tested drugs in the treatment of infection caused by <i>Naegleria</i>	
<i>fowleri</i>	136
5.6	Rationale and experiments of our study projected to test the drugs in cancer cell lines ...	137
5.7	Summary and Conclusion:	137
5.8	Publications and their impact:	138
5.9	Future Directions:	139
References:	140

Part 2: Published Work

(in order of publication date)

1. **Baig AM, et al., 2013:** Baig AM, Iqbal J. Khan NA. (2013). *In vitro* efficacy of clinically available drugs against growth and viability of *Acanthamoeba castellanii* keratitis isolate belonging to the T4 genotype. *Antimicrobial Agents and Chemotherapy*. 05/2013; DOI: 10.1128/AAC.00299-13
2. **Kulsoom H, et al., 2014:** Kulsoom H, Baig AM, Siddiqui R., and Khan NA. (2014). Combined drug therapy in the management of granulomatous amoebic encephalitis due to *Acanthamoeba* spp., and *Balamuthia mandrillaris*, *Experimental Parasitology*. 04/2014; DOI: 10.1016/j.exppara.2014.03.025 iv
3. **Baig AM, et al., 2016:** Baig AM, Rana Z, Mohsin M, Vardah E, and HR Ahmad. (2016) "Forte of Bioinformatics Computational Tools in Identification of Targets of Digitalis in Unicellular Eukaryotes: Featuring *Acanthamoeba castellanii*". *EC Microbiology* 4.6 (2016): 831-844v
4. **Baig AM, et al., 2017:** Baig AM, Rana Z, Mohsin M, Sumayya T, and HR Ahmad. (2017). Antibiotic Effects of Loperamide: Homology of human targets of Loperamide with targets in *Acanthamoeba* spp., *Recent Patents on Anti-Infective Drug Discovery* 12 (1). April 2017, DOI: 10.2174/1574891X12666170425170544
5. **Baig AM, et al., 2017:** Baig AM, Rana Z, Tariq SS, Ahmad HR. (2017). Bioinformatic Insights on Target Receptors of Amiodarone in Human and *Acanthamoeba castellanii*. *Infect Disord Drug Targets*. 2017;17(3):160-177;
6. **Baig AM, et al., 2017:** Baig AM, Ahmad HR. (2017). Evidence of an M1-Muscarinic GPCR homolog in unicellular eukaryotes: featuring *Acanthamoeba* spp. bioinformatics 3D-modelling and experimentations. *J Recept Signal Transduct Res*. 2017 Sep 7:1-9
7. **Baig AM, et al., 2017:** Baig AM, Rana Z, Tariq S, Lalani S, Ahmad HR. Traced on the Timeline: Discovery of Acetylcholine and the Components of the Human Cholinergic System in a Primitive Unicellular Eukaryote *Acanthamoeba* spp. (2017). *ACS Chem Neurosci*. 2017 Oct 23. doi: 10.1021/acscchemneuro.7b00254
8. **Baig AM, et al., 2017:** Baig AM and Khan NA: (2017). Apoptosis in *Acanthamoeba castellanii* belonging to the T4 genotype. *Journal of Basic Microbiology*. 2017; Article ID: JOBM2073; DOI: 10.1002/jobm.201700025
9. **Baig AM, et al., 2018:** Baig AM, Rana Z, Sumayya T, and HR Ahmad; (2017); Evolution of pH Buffers and Water Homeostasis in Eukaryotes: Homology between humans and *Acanthamoeba* proteins *Future Microbiol*. 2018 Feb; 13:195-207. doi: 10.2217/fmb-2017-0116
10. **Baig AM, et al., 2019:** Baig AM, Rana Z, Waliani N, Karim S, Rajabali M. Evidence of human-like Ca²⁺ channels and effects of Ca²⁺ channel blockers in *Acanthamoeba castellanii*. *Chem Biol Drug Des*. (2019), r;93(3):351-363. doi: 10.1111/cbdd.13421. Epub 2019 Jan 29. PubMed PMID: 30362253.

Part 1: Commentary

List of tables:

Table 1. <i>Acanthamoeba</i> genotypes.....	6
Table 2. Taxonomical Classification of <i>Acanthamoeba</i> spp.....	8
Table 3. Organ involvement, signs/symptoms, predispositions, and prognosis of <i>Acanthamoeba</i> infections.....	18
Table 4. Drugs approved by the regulating authorities.	33
Table 5: Published papers on human-like receptors and proteins targeted <i>in vitro</i> by drugs in <i>Acanthamoeba</i> trophozoites and cysts.	88

List of figures:

Figure 1: Global burden of parasitic diseases.....	2
Figure 2. Transmission electron microscope (TEM) of <i>A. castellanii</i>	5
Figure 3. Interaction between <i>Acanthamoeba</i> and Microbial Pathogens.....	12
Figure 4. <i>Acanthamoeba</i> keratitis cases at Moorefield's Hospital (1984-2016).....	13
Figure 5. Infections caused by pathogenic genotypes of <i>A. castellanii</i>	17
Figure 6. Current Drugs used in AK and the ODAK report 2017.	21
Figure 7. A Workflow of Drug Design Approach.....	25
Figure 8. Amino acid sequence homology and structure of glucokinase.....	27
Figure 9. Calcium-dependent cellular processes in <i>A. castellanii</i>	29
Figure 10. Molecular targets hypothesized in <i>Acanthamoeba castellanii</i> to be tested by drugs.	53
Figure 11 Effects of drugs tested in <i>Acanthamoeba</i> trophozoites.	55
Figure 12. Results of drugs tested <i>in vitro</i> in trophozoites of <i>A. castellanii</i>	57
Figure 13. Effects of drugs against cysts: Encystation blockage and activity against cysts in <i>A. castellanii</i>	57
Figure 14. Effects of drugs used in combinations <i>A. castellanii</i> for 24h.....	60
Figure 15. Amoebistatic effects of Amlodipine and Gabapentin in <i>A. castellanii</i> trophozoites.	61
Figure 16. Effects of different doses of loperamide in <i>A. castellanii</i> trophozoites.....	63
Figure 17. Effects of different doses of nifedipine and verapamil in <i>A. castellanii</i>	63
Figure 18. Fura-2AM staining in <i>Acanthamoeba</i>	65
Figure 19. <i>A. castellanii</i> with Ca ²⁺ chelating agents stained with Fura-2AM	66
Figure 20. Amoebistatic and amoebicidal effects of amiodarone.....	68
Figure 21. Effects of carbonic anhydrase inhibitor on <i>Acanthamoeba castellanii</i>	69
Figure 22. Immunostaining with anti-human mAChR1 antibody.....	70
Figure 23. Colorimetric assay for acetylcholine (ACh) detection	72
Figure 24. mAChR antagonists affect the growth and viability of <i>Acanthamoeba</i> trophozoites	73
Figure 25. Effects of mAChR agonist in <i>Acanthamoeba</i> trophozoites.....	74
Figure 26. Effects of KCL and VGCC blocking drugs on Fura-2 AM staining in <i>Acanthamoeba</i> trophozoites.....	75
Figure 27. LDH assays on 1x10 ⁶ <i>A. castellanii</i> trophozoites incubated with and without drugs.....	77
Figure 28. Programmed cell death in <i>Acanthamoeba</i> trophozoites.....	79
Figure 29. 20x Images of loperamide treated <i>A. castellanii</i> trophozoites:	80
Figure 30. Transcriptomics of human-like proteins that were hypothesized as drug targets in <i>Acanthamoeba</i> trophozoites.....	91
Figure 31. Reverse transcription-polymerase chain reaction (RT-PCR) with Real-time polymerase chain reaction (qPCR)	93
Figure 32. BLASTp results of <i>Acanthamoeba</i> protein ACA1_167020.....	96
Figure 33. Highlights of the Ion-trans domain in the ACA1_167020 gene and its phylogenetics.....	97
Figure 34. BLASTp results of ACA1_092610.....	98

Figure 35. Evolutionary distribution of the Ion-trans 2 domain in ACA1_092610.	100
Figure 36. BLASTp results and distribution of VGCC alpha2/delta1 across species.	101
Figure 37. BLASTp results, Evolutionary origins and functional predictions of <i>Acanthamoeba</i> CaM.	102
Figure 38. BLASTp results, sequence alignments, and Phylogenetic of ACA1_153000.	104
Figure 39. Sequence alignments of human and <i>Acanthamoeba</i> enzymes.	105
Figure 40. BLASTp results, Phylogenetic and functional predictions of ACA1_202400 K+ channel protein.	107
Figure 41. Multiple sequence alignment, evolutionary distribution, and functional predictions for ACA1_108830.	107
Figure 42. BLASTp results, conserved domains, and evolution of Cation_ATPase family.	109
Figure 43. MSA of <i>Acanthamoeba</i> carbonic hydratase and its evolutionary origins.	110
Figure 44. Homology Modelling of ACA1_167020.	112
Figure 45. Models developed for <i>Acanthamoeba</i> protein ACA1_092610.	113
Figure 46. Homology modeling of <i>Acanthamoeba</i> ACA1_270170.	114
Figure 47. Homology modeling of ACA1_366720 a putative CaM in <i>A. castellanii</i>	115
Figure 48. Homology modeling of <i>Acanthamoeba</i> ACA1_153000.	116
Figure 49. Alignment of the Model and template developed for ACA1_153000 hypothetical protein. .	117
Figure 50. Homology modeling of <i>Acanthamoeba</i> enzymes involved in the cholinergic cascade.	118
Figure 51. Homology modeling of <i>Acanthamoeba</i> ACA1_202400 K+ channel protein.	120
Figure 52. Homology modeling of <i>Acanthamoeba</i> protein ACA1_313610.	121
Figure 53. Homology modeling of <i>A. castellanii</i> carbonic anhydratase and major intrinsic protein (MIP).	123
Figure 54. Homology modeling of <i>Acanthamoeba</i> ACA1_175250 cytochrome c, putative.	124
Figure 55. Molecular docking of loperamide on the templates generated for <i>Acanthamoeba</i> proteins.	125
Figure 56. Molecular docking of amlodipine on templates generated for <i>Acanthamoeba</i> proteins. ...	127
Figure 57. Molecular docking of atropine on a template for ACA1_153000.	128
Figure 58. Molecular docking of amiodarone on template generated for <i>Acanthamoeba</i> proteins. ...	129

List of abbreviations

Abbreviation	Definition
ACE	Atomic contact energy
ACh	Acetylcholine
AIDS	Acquired Immune Deficiency Syndrome
AK	<i>Acanthamoeba</i> keratitis
AMB	Acetylcholine muscarine binding
AQP	Aquaporin
ATCC	American Type Culture Collection
ATP	Adenosine triphosphate
AZM	Acetazolamide
BAE	Balamuthia amoebic encephalitis
BEA	Brain-eating amoeba
BZA	Brinzolamide
CA	Carbonic anhydrase
CaM	Calmodulin

ChEMBL	Chemical database European Molecular Biology Laboratory
CO ₂	Carbon dioxide
CSF	Cerebrospinal fluid
CPZ	Chlorpromazine
EDTA	Ethylenediaminetetraacetic acid
FDA	Food and Drug Administration
FLA	Free-living amoeba
GAE	Granulomatous Amoebic encephalitis
GARD	Genetic and rare disease
GCCP	Good Cell Culture Practice
GPCR	G-protein coupled receptor
GPCRs	G-protein coupled receptors
GVR	Grand View Research
HIV	Human Immune deficiency Virus
KCL	Potassium chloride
LD ₅₀	Median lethal dose
mAChR1	Muscarinic Acetylcholine Receptor subtype-1
mAChRs	Muscarinic Acetylcholine Receptors
MBP	Mannose-binding protein
MCC	Minimum cytotoxic concentrations
MIC	Minimum inhibitory concentration
MS	Mass spectrophotometry
Na-K ATPase	Sodium Potassium Exchanger
NIH-US	National Institutes of Health United States
NMR	Nuclear Magnetic Resonance
NTDs	Neglected tropical diseases
ODAK	Orphan drugs for <i>Acanthamoeba</i> keratitis
ODs	Orphan drugs
PBS	Phosphate Buffer Saline
PC	Patient compliance
PCD	Programmed cell death
PHMB	Polyhexamethylene biguanide
PI	Propidium iodide
PYG	Peptone-Yeast-Glucose
qRT-PCR	Quantitative Real-Time Polymerase Chain Reaction
rRNA	Ribosomal RNA
TB	Tuberculosis
TEM	Transmission electron microscope
Uniprot	Universal protein knowledgebase

Acknowledgments and remarks:

I am grateful to Professor Timothy Paget and Dr. Lewis Bingle for their guidance in applying for a Ph.D. via published work. Both, Dr. Timothy Paget and Dr. Lewis Bingle guided me in writing the commentary for which I can't thank them enough. I am deeply indebted to Professor Naveed Khan for igniting my interest in the biology of eukaryotes. It is his mentoring, support, and encouragement which has helped me in keeping my research focused on the search for novel drug targets in *Acanthamoeba* spp. I would like to thank my mentor and supervisor at Aga Khan University, Dr. HR Ahmad, who has been an immense source of inspiration during preparation for my Ph.D. via published work. My special thanks to Professor and Associate Vice Provost Dr. Farhat Abbas, who has encouraged my passion for research and discovery. I extend my gratitude to my loving wife, Misbah, for her love, care, and support. Finally, I would like to dedicate my work to my parents, particularly to my mother from whom I have inherited my mitochondrial aptitudes of remaining positive and the quest for real discoveries.

Abstract:

Acanthamoeba castellanii is a free-living amoeba that exists in two different forms, the trophozoite, and the cyst. *A. castellanii* is known to cause two rare infections: *Acanthamoeba* keratitis (AK), a disease where the parasites infect the cornea, and a central nervous system (CNS) infection, known as granulomatous amoebic encephalitis (GAE). Patients with AK often lose significant vision in the infected eye and, if both eyes are infected, may lead to blindness. The other infection caused by this parasite, GAE, has a mortality rate of around 95%. The current chemotherapeutic drugs have not been able to reduce the morbidity and mortality associated with AK and GAE and the cost of *de-novo* drug development for such rare diseases has led to the development of alternative approaches for the identification of drug candidates. This is the driving force for the work presented in this thesis and is the overarching theme for the papers included in this work. The publications contributing to this thesis describe work on the discovery of novel drug targets in *Acanthamoeba* and the use of this information to identify drugs that could be re-purposed for the treatment of AK and GAE. *Acanthamoeba castellanii* was shown to express human-like calcium channels, calcium regulating adapter proteins, G-protein coupled receptors and muscarinic receptor-like proteins that are needed for growth and proliferation. Bioinformatic analysis based around amino acid sequence homology, modeling, drug docking studies and transcriptomic profiles of *Acanthamoeba* revealed these proteins as possible drug targets. There are currently a range of drugs that are antagonists for these targets in humans and these are used for a variety of non-infectious disease presentations. Our research studied loperamide, amlodipine, digoxin, amiodarone, anticholinergic agents like procyclidine, dicyclomine and atropine. Studies were able to show that these drugs have activity against trophozoite and cystic forms of *Acanthamoeba* spp. and that many work via disrupting calcium homeostasis. These drugs are fully characterised and their profile of adverse effects and the margin of safety and toxicity is well known. These drugs could now be evaluated for their clinical utility for the treatment of AK and GAE. This is much faster than for traditional novel drug discovery. Thus, the major conclusion from this body of work is that the repurposing of drugs, already in clinical use for the treatment of non-infectious diseases in humans, will provide an alternative and viable option in drug development against AK and GAE.

1 Background

1.1 Global burden of parasitic diseases

Diseases caused by parasites are known to affect millions of individuals worldwide with high morbidity and mortality rates. However, they have been largely neglected for drug development because they largely affect underdeveloped countries (Figure 1). Parasitic diseases cause an enormous burden on the economic growth of the affected countries and thus the need to devise prevention and treatment strategies is pressing. Most of the current drugs used in the treatment of parasitic diseases are decades old and have several limitations, like reduced patient compliance due to adverse effects, prolonged duration of chemotherapy, and the emergence of drug resistance [1-4]. There is paucity in the discovery of novel and safer drugs for diverse parasitic organisms that cause diseases in humans. Hence there is a need to revive the drug development pipeline for even common parasitic diseases like malaria which is increasing yearly as noted between 2015 and 2018 [5]. With about 1 in 6 individuals worldwide experience some form of parasitic disease, it is alarming to note that currently, we have no licensed vaccine for any human parasitic pathogen. Infection with *Entamoeba histolytica*, resulting in amoebic colitis and liver abscesses, is the second leading cause of death resulting from a parasitic infection. *E. histolytica* is estimated to infect one-tenth of the worlds' population amounting to about 500 million people [6].

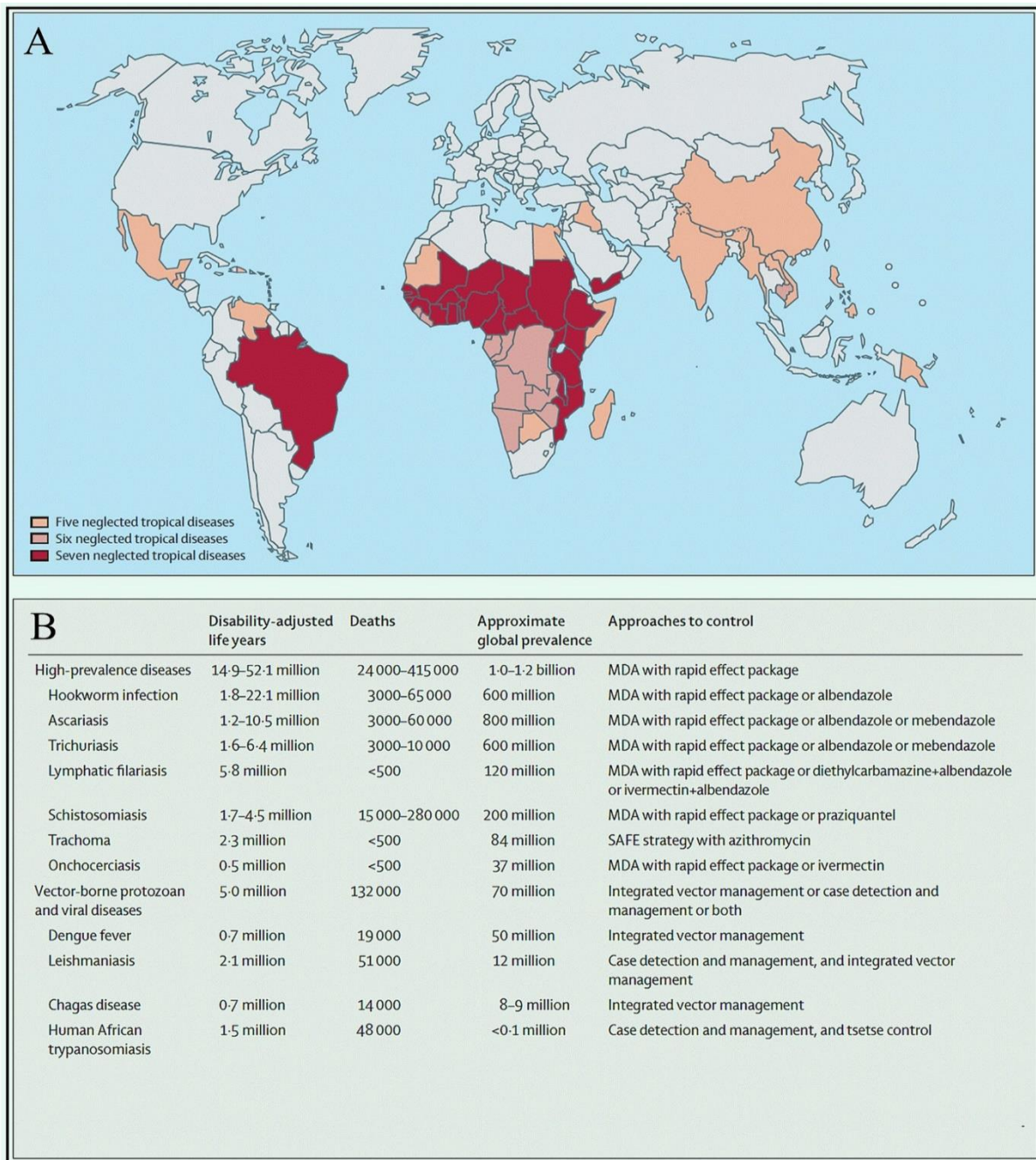


Figure 1: Global burden of parasitic diseases.

(A) Geographic overlap and distribution of the seven most common neglected parasitic diseases (red-areas in the map). Data from Hotez and WHO. (B) High-prevalence and other vector-borne neglected tropical diseases [Adapted from Hotez PJ, Fenwick A, Savioli L, Molyneux DH. Rescuing the bottom billion through control of neglected tropical diseases- Reference # - 7].

1.1.1 Challenges in antiparasitic drug discovery

Parasitic diseases affect millions of people worldwide (Figure 1) and result in significant morbidity, mortality, and devastating socioeconomic consequences. Few, if any, of the currently available drugs pass through a discovery-stage screening process at present, let alone preclinical and clinical development. It is puzzling yet to see the development of a new generation of more effective and safer antiparasitic drugs for which the answer primarily lies in economics [8]. Parasitic diseases, although globally massive in their impact, mainly affect poor people in underdeveloped regions which are not viewed as viable target markets by the pharmaceutical industry, particularly in today's post-merger climate. Generally, preclinical models tend to be more predictive, and human clinical trials are not more complicated or costly than those for other non-infectious chronic disorders. For example, the danger of failure in Phase II clinical trials is estimated to be ~50% for a new antimalarial, which is lower than the corresponding risk for a non-infectious disease [9]. Current drug discovery has not fully utilized the new knowledge of parasite genome sequences, freely available from online databases, and the insights that can be obtained from parasite genomics and transcriptomics into the novel, vigorous chemical clues that can form the basis of innovative drug discovery [10].

1.1.2 Mounting interests in orphan drugs for orphan diseases

According to the US National Institutes of Health (NIH-US), there are close to 7,000 described rare diseases. In the United States, a disease is considered to be 'rare' if it affects fewer than 200,000 individuals, and in the European Union, it is defined as having a prevalence of fewer than 5 in 10,000 people. One of the most central resources for orphan drugs and diseases in Europe is Orphanet, a European society that involves about 40 countries globally [11, 12]. It defines "orphan drugs" as "drugs envisioned to treat diseases so rare that the drug development industries are reluctant to develop them under usual marketing conditions." Orphan diseases include a wide range of infectious and non-infectious disease states [11]. Examples of such parasitic diseases include American trypanosomiasis (which affects more than 13 million

people), Leishmaniasis (which affects more than 12 million people), and lymphatic filariasis (which affects about 120 million people).

It is only recently that rare diseases and orphan drug development have provided attractive opportunities for pharmaceutical companies. They offer advantages such as quicker development timelines, less time spent in research, low development expenses, a higher likelihood of clinical and regulatory success, premium pricing, lower marketing costs, and a lower risk of generic competition. More recently, several pharmaceutical companies such as Pfizer and GlaxoSmithKline, have formally been incorporating the orphan drug model by launching policies for treating rare diseases through partnerships and acquisitions [13]. Recently, orphan diseases have become attractive to the industry because of the pricing and the potential to generate significant revenues in drug markets. Although early on the majority of approved orphan drugs were developed in biotech companies, big pharma has been responsible for a growing number of approvals — from 30-35% in 2000–2002 to 50-56% in 2006–2008 [14]. The following paragraphs highlight the biology and infections caused by *Acanthamoeba* spp. and drug development in the context of these infections as orphan diseases.

1.2 *Acanthamoeba* species: Biology, pathogenesis, and infections

Pathogenic and opportunistic free-living amoebae (FLA) such as *Acanthamoeba* spp., *Balamuthia mandrillaris*, and *Naegleria fowleri* are aerobic, mitochondriate, eukaryotic protists that occur worldwide and can potentially cause infections in humans and other animals [15-17]. Some pathogenic genotypes (Table-1) can intermittently invade the mammalian hosts and cause diseases [18-20]. These FLA are classified (Table- 2) under supergroup and thrive naturally in the environment in cystic (Figure 2 A) and trophozoite forms (Figure 2 B)

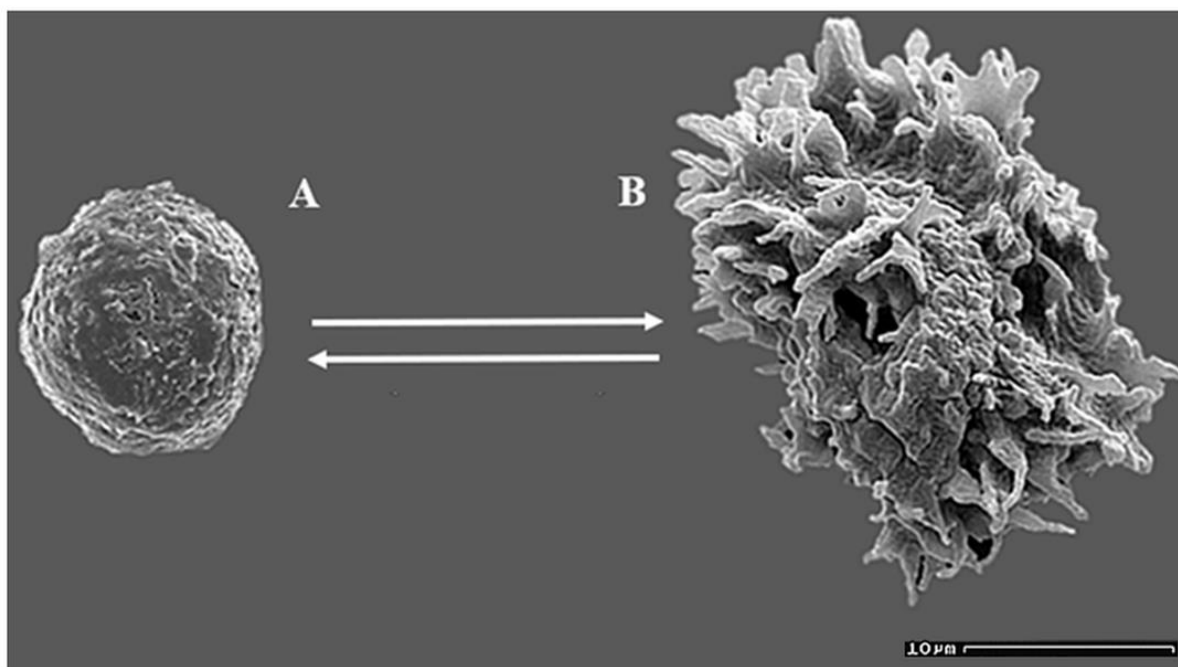


Figure 2. Transmission electron microscope (TEM) of *A. castellanii*

An encysted stage (A) and the trophozoite form (B) of *Acanthamoeba castellanii*. Note spiny surface projections, termed acanthopodia in the trophozoites form [Figures courtesy: (cyst), Khan NA and (trophozoite), Maritza Omaña-Molina [16, 42]]

1.2.1 Genotypes of *Acanthamoeba*

Dr. Thomas Byer classified *Acanthamoeba* based on rRNA gene sequences. Based on the sequence information, *Acanthamoeba* was classified into 12 different genotypes, termed T1 to T12. In 1999, Horn et al. identified two more genotypes, T13 and T14 [21], whereas Hewett *et al.* in 2003 proposed the T15 genotype of *Acanthamoeba* [22]. Recently, new genotypes particularly significant to human diseases have been reported and the genotypes have been extended to a total of 20 groups (Table 1).

Table 1. *Acanthamoeba* genotypes

Known *Acanthamoeba* genotypes and their associations with human diseases, i.e., keratitis and granulomatous encephalitis. *this genotype has been most associated with both diseases. ^ basis of T2 division into T2a and T2b has been proposed by Maghsood et al. [23]. NA - no disease association has been found yet.

<i>Acanthamoeba</i> genotypes	Human disease association
T1	Encephalitis
^T2a	Encephalitis - Keratitis
^T2b	NA
T3	Keratitis
T4*	Encephalitis - Keratitis
T5	Encephalitis - Keratitis
T6	Keratitis
T7	NA
T8	Keratitis
T9	NA
T10	Encephalitis - Keratitis
T11	Keratitis
T12	Encephalitis
T13	NA
T14	NA
T15	Keratitis
T16	NA
T17	NA
T18	Encephalitis
T19	NA
T20	NA

1.2.2 Classification of *Acanthamoeba* species

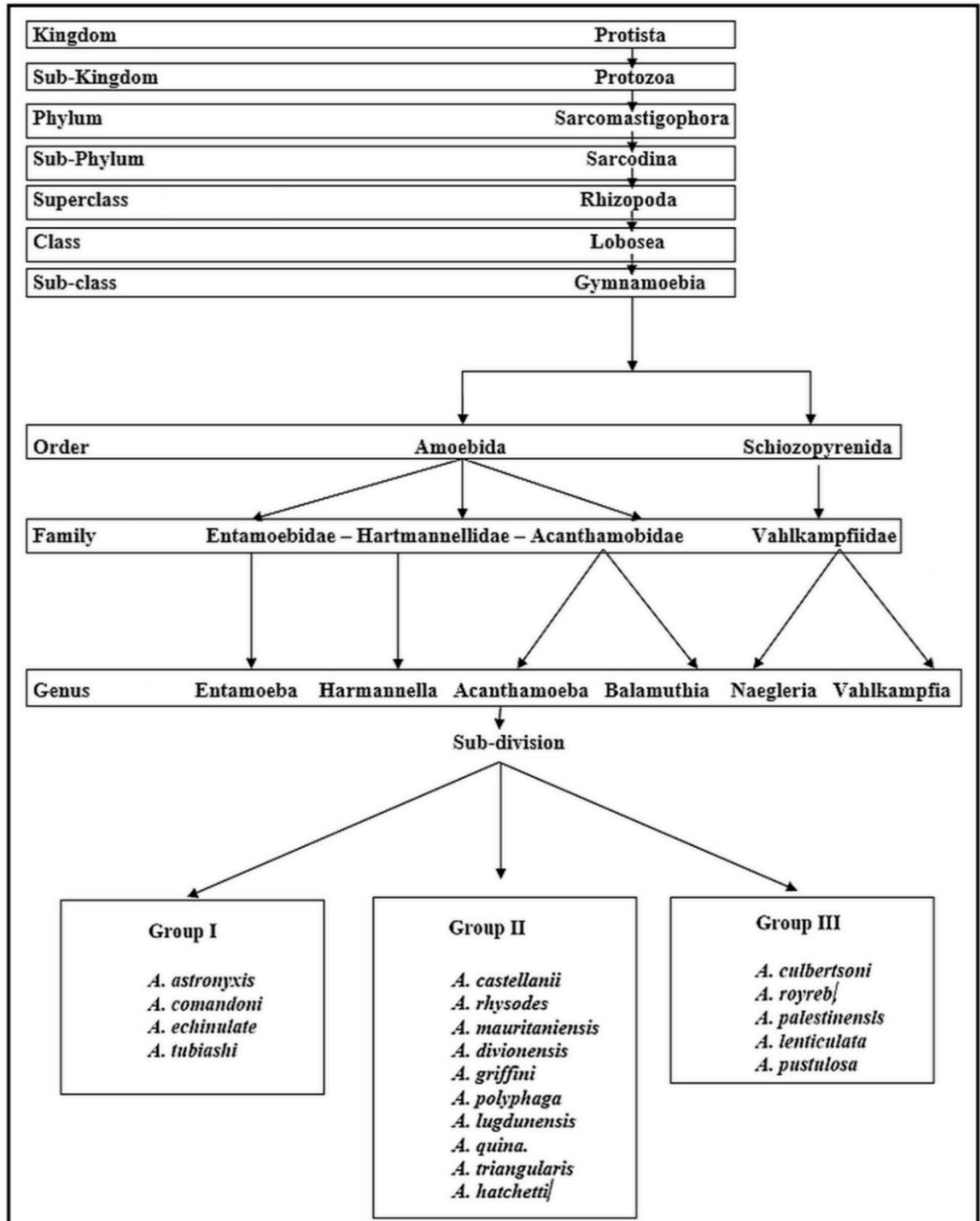
Acanthamoeba spp. was first reported by Castellani in 1930 when he reported the presence of an amoeba as a contaminant in the cultures of *Cryptococcus pararoseus* [18, 20]. Based on rRNA sequencing, it is estimated that amoebae diverged from the mainline of eukaryotic descent, about 1.2×10^9 years ago [24, 25]. Microscopic identification of *Acanthamoeba* is relatively easy due to the presence of spiny surface projections, termed acanthopodia, on trophozoites (Figure 2 B), and cystic form (Figure 2 A). In protists (plant-like) amoebae, such as *Acanthamoeba*, food/particulate ingestion occurs via phagocytosis (receptor-mediated process) or pinocytosis (through membrane invaginations) [26, 27]. The genus *Acanthamoeba* was established in the year 1931 by Volkonsky [28]. *Acanthamoeba* is placed in the Family Acanthamoebidae (Table-2) based on molecular analysis of 16S-like rRNA genes [25]. However, the identification of these amoebae using morphological criteria at the species level has been difficult. *Acanthamoeba* spp. were placed into three morphological groups (I, II, and III) based on cyst size and shape. Nevertheless, the classification of *Acanthamoeba* based on morphological characteristics of the cyst wall has proved unreliable because cyst morphology can change depending on culture conditions [29-32]. The genus *Acanthamoeba* comprises several species, (Table-2) historically assigned to one of the three groups of 18S ribosomal RNA (rRNA) gene [32] and (18S rDNA) sequences.

1.2.3 Free-living amoebae (FLA)

FLA have attained significance in the scientific world over the past few decades due to their ability to cause severe and sometimes fatal infections in humans and animals and the varied roles they play in the ecosystem [34-36]. Though these amoebae are free-living organisms, they can occasionally invade a host like animals and humans [29, 31, 32]. The term FLA is largely used to denote facultative pathogenic amoebae of the genus *Acanthamoeba*, *Balamuthia*, and *Naegleria*. These FLA are mitochondriate, aerobic, unicellular eukaryotic protists [36-38]. Culbertson et al., in 1959 were first to report the pathogenic potential of *Acanthamoeba* that was

demonstrated to exert cytopathic effects on monkey kidney cells *in vitro* and killed laboratory animals *in vivo* [29].

Table 2. Taxonomical Classification of *Acanthamoeba* spp. Taxonomical Classification of *Acanthamoeba* spp. [Reproduced with permission of Khan NA. Ref # [16] and Classification of *Acanthamoeba*. G.S. Visvesvara-1991 Ref # [33]-Suppl-5]



1.2.4 First report of *Acanthamoeba* spp. as an FLA

Round or oval in shape, cells with a diameter of 13.5 - 22.5µm with pseudopodia were reported by Castellani in the year 1930. While working with the fungus *Cryptococcus pararoseus*, Castellani observed and considered these amoebae as contaminant organisms that had amoeboid motility [16-18, 20].

1.3 Life cycle

Depending upon the environmental, nutritional, and chemical milieu, *Acanthamoeba* spp. exists in either an encysted stage (Figure 2 A) or its infective trophozoite stage (Figure 2 B).

1.3.1 Cyst stage

When *Acanthamoeba* trophozoite encounters hostile environmental conditions such as significant variation in pH, temperature, or nutritional availability, a process of cell differentiation called encystation occurs which leads to the formation of cysts (Figure 2 A) [36, 38, 39].

The mature cyst of *Acanthamoeba* is composed of a double-walled structure consisting of an inner (endocyst) layer and an irregular outer (ectocyst) layer [40, 41]. Cysts of *Acanthamoeba* are on an average of 10-15µm in diameter (Figure 2 A). Pores, also called ostioles, are present at different sites in the cysts.

1.3.2 Trophozoite Stage

Acanthamoeba exists in trophozoites (Figure 2 B) form if it is provided with an optimal nutrient source, temperature around 37°C, neutral pH, and osmolarity ~70 mOsmol. In the trophozoite form, *Acanthamoeba* divides by binary fission [24]. The trophozoite is usually about 25 µm in diameter but can be as small as 15 µm and larger forms can be 35 µm [18, 34, 36-38]. The trophozoite stage is recognized by the presence of thorn-like projections called acanthopodia on its cell surface that assists in adhering to surfaces, holding the prey before phagocytosis and motility [37, 38].

1.3.3 Cell biology of *Acanthamoeba* spp.

Acanthamoeba trophozoites possess a single nucleus that is about 1/6th the size of the trophozoite. The nucleus in the trophozoites, like that of any other eukaryotic cell, is enclosed within a nuclear membrane [43]. The pores present on this membrane are termed nuclear pores. The other prominent structure present inside the nucleus is the nucleolus. The cytoplasm constitutes the major portion of the cell and contains typical eukaryotic organelles. It possesses a large number of fibrils, glycogen, and lipid droplets [39, 43]. *Acanthamoeba* also possesses endoplasmic reticulum and the Golgi complex [43, 44]. The trophozoite contains numerous mitochondria that are primarily involved in energy production through adenosine triphosphate (ATP) generation [43]. Under normal conditions, cells divide asexually through binary fission; however, the generation time differs, from 8 to 24h, for isolates belonging to different genotypes [44].

1.3.4 Feeding in *Acanthamoeba* spp.

Acanthamoeba trophozoites are considered a major bacterial consumer [45]. In the natural environment, *Acanthamoeba* feeds on diverse microorganisms [46] through the process of phagocytosis [47] whereas liquids are ingested through pinocytosis [48]. The intake of food occurs by the projection of acanthopodia, food cup formation, and subsequent phagocytosis [26, 27]. During this process, *Acanthamoeba* surrounds the particle to be ingested with its plasma membrane followed by a flask-like invagination forming a phagosome (Figure 3) [49]. The phagosome then fuses with the lysosome to form a phagolysosome (Figure 3) to digest the ingested substance with the help of hydrolytic enzymes [50, 51]. In pinocytosis (Figure-7 A, empty invaginations), solutes, and mediums are ingested through membrane invaginations [49]. The calculated volume of fluid uptake during the process of pinocytosis is 2 μ L per 10⁶ cells at 30°C, while no pinocytosis occurs at 0°C. The uptake of organic material from the culture medium through pinocytosis is around 60 μ g per 10⁶ cells per hour [49].

1.3.5 Interaction between *Acanthamoeba* and other Microbial Pathogens

Acanthamoeba (Figure 3 A, B) also serves as a host, acting as a 'trojan horse', for pathogenic organisms (Figure 3. vacuoles C, D) such as *Vibrio cholerae*, *Burkholderia cepacia*, *Listeria monocytogenes*, *Escherichia coli* O157, *Mycobacterium Bovis*, and *Mycobacterium avium*, allowing them to replicate and survive inside it and thus also serving as a means for transmission and dispersal of the pathogenic microbes [17, 37, 38]. The cytosolic locations of these microorganisms (Figure 3 C, D) protect them from immune destruction conditions. Studies have also suggested that there are a variety of interactions where lateral gene transfers occur between the host and the ingested microbe [11]. Interaction of pathogens with *Acanthamoeba* has shown an induction and maintenance of virulence factors that increase microbial pathogenicity of *E.coli* [37, 38]. Interaction of the *Acanthamoeba* with microbes is correlated with the observation of higher

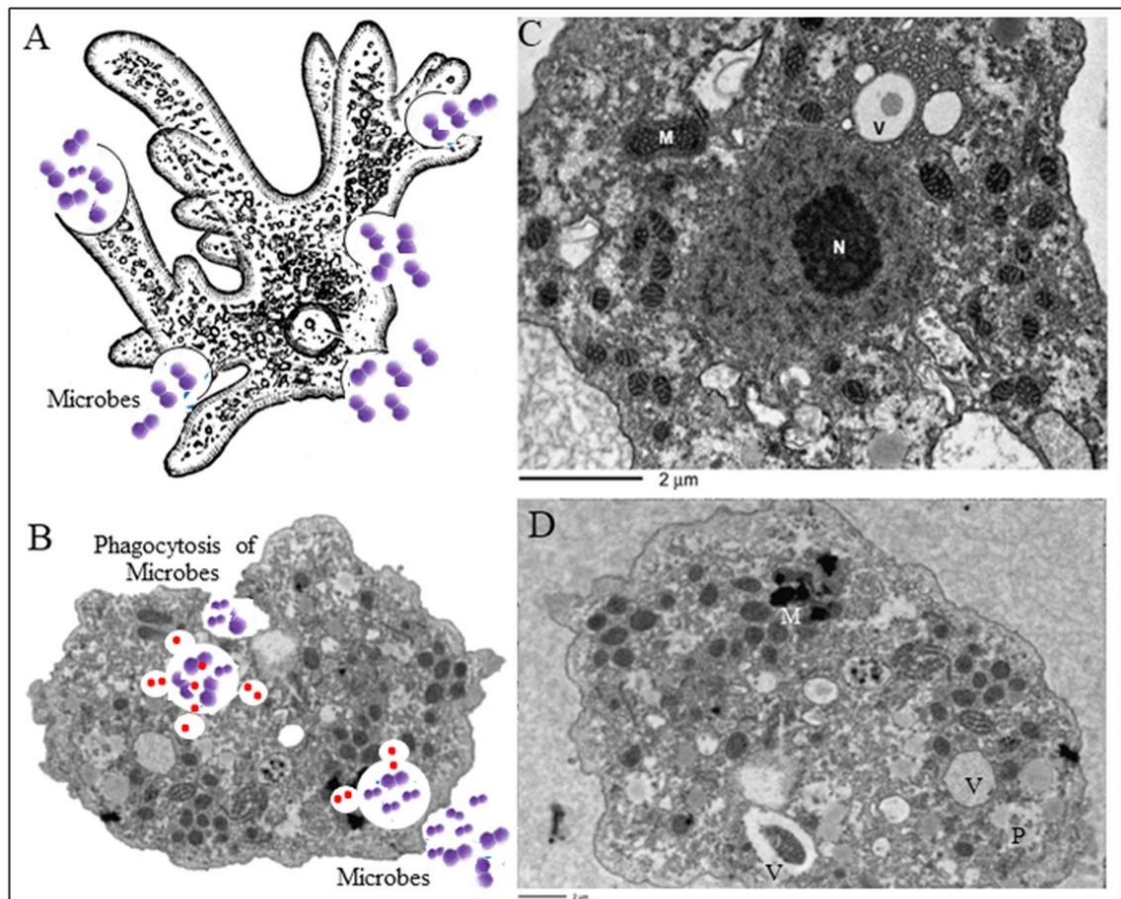


Figure 3. Interaction between *Acanthamoeba* and Microbial Pathogens

Schematic diagram showing phagocytosis of the microbe (purple) by *Acanthamoeba* trophozoite (A) with the formation of intracellular phagosomes and phagolysosomes (white circles with enzymes as red dots) (B). Transmission electron micrographs of *Acanthamoeba* trophozoite with phagosomes and vacuoles (M is mitochondria, N is a nucleus and V is the vacuole) (C-D). **[Images B-D were acquired from the book “Biology and Pathogenesis of *Acanthamoeba*”, with permission of Khan NA Ref-# [38]].**

gene numbers and the DNA content of amoeba-resistant microorganisms. The organisms escape the microbicidal action of the FLA. via mechanisms similar to the ones that come in play during the survival of Mycobacterium within the macrophages [52, 53]

1.4 Epidemiology of *Acanthamoeba* Infections

Acanthamoeba spp. is an opportunistic protist pathogen, which can be found in soil, air, and water samples and as a commensal in human nasopharynx [16, 17, 37]. *Acanthamoeba* can survive in freshwater, humidifiers, sewage, beach sands, home aquaria, flowerpot soils, hospital environment, dental and dialysis unit, and contact lens cleaning liquids [15-17, 38]. *Acanthamoeba* spp. can tolerate a wide range of temperature, salinity, osmolarity, and pH extremes which permits them to survive in tissue culture, mammalian body fluid, and distilled water. If the surrounding conditions turn hostile, it assumes a cystic form to re-emerge as trophozoite when the conditions turn favorable [17, 37]. The infections caused by the pathogenic genotypes (Table-1) are ocular keratitis, encephalitis, sinus, and wound infections detailed below.

1.4.1 *Acanthamoeba* Keratitis (AK)

AK is a non-fatal infection of the human cornea but is nonetheless disabling as it causes blindness if untreated and is reported mostly in contact lens users. Around 8 species and the T3, T4, T5, T6, T8, T10, T11, and T15 genotypes of *Acanthamoeba* (Table 1) have been reported to cause AK [13, 54]. The recreational water sources such as lakes, ponds, and swimming pools are environmental sources of *Acanthamoeba* and related FLA infections. In Italy, the presence of *Acanthamoeba* genotypes T3, T4, and T15 were reported in water samples collected in the regions

of Lazio and Puglia, where they were connected to reported cases of AK [55, 56]. The incidence rate of AK varies between different countries. An incidence rate of 0.33 per 10,000 contact lens wearers is reported in Hong Kong, 0.05 /10,000 in Holland, 0.01 /10,000 in the United States, 0.19/10,000 in England, and 1.49 /10,000 in Scotland [16, 38]. In the year 2004, it was estimated that 2% of the total world population, nearly ~ 120 million people, wore contact lenses which estimates the population susceptible to AK [16, 55, 57, 58]. Cysts of *Acanthamoeba* species can withstand drying and thus transport by water and air is possible. Most of the AK cases in the UK have a history of contact lens use [99, 100] and the use of contaminated water to clean the contact lenses may be the predisposing factor [55, 57]. The high-risk factors for AK are wearing contact lenses for extended periods, non-sterile contact lens rinsing, corneal trauma, biofilm formation on the contact lens, and swimming in contaminated water while wearing contact lens [57, 58]. An outbreak of AK and the prevalence of AK in a study (Figure 4) shows a rising trend in this corneal disease in the past 3 decades.

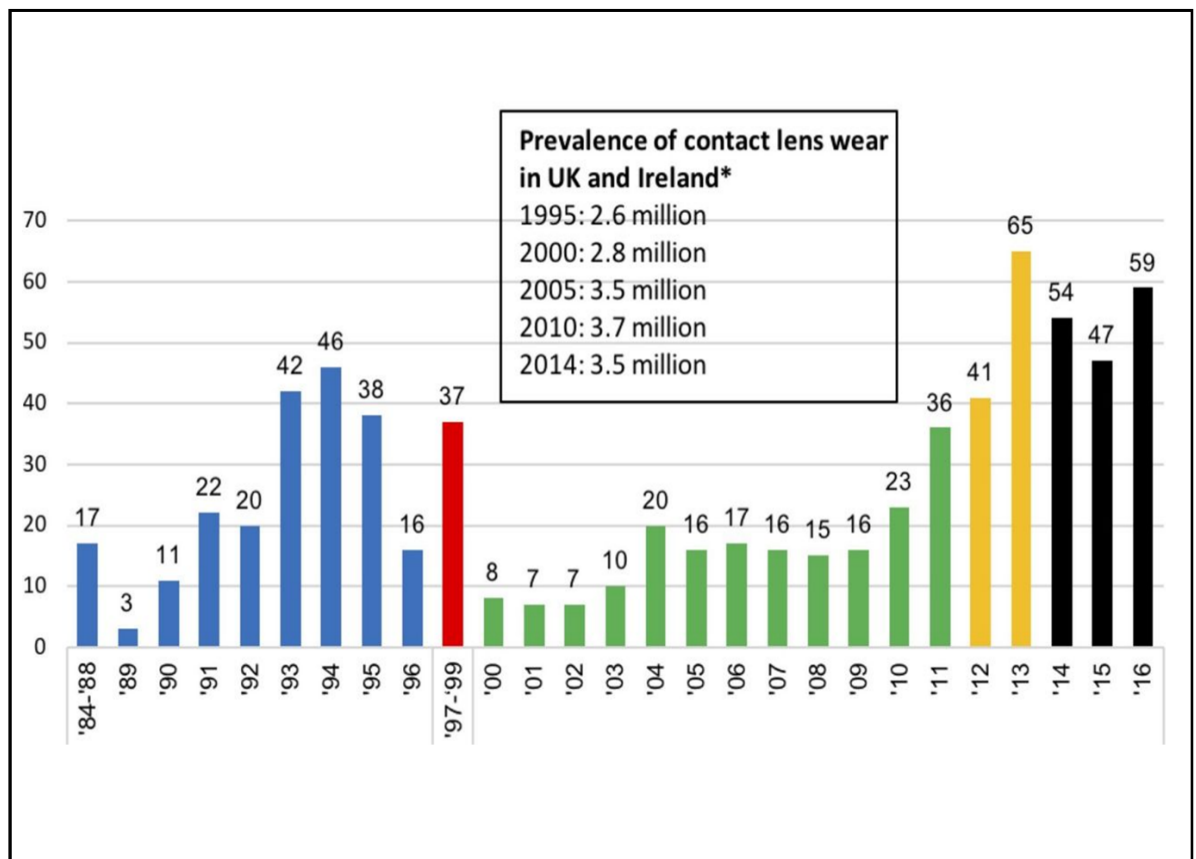


Figure 4. *Acanthamoeba* keratitis cases at Moorefield's Hospital (1984-2016).

The data reported from Moorfields hospital is shown that spreads over 33 years with a total of 709 cases of AK. The different periods (x-axis) are labeled and the cases reported (y-axis) by color in the figure. Each color represents a different data collection method like microbiology laboratory, electronic database / published reports, and data available from a national survey, etc. Insert box is the national data *. [Adapted from Ref # [55]].

Commonly, only one eye is involved but bilateral keratitis has also been reported. *Acanthamoeba* transmission into the cornea is dependent on its virulence and the physiological state of the cornea. Corneal traumatism is a prerequisite in keratitis in non-contact lens wearers and for individuals with AK, the trauma of the cornea is implicated in 85% of contact lens wearers. Genotyping (Table-1) has allowed the identification of six isolates of the T4 and one of the T8 genotypes in Hungary recently [59]. Between the period of 2002-2017, 111 confirmed AK cases were identified, including 75 (67.6%) in Iowa residents in the US alone [60]. Non-contact lens-related cases of AK related to contaminated water have also been on the rise in south-east Asian countries. An outbreak of AK in 2010-2011 with an incidence threefold higher than in 2004-2009 has been reported [55]. Risk factors for AK were: poor contact lens hygiene, deficient hand hygiene, and use of contact lenses while swimming or bathing.

1.4.2 Granulomatous Amoebic Encephalitis (GAE) Caused by *Acanthamoeba* spp.

GAE is a rare infection of the central nervous system (CNS) that has a very high mortality rate [38, 61, 62]. Another worrying aspect of the relevance of diseases related to *Acanthamoeba* spp. in humans is the recent occurrences of GAE in patients with solid organ transplantation [63] and patients with systemic lupus [64]. There have been a total of about 500 cases of GAE worldwide to date, the exact figure is likely to be far higher, with less than 10 % survival rate [62, 64]. The infection is commonly seen to affect individuals with a weakened immune system. GAE is an opportunistic and fatal disease, which affects immunocompromised or debilitated hosts (particularly patients with HIV/AIDS, diabetics, or those who have undergone organ transplantation). Studies from around the world have reported genotype T4 to be the predominant genotype while less frequent genotypes were T1, T2, T5, T10, and T18.

The involvement of the CNS is secondary to a primary site infection, which commonly is a wound or a sinus infection.

1.4.3 Cutaneous and respiratory infections

Skin infections caused by *Acanthamoeba* can appear as reddish nodules, skin ulcers, or abscesses in the skin (Figure 5, B) [62]. The respiratory infection caused by *Acanthamoeba* spp. are not common, but sinus infections have been reported with *A. castellanii* [65, 66]. The skin lesions morphologically give no clues towards *Acanthamoeba* spp. as the causative agent. Typically, the skin lesions follow a protracted course with little signs of healing by regeneration or scar. They appear as chronic ulcers that have an irregular margin and cloudy base [67] (Figure 5, C).

1.4.4 Pathogenesis of *Acanthamoeba* Keratitis

Of the predisposing factors described above [55, 68], corneal trauma caused by contact lens followed by the use of the lenses that are soaked in water or cleaning solutions contaminated with *Acanthamoeba* are known to cause AK [55]. Initial pathogenesis in AK involves adherence of the amoebae to the host cells (cornea, vascular endothelium, and stratified squamous epithelium of the skin) followed by invasion and damage [16, 55, 57, 58]. Several proteins including mannose-binding protein (MBP) [67, 69] and cell adhesion molecules like integrins have been reported to facilitate adhesion of the trophozoites to corneal epithelium [70]. Once the trophozoite forms colonize the cornea, the metalloproteinase and diverse enzymes produced by the trophozoites imitate a cascade of events that helps in the invasion of the parasite into the deeper layers of the cornea. Corneal opacities develop commonly (Figure 5 A) which reflect the morphological results of the vision-threatening keratitis caused by *Acanthamoeba* spp. In advanced AK, the involvement of deeper layers of the eye has been reported with complications requiring surgical interventions. The neovascularization from the sclero-corneal junction (limbus) further intensifies the inflammation by pouring inflammatory cells into the cornea. As this infection occurs usually in an immunocompetent host, a granulomatous reaction could significantly contribute towards corneal damage. The ring abscesses are seen to first develop

along the limbus, a region from where the blood vessels are known to neo-vascularize the cornea in keratitis [71].

1.4.5 Pathogenesis of GAE

GAE is the CNS manifestation of *Acanthamoeba* infection. How the *Acanthamoeba* trophozoite spread from the primary site to the bloodstream to cause GAE is not completely understood yet [38, 61, 62], but an invasion of the circulation followed by dissemination to the CNS may be the underlying pathway. The human immune system mounts a chronic inflammatory granulomatous response instead of an acute inflammatory reaction to the presence of *Acanthamoeba* trophozoite in the tissues [72]. A granulomatous response tends to form to wall-off *Acanthamoeba* trophozoite and prevent further spread in the body. This granulomatous inflammatory response is the result of a Type-IV hypersensitivity reaction and for mounting such an immune response, the individual should be in a complete or partial immunocompetent state. Penetration across the BBB possibly involves adhesion of the trophozoites to the endothelium followed by the movement of the trophozoites in between the endothelial cells or after causing direct damage to the endothelium [61, 62, 73]. The mechanism of cellular damage in GAE is known to involve a combination of cellular damage caused by cytotoxic enzymes of *Acanthamoeba* and the inflammatory cytokines released by macrophages within the granuloma [72].

1.5 Clinical Features of *Acanthamoeba* infections

1.5.1 *Acanthamoeba* Keratitis

Individuals affected with AK often complain of redness of the eyes, ocular pain, blurred vision, photophobia, irritation in the eye, and excessive lacrimation (Table-3) [37, 55, 67, 74]. As these symptoms resemble other common eye infections, an early diagnosis is often missed which is essential for effective treatment of *Acanthamoeba* keratitis. AK progresses to produce a ring of abscess at the sclero-corneal junction (limbus) [74, 75] (Figure 5 A-2). Untreated AK leads to uveitis, corneal damage, and blindness by progressing to the deeper layers of the cornea [16, 17, 74].

1.5.2 Skin and Wound infection

Skin infections caused by *Acanthamoeba* can appear as reddish nodules, skin ulcers with a dirty base, or abscesses in the skin (Figure 5, B, C). Secondary bacterial infections in immunocompromised patients may be seen [76]. Both, trophozoite and cystic forms of *Acanthamoeba* spp. are found in the contaminated wounds, which via the bloodstream reach the CNS to cause GAE (Figure 5- B-G).

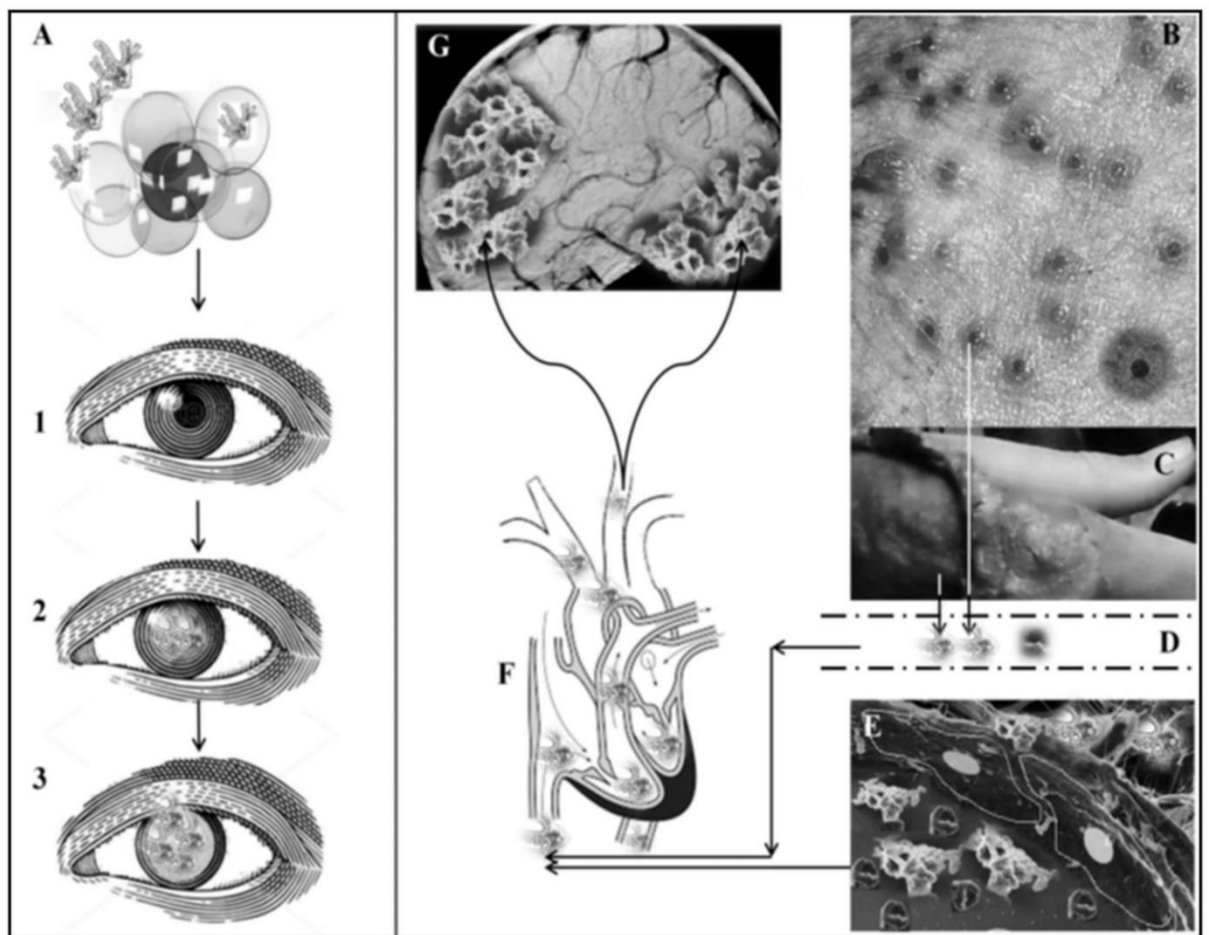


Figure 5. Infections caused by pathogenic genotypes of *A. castellanii*

Acanthamoeba trophozoites contaminate the contact lenses (A). Wearing infected contact lenses leads to AK which causes corneal opacity and blindness (1-3). Trophozoites from wounds (B-C) enter circulation (D-E) and travel to the brain via blood pumped by the heart (F) to infect the CNS by traversing the BBB. [Adapted from Ref # [67]].

1.5.3 Sign and symptoms in GAE:

In GAE, clinical symptoms (Table-3) include headache, mental status changes, vomiting, photophobia, apprehension, fever, lethargy, cranial nerve palsies, hemiplegia, stiff neck, loss of coordinated movements, increased intracranial pressure, and lack of speech. Terminal stages include comatose state, fits, and respiratory arrest causing death [77-81]. Widespread body infections may occur after organ transplantations in humans [79]

Table 3. Organ involvement, signs/symptoms, predispositions, and prognosis of *Acanthamoeba* infections [Adapted from Baig AM 2018, book chapter Ref# [67].

Infections caused by <i>Acanthamoeba</i> spp.	Predisposing conditions and source	Clinical Features	Prognosis and Outcome
1. Cornea - <i>Acanthamoeba</i> keratitis (AK)	1. Corneal trauma caused by contact lens or other physical causes 2. Contact lens contamination. 3. Swimming and showering with contact lenses.	<ul style="list-style-type: none"> • Redness of the eyes • Ocular pain • Blurred vision • Photophobia • Irritation in the eye • excessive tears • Opacity of cornea • Corneal ulceration • Uveitis 	<ul style="list-style-type: none"> • Poor prognosis without treatment. • Blindness is common without treatment
2. Brain and spinal cord - Granulomatous amoebic encephalitis (GAE).	1. Immunocompromised states, like AIDS and corticosteroid therapy. 2. Skin lesions, infected wounds, post-transplantation of organs, infected air-sinuses. 3. Severe malnutrition	<ul style="list-style-type: none"> • Fever • Headache • Vomiting • Apprehension • Photophobia, • Cranial nerve palsies • Paralysis of one side of the body • Stiff neck • Aphasia • Ataxia • Raised intracranial pressure 	<ul style="list-style-type: none"> • Very poor with death occurring due to brain stem herniation and respiratory arrest.

3. Skin	<ul style="list-style-type: none"> Contaminated water, soil. 	<ul style="list-style-type: none"> Multiple or single broad-based ulcers of the skin and sinus mucosa Thick margins around a central dirty ulcer base. Fever and pain at the site on skin or over the air-sinus 	<ul style="list-style-type: none"> Poor – Many cases continue to become chronic ulcers on the skin.
4. Air sinuses	<ul style="list-style-type: none"> Immunocompromised state, like AIDS and corticosteroid therapy. 	<ul style="list-style-type: none"> Nasal congestion and discharge Super-infection. 	<ul style="list-style-type: none"> Moderate – In cases of air-sinuses

1.6 Diagnosis of *Acanthamoeba* Infections

Acanthamoeba infections are difficult to diagnose because of their clinical similarity with infections caused by bacterial and fungal microorganisms [72, 82, 83]. For example, GAE is caused by *Acanthamoeba* spp. resembles fungal or tuberculous encephalitis [16, 17, 37, 38]. AK caused by *Acanthamoeba* is akin in its morphology to bacterial corneal keratitis [84-87] and wound infections appear to be similar to tuberculous or fungal ulcers [67]. Absolute diagnosis of *Acanthamoeba* infection and its genotyping involves methodologies like RT-PCR [74] and immunostaining with *Acanthamoeba* specific antibodies. Additionally, the diagnosis of the amoebal origin of infection requires microscopic examination and culturing in a specialized growth medium [75]. Radiological imaging like CT scans and MRIs are only helpful in showing the location of the lesions in GAE but do not provide a definitive clue towards the diagnosis [17]. In cases with AK and skin lesions, the culture of the biological fluids from the lesion and in cases of GAE, the CSF microscopy, culture, RT-qPCR helps in establishing *Acanthamoeba* as the causative agent [17, 76, 79]. Long periods pass to resolve the diagnosis which is complicated by the time taken in resolving other diseases that are considered in the differential diagnosis [37, 38, 63, 72, 88, 89]. Culture remains the gold standard of laboratory diagnosis of *Acanthamoeba*, but several PCR-based techniques are currently available that can accurately diagnose *Acanthamoeba* with certainty [17, 74]. The tentative diagnosis of AK can often be made by *in vivo* confocal microscopy as *Acanthamoeba* cysts appear as hyperreflective, spherical structures that are usually well defined because of their

double-wall, but due to varying cyst morphology, a diagnostic identification is not forthright [90].

1.7 Treatment of AK and GAE

The drugs used in the treatment of AK and GAE consist of a combination of various chemical agents, for example, azoles, amphotericin-B, rifampin is given in GAE, and mostly biocides in AK (Figure 6), that target *Acanthamoeba* specific enzymes and proteins. With the above-mentioned drugs, the morbidity associated with AK and mortality associated with GAE is yet to prove their efficacy. Though drugs that target human-like cellular receptors and proteins have shown to be amoebistatic and amoebicidal in FLA [108] including *Acanthamoeba* spp, their targets remain to be elucidated. The drugs tested *in vitro* in the past included chlorpromazine and other phenothiazine compounds prescribed in non-infectious human diseases [90] which are yet to be tested in AK and GAE.

1.7.1 Main reasons behind the failure of treatment in AK

The management of AK has remained problematic and even with a combination of several drugs, the outcome remains poor. The factors that have contributed towards a failure of treatment and poor outcomes include

1. Frequent instillation of drugs in the form of eye drops that is difficult to follow.
2. A longer period of the drug treatment regimen that extends to a duration of 12 months plus.
3. The inability of the drugs to exert their action on trophozoites as the drug escapes the eye after instillation through tears.
4. Irritant effects of the drugs on the eye.
5. The transformation of trophozoites into cysts to resist the drugs.
6. lack of interest in drug development due to the rarity of the disease.

1.7.2 *Acanthamoeba* Infections as Orphan Diseases

The World Health Organization defines orphan/rare diseases as ‘all pathological conditions that affect 0.65-1 out of every 1000 inhabitants.’ The EU defines a rare disorder as one with a prevalence of 5:10,000 Europeans. Of the diseases caused by *Acanthamoeba*, AK with a # ICD10: B60.1+ H19.2 is listed as an orphan disease at Orphanet Rare Disease Platform [91, 92]. Although the incidence of AK infections in humans is low, they are notoriously difficult to treat [93]. NIH lists AK and GAE under the heading of genetic and rare disease (GARD) and has a web portal that provides information on the infections caused by *Acanthamoeba* spp. [91, 94]. Recognizing AK as a rare disease, orphan drug trials are now active in countries like the UK, Italy, and Belgium. The fact that AK and GAE are very difficult to treat makes the discovery of orphan drugs against these infections challenging.

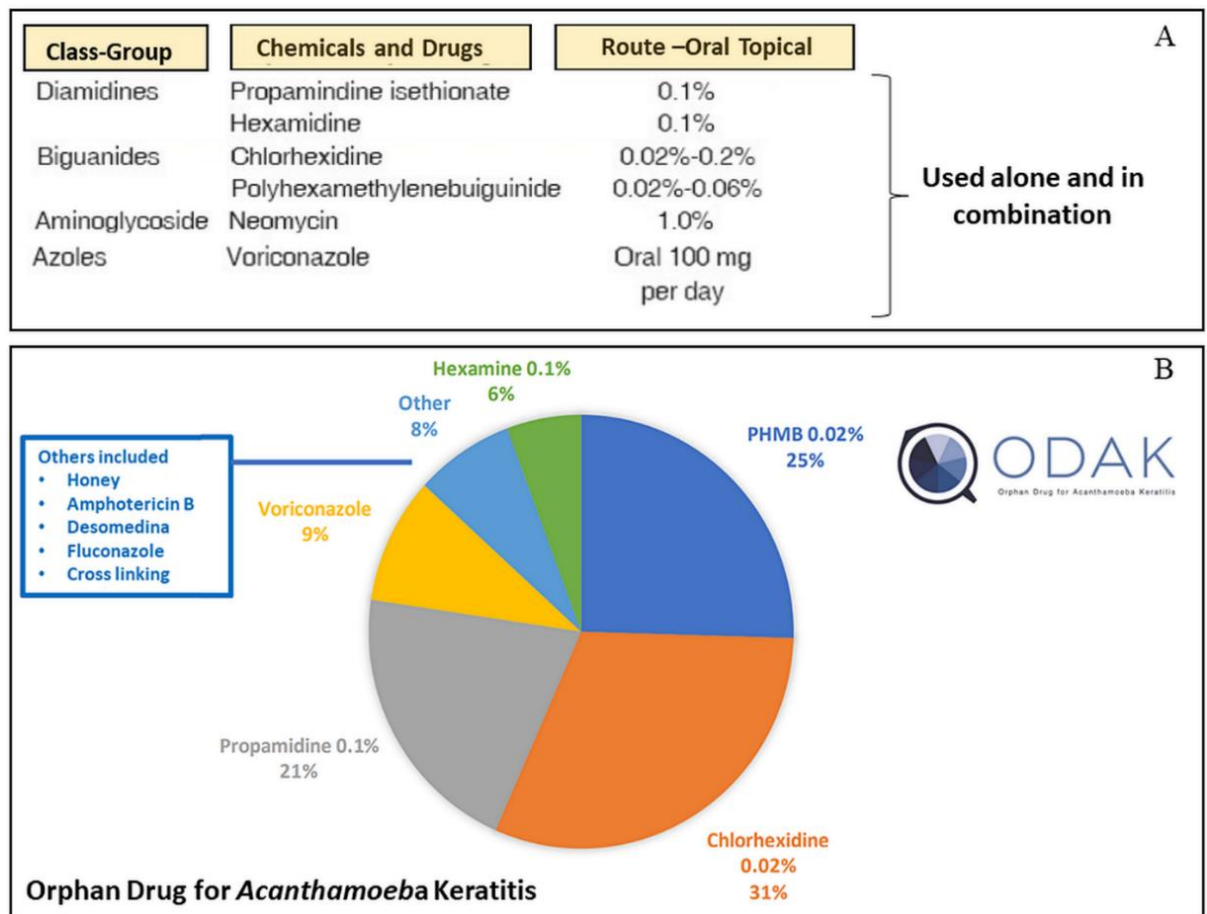


Figure 6. Current Drugs used in AK and the ODAK report 2017.

(A) Different drugs and biocides are used alone and in combination via the topical route (eye drops) and orally in AK for months. (B) A range of off-label drugs tested in ODAK trials is shown that were tested in *Acanthamoeba* keratitis in a report published in 2018 by Orphan drug for *Acanthamoeba* keratitis (ODAK). [Adapted from Ref # [95].

1.7.3 Orphan drug development in *Acanthamoeba* infections

The orphan drugs by definition are pharmaceutical agents developed to target a rare disease. The development of orphan drugs for AK is much needed as it has been on the rise in the past decade (Figure 4) [91-93]. In this regard, Orphan Drug for *Acanthamoeba* Keratitis (ODAK) (Figure 6), a European research project, has investigated the safety and efficacy of polyhexamethylene biguanide (PHMB) eye drops to provide the basis for marketing and authorization of this agent [95, 96]. Moorfield's Eye Hospital, in the UK, has reported on clinical trials for the effectiveness of PHMB and other off-label drugs in AK [55, 56, 58].

Another example of an orphan agent is the drug miltefosine that was designated to be an orphan drug in the management of AK by the FDA [55]. This agent has also been used to treat GAE caused by a related free-living amoeba called *Balamuthia mandrillaris* and primary amoebic encephalitis caused by *N. fowleri*. Recently, it has been used to treat refractory cases of AK [97].

1.7.4 Key reasons behind the failure of treatment in GAE caused by *Acanthamoeba* spp.

Though the treatment of GAE is hindered by the difficulties in rapid and authentic diagnostic tests, the management of GAE is problematic mainly due to:

1. The restriction offered to the drugs by the blood-brain barrier (BBB) remains a real obstacle even when given via intravenous route [17, 37, 38].
2. The resistance of the cystic forms to the chemotherapeutics agents.
3. The inability of the drugs to penetrate the lesion due to the lipid solubility of the drugs.
4. Neurotoxicity associated with the drugs used in GAE.
5. Lack of interest in new drug development in GAE due to its rarity.

1.7.5 Lack of drug development for the treatment of GAE

As GAE caused by pathogenic strains of *A. castellanii* (Table 1) is a rare disease, there has been a paucity in drug development for this fatal encephalitis. Even after 6 decades of the first reports of GAE, the mortality rate has remained static for this infection. With the single exception of miltefosine, all the remaining drugs are either conventional anti-fungal drugs or broad-spectrum antibiotics. Even with miltefosine, the success rates in GAE are yet to prove its efficacy.

1.8 Drugs with the potential to be orphan drugs in infections caused by *Acanthamoeba* spp.

The phenothiazine group of drugs has been experimentally used against FLA *in vitro* in the past [98] and other members of this group of neuroleptics stand a chance of being repurposed, but the precise cellular targets of these drugs are not known. A list of diverse biocides [95] and drugs like miltefosine [55] have shown the potential to become orphan drugs and have the advantage of already being used in humans, but the drugs used in AK need to be evaluated for ocular safety, patient compliance, and activity against cystic forms of *Acanthamoeba* spp. For GAE, there is a need to test drugs already prescribed for neurological diseases against pathogenic genotypes of *Acanthamoeba* known to cause GAE (Table-1).

1.9 Use of Bioinformatics computational tools in anti-parasitic drug target discovery

The use of bioinformatics (a discipline in which biology, computer science, and information technology are merged) computational tools in drug target discovery have played a fundamental role. Pharmaceutical companies have boosted their ability to find novel molecular targets and chemical compounds that can bind these targets by exploring the retrievable chemical and biological data accessible from diverse databases [99-101]. As the knowledge of the molecular basis of biological systems evolves, the tools for storing and analyzing the data on molecular targets have been amplified as well.

1.9.1 In silico screening in the discovery of Antiparasitic drugs

In silico drafting or pre-screening of the chemical compound may also be a beneficial approach for the identification of novel drug leads for parasitic infectious diseases. In silico methods take advantage of modern high-performance computing as well as the vast amount of publicly available pharmacological, biological, and chemical data. Databases, such as PubChem [100], Drug Bank [101], and ChEMBL [99] contain information that can be retrieved and manually curated from the freely available literature to guide compound selection (Figure 7). One example, one the forte of data mining used to identify drug repurposing possibilities was in the case of *Cryptosporidium parvum*, a protozoan that commonly causes opportunistic infections in immunocompromised hosts [102]. Network-based in silico approaches use the methods of systems biology and bioinformatics to directly compare host responses to pathogens and drugs [103]. Another example in this regard is the work of Chavali *et al.*, [104], who used metabolic modeling to generate a list of 15 genes and 8 double-gene combinations predicted to be relevant targets for the neglected tropical disease caused by the parasite *Leishmaniasis major*. Astemizole was introduced in 1983 as a non-sedating selective H1-histamine receptor antagonist for the treatment of allergic rhinitis [103, 105, 106]. In 2006, a screen of the Johns Hopkins Clinical Compound Library (JHCCL) for inhibitors of *P. falciparum* identified the antihistamine astemizole as an effective agent against chloroquine-sensitive and multidrug-resistant parasites in mouse models of malaria [103]. Another success story comes from a recent repurposing campaign for inhibitors of *Entamoeba histolytica*, a protozoan intestinal parasite and the causative agent of human amoebiasis. Debnath *et al.* [107] devised and validated a suitable HTS that identified auranofin, an FDA-approved oral, gold-containing drug that has been in clinical use to treat rheumatoid arthritis for 25 years

1.9.2 Identification of Protein Targets in Parasites:

With the advances in computing bioinformatics computational tools, there have been improvements in the scientific research towards the identification of possible targets in pathogenic parasites by constructing an atomic-resolution model of the "target" protein from its amino acid sequence and an experimental three-dimensional structure protein [82, 83]. The selection of protein targets by predicting their three-dimensional structures has gained significance in drug development (Figure 7, left panel).

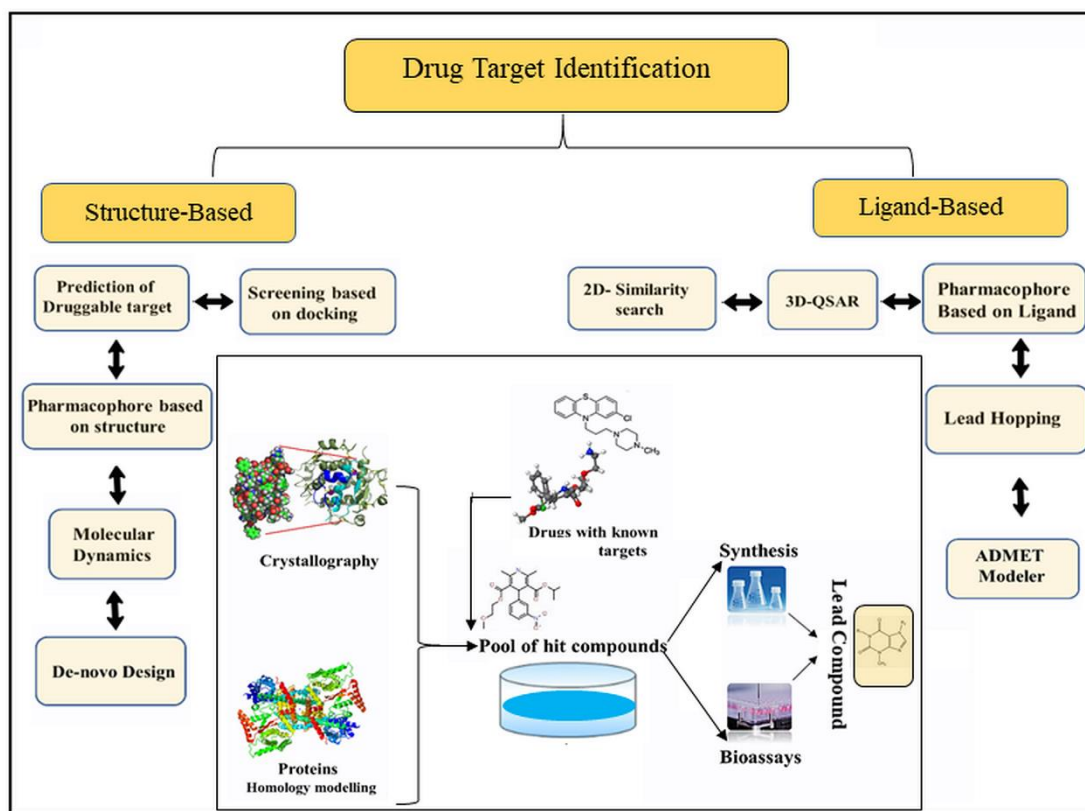


Figure 7. A Workflow of Drug Design Approach.

A workflow of classical structure and ligand-based drug design approach. The pipeline of bioinformatics computational tools that are used in drug discovery and facilitating repurposing of already approved drugs and compounds.

With the availability of diverse compound databases, this cost-effective structure-based or ligand-based strategy can significantly increase the efficiency of drug discovery and provide promising avenues to conquer life-threatening diseases. In the last decades, three-dimensional structures for over 50,000 proteins have been

deposited in the Protein Data Bank (PDB) [108]. Concerning antiparasitic drugs, various well-established protein targets had their structures solved, either by X-ray crystallography or NMR methods. The enzymes related to the shikimate pathway, several kinases, and nucleoside phosphorylases [109] are some examples of these parasitic protein targets. Additionally, knowledge obtained from the parasite genome databases has been modeled using experimentally determined structures as templates [110, 111]. Computational tools have been used to predict structural, functional, and immunological characteristics of the putative amino acid sequences of *Clonorchis Sinensis* (Chinese liver fluke) proteins like 14-3-3 protein and propionyl-CoA carboxylase that could be used as targets for affective parasitic infection control strategies [112]. Investigation of genomic databases and metabolic pathways delivers a useful conceptual framework for the identification of potential drug targets [113]. Extensively integrating complete genomic and proteomic data with other molecular databases via bioinformatics analyses has led to the development of novel, viable strategies for alternative treatments of Chagas disease caused by *Trypanosoma cruzi* [112, 113] and filarial infections of humans caused by *Brugia malayi*, *Wuchereria bancrofti*, *Loa loa* and *Onchocerca volvulus* [114]. The availability of the genome sequence provides a wide range of novel targets for drug design against the drug-resistant malaria parasite in which gene regulated parasite metabolism and organelle function could be attractive targets [115]. In other similar studies, protein homology modeling and molecular dynamics simulation study have helped in the identification of potential drug targets in *Plasmodium falciparum* [116]. In other unicellular eukaryotes, such as *Naegleria fowleri*, exploiting the differences present between enzymes of vital metabolic pathways has been suggested to synthesize antiamebic drugs. An example of this approach is shown with an example of glucokinase in *Naegleria fowleri* (Figure 8).

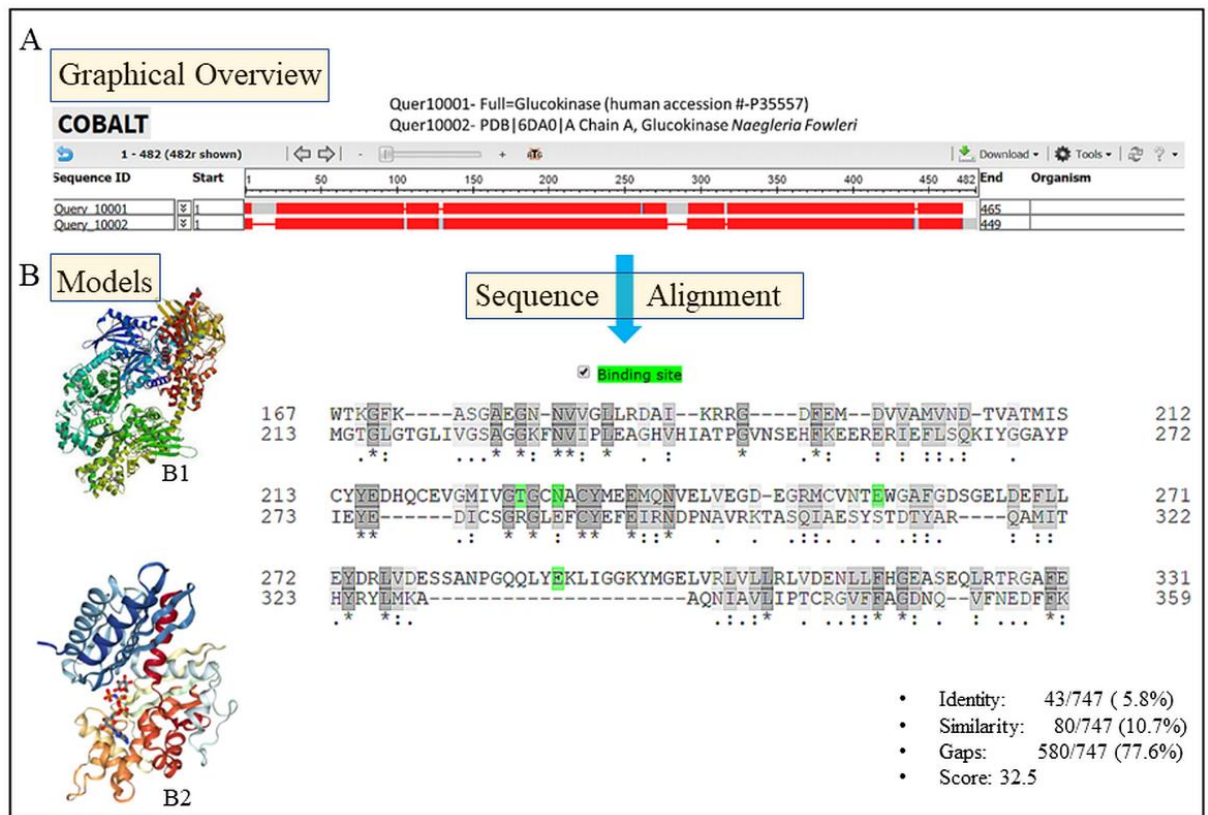


Figure 8. Amino acid sequence homology and structure of glucokinase.

(A) Sequence similarities of amino acids of glucokinase of humans (Quer-10001) and *Naegleria fowleri* (Quer-10002) show the regions of similarities (shaded letters) and dissimilarities (non-shaded alphabets) between 2 enzymes (arrows in the middle) that offer a chance to synthesize specific inhibitors of *Naegleria fowleri* glucokinase. Identities, similarity, gaps, and the score of alignment are shown (lower-right) (B) Template-based models developed for humans glucokinase (B1) and glucokinase in *Naegleria fowleri* (B2). [Retrieved from NCBI, Uniprot, and SWISS-MODEL databases].

Identification of homologs and computational analyses using various bioinformatics tools have identified over 250 targetable putative ubiquitin-proteasome pathway proteins in the *T. cruzi* proteome along with their homologs in other *Trypanosoma* species [117]. The utility of the transcriptomes, proteomes, metabolomes, protein sequence and structure as well as protein-ligand interactions [101, 108, 118, 119] data in the identification of novel molecular targets in disease-causing parasites is illustrated by the fact that the global computational biology market size is expected to

reach USD 13.6 billion by 2026, according to a new report by Grand View Research, (GVR) Inc.[120, 121].

1.9.3 Molecular Docking:

Molecular docking is a computational methodology that estimates the conformation of a receptor-ligand complex. It can also be defined as a simulation process where a ligand engagement position is estimated in a predicted or pre-defined binding cleft or site in a molecular target. Molecular docking is a tool to predict receptor-ligand complexes where a library of several compounds is “docked” against one drug target. The source of these chemical compounds has already been described in the previous sections. Speed and accuracy are key features for obtaining an induced-fit (near ideal) result in docking simulations. There are several docking programs such as DOCK [122], AUTODOCK [123, 124], GOLD [125, 126], FLEXX [127, 128], ZDOCK [129], M-ZDOCK [130], MS-DOCK [131], Surflex [132], MCDOCK [133] and PatchDock (detailed in chapter-3).

1.9.4 The rationale of the study presented in published work

The rationale of the published studies pivots around the hypothesis that, being eukaryotes, humans and *A. castellanii* share similarities in proteins and conserved pathways specifically that mediate calcium (Ca^{+2}) signaling (Figure 9), which can be exploited to bring imbalances in the calcium homeostasis in this protist pathogen. Conceived from the Greek terminology “*Amoeba Proteus*”, referring to the God of changing shapes, it was hypothesized that paralyzing the motility, phagocytosis, cell division, and diverse calcium-dependent physiological functions (Figure 9, highlighted text) in *A. castellanii* by drugs that directly or indirectly act on human-like receptor and ion-channels could prove to be amoebicidal and cysticidal in *Acanthamoeba* spp. Already in use drugs like loperamide, amlodipine, digoxin, procyclidine, dicyclomine, prochlorperazine, and haloperidol were tested initially that to observe if they exhibited antiproliferative effects followed by evidence of the presence of voltage-gated calcium channels (VGCCs) like proteins, calmodulin (CaM), and other possible calcium channels that are coupled with receptors in *Acanthamoeba castellanii*. Non-antibiotic

drugs like the phenothiazine group of neuroleptic drugs have been tested in *A. castellanii* in the past without the evidence of specific cellular targets of the aforementioned drugs [98].

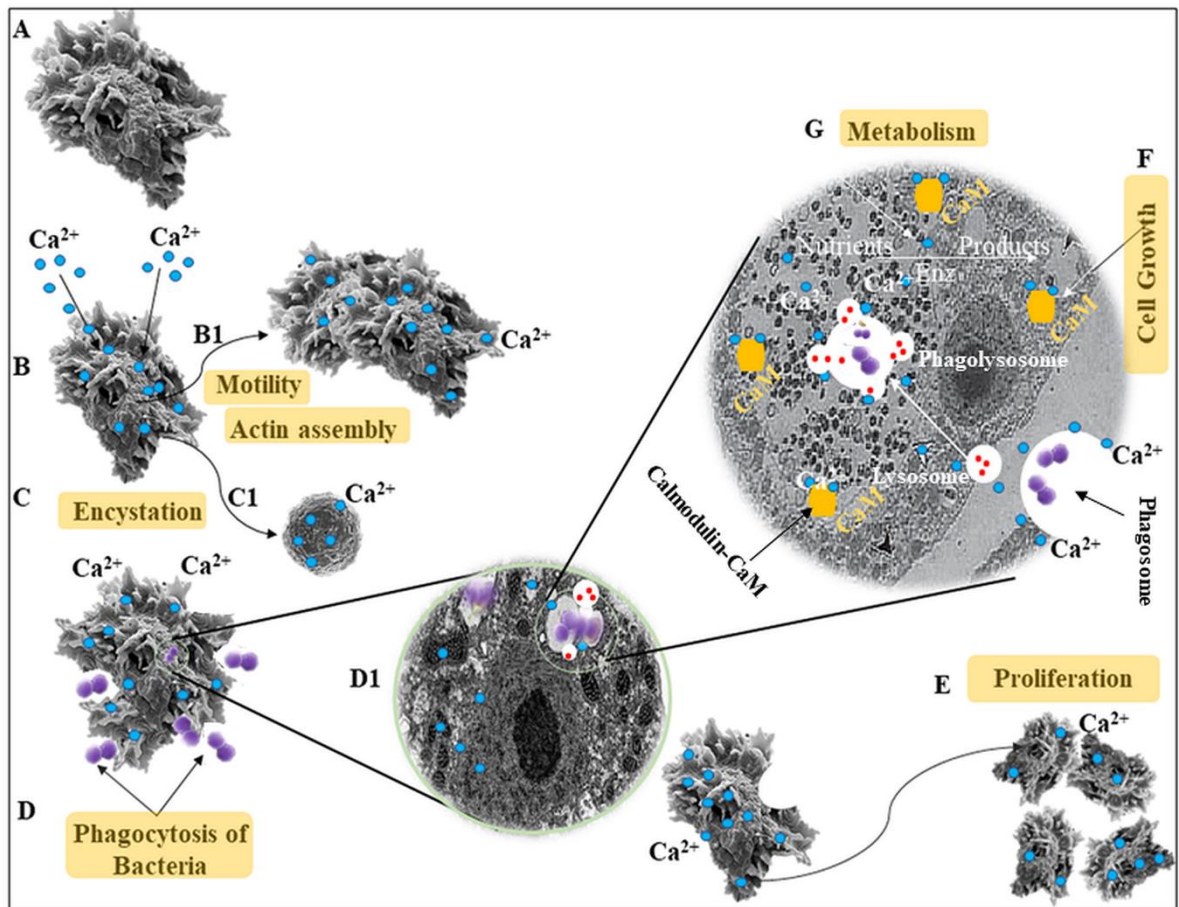


Figure 9. Calcium-dependent cellular processes in *A. castellanii*.

(A) *Acanthamoeba* spp. uses calcium to carry out physiological processes (B-G) that include motility (B1), encystation (C1), phagocytosis, and digestion of the ingested nutrients and bacteria. Processes like cell division, metabolism, and growth all use calcium (blue dots). Note calmodulin (CaM: yellow circles) dependent cellular processes that are executed after the formation of the Ca-CaM complex. Lysosomal fusion with pouring of the enzymes (red dots) into the phagosome is also Ca^{+2} dependent.

Making the use of post-genomic methodologies like proteomics, and transcriptomics, the present study used bioinformatics computational tools seeking sequence similarities, homology modeling, and drug docking predictions to provide the evidence of human-like proteins that were possibly targeted by drugs used *in vitro* in *Acanthamoeba* spp., affecting the viability and growth of this protist pathogen.

The methodology employed in the studies used the human proteins and receptors (that are targets of the drugs experimented) as model molecules that were explored in the genome of *A. castellanii* to find their homologs (detailed in chapter-4). This method uses the amino-acid sequence of a human protein to find a match in the *Acanthamoeba* genome. Candidate *A. castellanii* (T4 genotype) encoded proteins were selected based on their sequence similarities with human proteins, ligand sharing, and functional attributes were then investigated by homology modeling. Additionally, drug docking programs available in online databases were used to determine the stability and drug docking prediction for the drugs used in the experiments on the selected *A. castellanii* proteins. This methodology was intended to provide a possible explanation for the drug effects observed in the past with drugs like chlorpromazine (CPZ) [98] and other non-antibiotic drugs belonging to the phenothiazine class experimented in *Acanthamoeba* spp.

1.9.5 Aims of the study:

Specific aims of the research and papers published in the past 8 years were to:

1. Demonstrate the activity of directly and indirectly acting Ca^{+2} ion modulating drugs exerting *in vitro* amoebicidal, amoebistatic, and cysticidal effects in *A. castellanii*.
2. Determine amoebicidal and amoebistatic effects of human-like muscarinic receptors blocking drugs in *A. castellanii*.
3. Demonstrate the types of cell death induced by drugs affecting Ca^{+2} homeostasis in *A. castellanii*.
4. Identify primitive forms of human-like two-pore (TPC) VGCCs, L-types VGCCs, CaM, G-protein coupled receptors (GPCRs), cholinergic transmission, and human muscarinic receptor-like proteins in *A. castellanii*.
5. Show docking prediction of the drugs tested in *Acanthamoeba* spp. over the templates of the proteins developed for the trophozoite forms of *A. castellanii*.

Details of the methods used (Chapter-2), the results of experimental assays (Chapter-3) along with the evidence of the possible molecular targets and docking predictions (Chapter-4) are detailed in subsequent sections.

2 Material and Methods

In this section, details of the material and methods used in the series of papers submitted for the consideration of Ph.D. by published work are itemized. A detailed material and method section is also described in each published paper attached in part-2 of this thesis.

Section -1

2.1 Experimental Assays

2.1.1 List of the Drugs used in experiments:

Testing drugs and chemical compounds that exhibit *in vitro* amoebicidal and cysticidal effects in *A. castellanii* and are already approved by drug regulating authorities can offer an opportunity to re-purpose them after testing them in human clinical trials against AK and GAE. In vitro drug assays were performed with drugs that are already in clinical use in *A. castellanii* trophozoites and cysts to test amoebicidal and cysticidal effects. The published papers show the effects of selected drugs with the rationale that disturbing Ca^{2+} homeostasis by targeting Ca^{2+} ions transport, intracellular Ca^{2+} dependent adapter proteins, and receptors coupled with Ca^{2+} influx could affect the viability and growth of *A. castellanii*. Drugs that directly and indirectly affect the Ca^{2+} homeostasis like loperamide, amlodipine, digoxin, haloperidol, amiodarone, apomorphine, procyclidine, prochlorperazine, and other FDA approved drugs were selected from a large list of chemical compounds to be tested alone and in combinations in *A. castellanii* belonging to the T4 genotype (Table-4). All chemicals were purchased from Sigma (Poole, Dorset, United Kingdom) unless otherwise stated. Among various drugs tested, amlodipine, nifedipine, verapamil, apomorphine, dicyclomine pirenzepine, and loperamide were purchased from Sigma Aldrich; procyclidine was purchased from Auden McKenzie Pharma; haloperidol was purchased from Searle Pharma Ltd.; amiodarone and prochlorperazine were purchased from Sanofi-Aventis, and digoxin was purchased from Glaxo-SmithKline.

Table 4. Drugs approved by regulating authorities.

Drugs approved by regulating authorities that were hypothesized to, directly and indirectly, affect Ca²⁺ ions hemostasis in *Acanthamoeba* spp. [Adapted and modified from Baig AM, 2013 [134] and Huma K, 2014[135]]

Drug	Clinical use	Mechanism of Action
Amlodipine } Nifedipine } Verapamil } Gabapentin }	Antihypertensive and in the treatment of Angina pectoris Diverse Neuralgias	Voltage-gated Ca ²⁺ Channel (VGCC) blockers of L-type, N-type, TPC and alpha2/delta-1 subtype
Procyclidine } Dicyclomine } Pirenzepine } Atropine }	Parkinsonism Relaxation of GIT smooth muscle In eyes for Mydriasis	Muscarinic receptor (mAChR) antagonists, relaxation of smooth muscles in GIT and eyes by affecting Ca ²⁺ influx
Haloperidol } Prochlorperazine } Promethazine }	Schizophrenia and acute psychosis Anti-emetic, nausea-vertigo and allergic reactions	D-Receptor, muscarinic receptor (mAChR) and histamine receptor antagonist
Apomorphine	Parkinsonism, Erectile dysfunction and Alzheimer's disease	D2-agonist 5HT-antagonist
Amiodarone	Various types of atrial and ventricular dysrhythmias	VGCC, beta adrenoreceptors and nuclear T3 receptor blocker
Acetazolamide	Heart failure; epilepsies; glaucoma	Carbonic anhydrase inhibitor affecting cellular pH and therefore ionic state of Ca
Etoposide Doxorubicin	Apoptosis inducer, Anticancer drugs	Inhibits DNA synthesis DNA strand breakage and inhibition
Loperamide	Various types of diarrhea of non-infectious type	Opioid receptor agonist, Calmodulin inhibitor, P/Q type Voltage-gated Ca ²⁺ channel blockers
EDTA } Pirenoxine } KCL }	Heavy metal poisoning Glaucoma	Ca ²⁺ Ions – chelators Opens Voltage-gated Ca ²⁺ Channel

2.1.2 *A. castellanii* cultures, amoebistatic, amoebicidal, encystation, and cysticidal assays.

The drug listed above (Table-4) were tested in the published work for their amoebistatic, amoebicidal, encystation blocking, and cysticidal effects and are detailed in the individual papers (part-2) and are described below.

2.1.3 *A. castellanii* cultures

A keratitis isolates of *A. castellanii* trophozoites belonging to the T4 genotype *A. castellanii* (Douglas) Page (ATCC[®] 50492[™]) GenBank: Accession # U07401.1, obtained from my mentor. They were grown in a growth medium (0.75% [wt./vol] proteose peptone, 0.75% [wt./vol] yeast extract, and 1.5% [wt./vol] glucose) (PYG) in T-75 tissue culture flasks at 37°C without shaking. The media were refreshed at an average of ~18 h before all the experiments. The *A. castellanii* trophozoites found adhering to flasks represented the healthy trophozoites forms and were collected by placing the flasks on ice for 30 min with gentle agitation and used in all experiments. The cell cultures and *in vitro* experiments were performed according to the standards of Good Cell Culture Practice (GCCP) [136] to ensure reproducibility, reliability, credibility, acceptance, and proper application of any results produced.

2.1.4 Amoebistatic and amoebicidal assays

1. To determine the amoebistatic activities of drugs, *A. castellanii* trophozoites were incubated in the growth medium PYG with different concentrations of drugs in 24-well plates at 30°C for 48 h. After this incubation, the amoebae were counted using a hemocytometer.
2. To determine the amoebicidal effect of drugs on *A. castellanii*, amoebicidal assays were performed. Briefly, *A. castellanii* trophozoites were incubated with different concentrations of drugs in phosphate-buffered saline (PBS) in 24-well plates. The plates were incubated at 30°C for 24 h. Following this incubation, amoeba viability was determined by adding 0.1% Trypan blue and determining the number of live (non-stained) and dead (stained) *A. castellanii* organisms using a hemocytometer. The

count from *A. castellanii* incubated with PBS alone was used as controls. Data are represented as the means and standard errors of at least three independent experiments performed in duplicate.

2.1.5 Cysticidal assays.

For cysticidal assays, encystation was induced by inoculating amoeba trophozoites on non-nutrient agar plates, and the plates were incubated for up to 7 days to allow trophozoites transformation into the cyst stage. After this incubation, each plate was flooded with 10 ml of PBS, and the cysts were scraped off the agar surface using a rubber scraper, yielding more than 99% cysts as determined by microscopy. The mature cysts were incubated in PBS with various concentrations of drugs for up to 24 h. After this incubation, the cysts were centrifuged for 10 min at 1,000 g, and the supernatants were aspirated, followed by the addition of 0.5 ml of PBS. This process was repeated 3 times to remove the extracellular drug. Finally, the cysts were resuspended in PYG medium and inoculated in 24-well plates (0.5 ml PYG medium/well). The plates were incubated at 30°C for 48 h, and the emergence of trophozoites was considered to indicate viable amoebae while the absence of excystation was considered a cysticidal effect **[Baig AM, 2013 [134]]**. In some experiments, plates were incubated for up to 2 weeks to observe the emergence of viable trophozoites.

2.2 Drug combination assays in *A. castellanii* spp. and *Balamuthia mandrillaris*.

2.2.1 Materials and methods

All drugs tested in assays, and their mode of action are indicated in Table 4.

2.2.2 Human brain microvascular endothelial cell culture

Primary human brain microvascular endothelial cells were grown in RPMI-1640 containing 10% fetal bovine serum, 10% NuSerum, 2 mM glutamine, 1 mM pyruvate, penicillin (100 U/ml), streptomycin (100 U/ml), non-essential amino acids, and vitamins as previously described [Huma K and Baig AM 2014[135]]

2.2.3 Cultures of *B. mandrillaris*

B. mandrillaris, originally sourced from the brain of a mandrill baboon were obtained from American Type Culture Collection, ATCC 50209. For routine culturing, 1×10^6 amoebae (suspended in 10 mL of RPMI-1640) were inoculated on the HBMEC monolayer in T-75 tissue culture flasks. The flasks were incubated in a 5% CO₂ incubator at 37 °C. The amoebae consumed HBMEC within 48 h and produced approximately 5×10^6 amoebae (>95% trophozoites), which were subsequently used for experiments performed.

2.3 Amoebicidal assays

For amoebicidal effects, *A. castellanii* were incubated with a different combination of drugs (Table 4 and below in result section) at various concentrations (100 µM to 1 mM) in phosphate-buffered saline (PBS) in 24-well plates (5×10^5 amoebae/mL/well). Plates were incubated at 30°C for 24 h. To determine the amoebicidal activity of drugs against *B. mandrillaris* trophozoites, amoebae (10^5 amoebae/0.5 mL/well) were incubated with different combinations of drugs (Table 4) at various concentrations (100 µM to 1 mM) in RPMI-1640. Plates were incubated in a 5% CO₂ incubator at 37

30°C for 24 h. After this incubation, amoebae were centrifuged for 10 min at 1000 μ g, and the supernatant was aspirated, followed by the addition of 0.5 mL of PBS. This process was repeated 3x to remove any extracellular drug. Finally, *B. mandrillaris* were resuspended in RPMI-1640 and inoculated in 24-well plates containing HBMEC monolayer as a food source. Plates were incubated in a 5% CO₂ incubator at 37°C for up to 48 h and the emergence of trophozoites was considered as viable amoebae, and the absence of amoebae, as well as intact HBMEC monolayer, was considered as non-viable amoebae [Huma K and Baig AM 2014[135]] In some experiments, plates were incubated for up to 2 weeks to observe the emergence of viable trophozoites.

2.4 Determination of Intracellular Calcium.

2.4.1 Material:

Fura 2-AM (CAS # F1221 - Thermo Fisher Scientific) was used which is a cell-permeable fluorescent probe for Ca²⁺ used to determine cytosolic Ca²⁺ that is metabolized *in vivo* to the active ligand Fura 2. Application: Fura 2-AM was used for measuring intracellular Ca²⁺ concentration. The fluorescent excitation maximum of the Fura-2 AM undergoes a blue shift from 363 nm (Ca²⁺-free) to 335 nm (Ca²⁺-saturated), while the fluorescence emission maximum is relatively unchanged at ~510 nm.

2.4.2 Fura 2-AM staining Method:

The *Acanthamoeba* trophozoites and cysts were seeded in six-well plates in a growth medium. Ringer lactate (2 mL) was added additionally to provide free Ca²⁺ in the media. Cells and cysts were then exposed to the drug (s) and were incubated for an hour at room temperature. After an hour, the cells and the cysts were collected, the supernatant was discarded, and cells were washed twice with phosphate buffer saline (PBS). In the case of the cysts staining with Fura 2 AM, the cysts were detached from the well plates and moved to the Eppendorf and centrifuged for 5 min at 2500 rpm. For both, trophozoites and cysts, a working solution of 5 μ M Fura-2 AM was prepared, and cells and cysts were suspended in it. Incubated cells and cysts were exposed to

Fura-2/AM for an hour at room temperature. The cells and the cysts were centrifuged and washed with PBS (x2) and resuspended in a fluorescent mounting medium. The cysts and the cells were then transferred to a glass slide, and coverslips were placed on it. In the case of KCL and Ca²⁺channel blocker coincubation assays, 20mM KCL was added 45 mins after the drug exposure and the trophozoites were centrifuged and washed 3x with PBS to remove excess KCL and drugs before resuspending them in the fluorescent mounting medium. Slides were left for an hour and observed under an Olympus fluorescent microscope at excitation spectra of 363 nm (calcium-free) and 340 nm (calcium complex) with fixed emission at 510 nm.

2.5 Immunostaining for Muscarinic Cholinergic Receptor in *A. castellanii*

2.5.1 Materials and Methods

An anti-human mAChR1 receptor antibody directed against the mAChR1 receptor was obtained from Millipore-Merck.

2.5.2 Immunostaining

Trophozoites forms of the *A. castellanii* were grown on coverslips in PYG overnight at 30°C. The cells were fixed with paraformaldehyde (4%) in 0.1M phosphate buffer saline (PBS) for 30 min. Endogenous peroxidase activity was quenched by incubation with 0.2% hydrogen peroxide in 0.1M phosphate buffer saline (PBS) pH 7.3 containing 0.2% Triton X-100 for 25 minutes at room temperature. After three washes with a blocking solution (50 mL of phosphate-buffered saline 0.02M PBS, pH 7.4/casein 2%), the cells were immersed with primary mAChR1 antibody (Merck-Millipore) directed against rat and human mAChR1 were incubated for 1 h 30°C at and then refrigerated overnight. Washing was then done thrice with 0.02M of phosphate-buffer saline. The reactivity of immune complexes was identified after co-incubation with horseradish peroxidase tagged conjugated goat anti-rabbit antibody (Chemicon Catalog # AP132P) for 1 h at room temperature and then refrigerating overnight. The trophozoites were then incubated with a solution of diaminobenzidine (DAB) at the concentration of 0.0125%, containing 0.05% nickel ammonium sulfate for 10 min at room temperature. Cells were then washed with 0.02M PBS, 4x for 10 min, and

mounted on coated glass slides, and dehydrated in an ascending series of ethanol concentrations as per manufacturer's instructions. An inverted microscope (Olympus) was used to obtain images. The slides were observed at 10x, 20x, and 40x magnifications. For positive controls, neurons and smooth muscle cells were stained and fat cells we used as negative controls.

2.6 ACh Detection in *A. castellanii* trophozoites

2.6.1 Materials and Methods

Dicyclomine and pirenzepine were from Sigma-Aldrich and were used to target mAChR subtypes. The drug pirenzepine is known to specifically target the human mAChR1 receptor subtype. The AChE inhibitor physostigmine was also purchased from Sigma-Aldrich, and Acetylcholine Assay Kit (colorimetric; catalog # STA-603 Cell Biolabs, Inc.) was obtained from Cell Biolabs.

2.6.2 Colorimetric Acetylcholine Assay for ACh Detection in *Acanthamoeba*

To assess the presence of ACh in *A. castellanii*, an ACh assay was run as per the manufacturer's protocol (Cell Biolabs). At 24 h before conducting the assay, the media were refreshed within a confluent culture flask harboring the cell lines. After the *Acanthamoeba* cells of a single flask were detached by ice shock treatment, they were centrifuged at a speed of 3500 rpm for 10 min. The pellet obtained was dissolved in chloroform/methanol (2:1, v/v) and centrifuged, followed by incubation for 1 h on an orbital shaker, with the addition of 1.25 mL of distilled water; centrifugation was done at 1000g for 10 min. The lower (chloroform) organic phase was collected, and the upper phase was re-extracted with chloroform/methanol/water (86:14:1, v/v/v).

Subsequently, the organic phases were combined, lyophilized in a vacuum centrifuge, and dissolved in chloroform/methanol/water (60:30:4.5, v/v/v). Another set of samples was produced by adding Physostigmine to the chloroform/ methanol before being used to suspend the cell pellet. Samples without Physostigmine were diluted to concentrations of 1:10, 1:50, 1:100, 1:500, and 1:1000. Samples with Physostigmine were diluted to concentrations of 1:50 and 1:400. These samples were mixed with

reagents using Acetylcholine Assay Kit (colorimetric; catalog # STA-603 Cell Biolabs, Inc.) to which superoxide dismutase was added as per manufacturer's protocol. The plate was read at an absorbance of 550 nm. The concentration of ACh standard curve was used to determine the particular concentrations in the samples through a regression line. The kit detection limit is 0.75 μ M. Androgen independent prostate cancer cell lines (PC3) were grown in flasks, and the growth media were refreshed 24 h before the experiment. The cells that were confluent on the floor of one flask were used. To detach the healthy PC3 cells from the floor of the flasks, trypsin was used. Samples were prepared and analyzed as described above for *Acanthamoeba* assays.

2.7 Apoptosis in *A. castellanii* belonging to the T4 Genotype

2.7.1 Material and Methods:

Digoxin [Lanoxin] was obtained by Glaxo-SmithKline. Acridine orange, Etoposide, and Loperamide were purchased from Sigma Aldrich and Merck-Millipore. ApopNexin V FITC Apoptosis kit (Cat# APT750) was purchased from Chemicon International and 7AAD (a fluorescent intercalator that undergoes a spectral shift upon association with DNA) was purchased from Invitrogen.

2.7.2 Immunofluorescence: Imaging Apoptosis at different intervals

Acridine orange (Sigma Aldrich) and Merck-Millipore (Annexin-V FITC) apoptosis kits were used to determine patterns of apoptosis and necrosis that occurred in the experiments that were carried out on healthy *A. castellanii* trophozoites at doses of 100-150 μ g/ml of loperamide. Acridine orange stains fragmented DNA in the cell undergoing apoptosis. The Acridine orange staining was done and visualized for early apoptotic changes at the 6th, 18th, and 24th hours. The trophozoites showing both, Annexin V and AO stains were considered to be exhibiting an apoptotic type of cell death at the time of staining. The manufacturer's kit contains Annexin-V in conjugation with FITC. The cells undergoing apoptosis uptake Annexin-V which stains the externalized phosphatidylserine, on the cell membrane, that occurs during apoptosis. Olympus IX71 inverted microscope was used and the images were compared by first observing them under normal light and then FITC. The Propidium iodide [PI], included

with the kit, was used to differentiate cells undergoing apoptosis with intact membranes from necrotic cells with damaged cell membranes. Necrotic cells that uptake the Propidium iodide [PI] was detected using a green/red filter with an excitation wavelength of 540/25 nm and an emission filter of 605/55 nm.

2.7.3 FACS Analysis

A. castellanii (1×10^6 cells/100 μ L) were loaded into FACS tubes. The amoebae were washed twice with 2 mL PBS and centrifuged at 1500 x g for 5min, and then poured out of the buffer from pellets containing trophozoites. *A. castellanii* trophozoites were then added to 100 μ L of flow cytometry staining buffer. Following this, 10 μ L of 7AAD was added to the staining solution to a control tube of trophozoites (2.0×10^6 trophozoites) to adjust flow cytometer settings for 7AAD. 7-AAD is known to enter late apoptotic or necrotic cells to stain DNA. After mixing for 30 minutes at 4°C in the dark, 7AAD fluorescence was determined using the FL-2, as staining alone with 7AAD was intended for the determination of the type of cell death. 10 μ L of the 7AAD staining solution was added to the cell samples treated with 40 μ g/ml of digoxin and incubated for 30 minutes at 4°C in the dark before the analysis. The trophozoite counting was optimized from a dot-plot of forward scatter versus 7AAD to measure cell death patterns induced by digoxin.

2.8 Detection of phosphatidylserine (PS) externalization in *Acanthamoeba*

PS exposure at the outer plasma membrane of apoptosis cells was detected by using ApopNexin V FITC. Briefly, HBMEC and/or *A. castellanii* trophozoites (5×10^5 amoebae/0.5 ml) were incubated with various concentrations of doxorubicin, melphalan, ethidium bromide, loperamide, dicyclomine, hydrogen peroxide (H₂O₂) for 16, 18, and 24 h in 24-well plates at 37°C (in a CO₂ incubator in the case of HBMEC). For HBMEC, cells were washed twice with 0.5 ml RPMI to remove excess drug and incubated with washed with PBS (thrice), and re-suspended in ApopNexin V FITC and propidium iodide in 1x binding buffer (10x binding buffer contains 0.1M HEPES, pH 7.4; 1.4M NaCl; 25 mM CaCl₂). HBMEC were incubated in cold for 1 h in dark. Finally, cells were washed thrice with PBS to remove the excess of the antibody and

visualized under a fluorescent microscope (Olympus BX43 microscope) using Infinity-1 camera and Lumenera software. For *A. castellanii*, amoebae were harvested at 16, 18, and 24 h by centrifugation as described above. Next, cells were washed with PBS (thrice), and re-suspended in ApopNexin V FITC and propidium iodide in 1x binding buffer and incubated in cold for 1 h in dark. Next, amoebae were washed thrice with PBS to remove excess antibody. The final cell pellet was re-suspended in PBS and visualized under an Olympus BX43 fluorescent microscope.

2.8.1 Cytotoxicity Assay - LDH release experiments

To determine the ability of the diverse drugs (Table-4) used in differential doses to induce cell death by cytotoxicity, LDH release assays were performed. Healthy trophozoite forms (1×10^6 /well) of *A. castellanii* were grown in PYG medium and exposed to different concentrations of drugs in 96-well plates at 30°C for 24 h. Following this incubation, the supernatants were collected and examined for cell cytotoxicity by measuring lactate dehydrogenase (LDH) release (cytotoxicity detection kit, Promega, Madison, Wisconsin, USA). Briefly, the supernatants were assessed for the presence of LDH, the release of which is considered as an estimate of cell death. The percentage of the release of LDH was calculated as: $(\text{LDH activity in the experimental sample [measured by optical density at 492 nm]} - \text{LDH activity in control samples}) / \text{total LDH activity release} \times 100 = \% \text{ cytotoxicity}$. Control samples were obtained from well plates in which *Acanthamoeba* trophozoites were incubated alone without any drug. Total LDH activity release was determined by total *A. castellanii* trophozoite lysis with 1% Triton X-100 for 30 min at 37°C.

Section 2.

2.9 Genome databases and bioinformatic computational tools in the identification of drug targets in *A. castellanii*.

2.9.1 Transcriptomics of *A. castellanii*.

Recently, the analysis of the RNASeq data for *A. castellanii* has been reported [137]. This study has presented the orthology association analysis and gene ontology (GO) description in conjunction with the gene expression estimation of different gene groups for *A. castellanii*. The expression of mRNA encoding proteins that were presumed as a drug target in *A. castellanii* was retrieved from the AmoebaDB database [137]. Once the expected molecular targets of the drugs were drawn (details below in the result section), the mRNA encoding the relevant proteins were retrieved and analyzed for their gene expression as compared to other protein encoded by *A. castellanii*.

2.10 Reverse transcription-polymerase chain reaction (RT-PCR) with Real-time polymerase chain reaction (qPCR)

2.10.1 Processing of *Acanthamoeba* trophozoites:

Acanthamoeba trophozoites were harvested from the T75 flask and shifted to 15ml falcon tubes. Cells were centrifuged at 2500rpm for 10 minutes. The supernatant was discarded, and the cells were re-suspended and washed with PBS thrice. After washing, cells were counted and 0.5×10^6 *Acanthamoeba* trophozoites were collected in a separate tube. These cells were then re-suspended in 40 μ L PBS and processed for mRNA extraction.

2.10.2 Processing and Treatment of PC3/DU145 with trifluoperazine:

0.5x 10⁶ prostate cancer cells, PC3, and DU145 cells were grown in 6 well plates for 24 hours in RPMI and DMEM respectively. The cells were then exposed to trifluoperazine 10, 20, 30, and 40 µg/mL and incubated at 37°C for 24 hours. After completion of the incubation period, cells were collected in Eppendorf tubes and centrifuged at 2500rpm for 10 minutes. The supernatant was then discarded and re-suspended in PBS. The cell pellet was washed with PBS three times and the supernatant was discarded. The PC3/DU145 cells were re-suspended in 40µL of PBS and used for mRNA extraction.

2.10.3 Extraction of WBCs:

The whole blood specimen in a heparin tube was obtained and an aliquot of 1ml blood into a 15ml conical centrifuge tube was prepared for lysis of the RBCs. The tube was filled with a fresh cold RBC lysis buffer. The tube was mixed gently by inverting the tube for ~10 minutes at room temperature until the liquid became clear red. The tubes were centrifuged at 4°C for 10 minutes at 300 x g. WBCs were washed with PBS and 10ml cold PBS was added as per manufacturer protocol. WBCs were counted and cells were adjusted to ~0.5x 10⁶/mL.

2.10.4 mRNA Extraction from *Acanthamoeba* trophozoites, PC3, and DU145 cells: Preparation of lysis buffer:

The mRNA catcher plus plate was used to extract mRNA from each sample. The PC3/DU145 cells, suspended in 40µL PBS, were loaded in mRNA catcher plus plate. An equal volume of lysis buffer was added to each well. The solution was mixed by pipetting in and out. After mixing the solution, the plate was incubated at room temperature for 45-60min. After incubation, the whole solution was dispensed out of wells. Wells were washed by dispensing 100µL of wash buffer for 1minute (x3). 80µL of elution buffer was added and the plate was incubated at 68°C for 5minutes and kept on ice immediately to cool down.

2.10.5 Detection of RNA concentration:

Nanodrop was used to analyze RNA concentration in the sample

2.10.6 cDNA synthesis:

15ng of RNA was used to form cDNA. The reaction mixture was prepared by adding dNTP and RT enzyme as per the manufacturer's protocol. The tubes were labeled for each sample. Following this, 15ng of RNA samples were added into their respective tube and 6.4 μ L from the reaction mixture was added to each tube. After adding all the reagents and samples, the total volume was brought up to 20 μ l with nuclease-free water, mixed gently, and centrifuged. The plate was incubated in a thermocycler and the temperature was set at 25°C for 10min, followed by 50°C for 30minutes. The reaction was terminated by heating at 85°C for 5 minutes and holding it at 4°C.

2.10.7 Real-Time PCR:

All the reagents were gently vortexed and centrifuged and tubes were labeled for each sample. 2 μ L of cDNA was added to the samples in the respective tube. Beta-actin was used as standard and it was run along with test samples. 13.24 μ L of regent was added from the reaction mixture in each tube. A volume up to 25 μ L was made with nuclease-free water, mixed gently, and centrifuged briefly as per the manufacturer's instructions. The thermal cycler was programmed according to the recommendations, samples were placed and the process was initiated.

2.10.8 qPCR Analysis:

The data were analyzed by using the Cq values obtained by qPCR. Results obtained from beta-actin was used to compare and analyze the results.

2.11 Methodology: Genomic, Transcriptomic, and Bioinformatics Computational Tools used in drug target discovery.

2.11.1 General sequence identification and similarity searches

Sequence identification and similarity search for *A. castellanii* proteins were done by using the Basic Local Alignment Search Tool for proteins (BLASTp). BLASTp was used to conclude the functional and evolutionary relationships between sequences as well as to help identify members of gene families [138-140]. The BLAST program uses a set of algorithms that attempts to find a fragment of a query sequence that aligns with that of the subject sequence and uses a heuristic algorithm [138, 140] which is designed to solve a problem in a faster and more efficient fashion than methods like FASTA. The EMBL-EBI automated server has a powerful cross-referencing and functional data retrieval capability and was used to generate the BLASTp results mainly, as resolving the functions of the query *Acanthamoeba* protein was important to relate it to the observed drug effects seen in the in vitro assays done in *A. castellanii*. Running a BLASTp in EMBL-EBI automated server is a multiple steps process and was used to generate results with function annotations (detailed below in results). BLASTp searches were done by submitting FASTA sequences of amino acids of a particular protein encoded in *Acanthamoeba* spp. The sequences of *Acanthamoeba* proteins encoded and expressed are designated as ACA1_ followed by unique ID (6-digit numbers) in the AmoebaDB.org database. In our study, these proteins are either identified as ACA1_xxxxxx or by name as annotated in the databases.

2.11.2 BLASTp: Scores and E-values

In BLASTp results, the scores describe the overall quality of the alignment between the query and the hit. Higher scores correspond to a higher-quality alignment and can be used to deduce similarity. To determine whether a score is good or just may be caused by chance, a statistical procedure is needed to assess its reliability. The e-value threshold is a statistical measure of the number of expected matches in a

random database. The e-value estimates how many times one expects to see such an alignment occur by chance and thus e-value along with scores on BLASTp searches for *Acanthamoeba* proteins allowed us to quantitatively assess the significance of the alignment that we have reported in many of our studies including **[Baig AM, 2017d [141]]**, **[Baig AM, 2017e [142]]**. The lower the e-value, the more likely the match is to be significant [138, 139, 143]. The e-values between 0.1 and 10 are generally dubious, and over 10 are unlikely to have biological significance [143]. In our studies, the *Acanthamoeba* proteins that had the highest scores and lowest e-values in BLASTp searches were selected for homology modeling and drug/ligand docking (detailed in result section).

2.11.3 PSI-BLAST

The PSI-BLAST algorithm is based on the standard BLAST algorithm. A query sequence is scanned against a database of sequences and high-scoring alignments are detected [138]. Multiple alignments of detected sequences are then used to construct a profile [140]. The PSI-BLAST algorithm is iterative which means that subsequent searches that detect related homologs are used to further refine the profile [138, 139]. In our studies, we used PSI-BLAST for *Acanthamoeba* protein (detailed in the result section) that had low sequence similarities but shared functional attributes with the human proteins that are known drug targets.

2.11.4 Multiple Sequence analysis (MSA) and alignment with functional annotations

While the pairwise analysis can be applied to the problem of finding homologs, it cannot (by itself) be used to conclude a family of sequences. MSA can reveal levels of similarity between sequences. Conserved regions might represent motifs that are essential for function [138, 144]. MSA is the foundation for the identification of functionally important regions, building a sequence profile for further sequence search, protein family classification, phylogenetic reconstruction, etc. [139, 145].

To this end, we needed to take all the members of a family into account to characterize sequence signatures caused by similarity in the fold, membrane topology, residues participating in the active site, or ligand binding by aligning the member sequences in one big alignment like in the case of VGCCs [Baig AM, 2019d [146]] and Aquaporin protein [Baig AM, 2018d [147]]. The automated servers in NCBI [138], Uniprot [143], EMBL-EBI, and NCBI that is hosted by the European Bioinformatics Institute (EBI) were used for MSA that are reported in my studies [Baig AM, 2018d [147]].

2.11.5 Evolutionary analysis of *A. castellanii* protein.

Our study attempted to not only provide evidence of finding a homolog of human protein in *A. castellanii* but also endeavored to trace the reported proteins on an evolutionary timeline. We used NCBI and Pfam automated servers, with the neighbor-joining (NJ) algorithm, for assessment of protein distance measures by the construction of rooted tree (rectangle cladograms) and sunbursts (circular tree). For example, a distance matrix calculation employed in the automated MSA tool in NCBI and Pfam webserver was used to generate an evolutionary analysis of the sequences of protein family AQP and superfamily MIP protein family. [Baig AM, 2018d [147]].

As the presentation of the complex proteomic data arising in evolutionary algorithms remains a challenge, treemaps (cladograms/dendrogram) and sunbursts forms (circular trees) shown in our studies helped us in visualizing such complex data. In our result sections, shown are treemaps and sunbursts (circular treemaps) developed in NCBI and Pfam servers (using neighbor-joining, NJ-method), that display important aspects of the evolutionary distribution of protein family and superfamily in between species.

2.11.6 Homology Modeling: Automated Protein Homology Modeling Servers

Homology modeling (or comparative modeling) depends on evolutionarily linked structures (templates) to create a structural model of a protein of interest (target). In automated web resources for homology modeling like Phyre² and SWISS-

MODEL[195], the process typically comprises the following steps: (i) template identification, (ii) template selection, (iii) model building, and (iv) model quality estimation. In summary, a library of experimentally determined protein structures is searched with sensitive sequence search tools to identify proteins that are evolutionarily related to the target protein [148]. The SWISS-MODEL server was used for the homology modeling of *A. castellanii* proteins, which interactively searched for templates, clustered them by sequence similarity, structurally compared alternative templates, and selected the ones to be used for model building. For some well-studied protein families, (like in our studies with VGCCs and mAChR) finding diverse numbers of templates for a target protein is not unusual [148]. Often, these represent different functional states or structures in complex with different ligands, the latter was more important to us (as mentioned above). In cases where evolutionarily conserved proteins like CaM, cytochrome-c, and adapter protein involved in the execution of intrinsic apoptotic pathway, homology modeling parameters like Qualitative Model Energy ANalysis (QMEAN) and Global Model Quality Estimation (GMQE) that access the model quality estimation [148] were considered as important parameters.

2.11.7 Annotation of ligands in SWISS-MODEL template library (SMTL)

In most crystal structures low molecular weight ligands are observed, but only some of those are functionally or structurally relevant for the protein [148]. Instead of their natural ligands, some structures contain synthetic analogs or inhibitors which occupy competitively the same binding site [148] as in the case of Tiotropium bound to human mAChR1 [Baig AM, 2017a, [149]]. SMTL implements a two-stage process to annotate biologically relevant ligands and synthetic analogs. The first stage uses a list of rules to automatically categorize the ligands based on their chemical identity.

2.11.8 Template search and selection

The STML was searched in parallel both with BLAST and Hhblits (online server for protein structure prediction that uses homology information) to identify templates and to obtain target-template alignments [148]. This feature in homology modeling in

SWISS-MODEL helped us to study the target-template alignments and use the templates for prediction of docking drugs (detailed in the result section)

2.11.9 Modeling of the Ligands:

Depending on the intended application of a model, selecting a different template than the top-ranked one might be necessary, e.g. to build a model of a protein in complex with a ligand rather than its apo form [148]. This template selection method was done in our study for example in the case of homology modeling of *A. castellanii* GPCRs that we postulated to have conserved ACh (agonist) and tiotropium (orthosteric antagonist) binding amino acid residues. Recently, the functionality of SWISS-MODEL homology modeling has improved with models of generation of oligomeric structures of target proteins that include evolutionarily conserved ligands such as essential cofactors or metal ions in the template-based models [148]. The implementation of the new web interface of SWISS-MODEL allowed an interactive comparison of alternative templates (as in the case of VGCC) and selection of those which are more suitable for the intended application of the model (e.g. based on the presence/absence of specific ligands).

2.12 Drug and Ligand docking predictions:

The task of calculating the interactions between a pair of molecules, usually a ligand /drug and a receptor, is usually referred to as docking (detailed in chapter-1). Molecular Docking is the method of molecular modeling that assesses the atomic-level interactions between a small molecule and a receptor-like enzyme or any other protein. [150]. Molecular Docking is a cost-effective, fast technique that has been an essential tool in the process of drug discovery as well as a complementary tool to many experimental biophysical techniques [151]. In the published papers, molecular dockings of ligands and drugs were carried out on the web-based PatchDock server [152]. PatchDock is based on object recognition and image segmentation techniques usually used in computer vision, as docking can be compared to the assembly of a jigsaw puzzle [153].

2.12.1 PatchDock: Molecular Docking Algorithms:

PatchDock [152] is a geometry-based molecular docking algorithm that is aimed to find docking transformations that yield good molecular shape complementarity. Docking transformations, when implemented, induce both wide-interface areas and small amounts of steric clashes. A wide-interface is ensured to include several matched local features of the docked molecules that have complementary characteristics to determine the contact area. The PatchDock algorithm divides the dot surface representation of the molecules into concave, convex, and flat patches. Then, complementary patches are matched to generate candidate transformations. Each candidate transformation is further evaluated by a scoring function that considers both geometric fit (contact area) and atomic contact energy (ACE) (an electrostatic and/or van der Waals energy loss due to the interaction between ligand or protein and solvent upon binding). Generally, ACE is the energy of replacing a protein-atom/water contact, with a protein-atom/protein-atom contact, and the more negative it is the more it is considered to favor a binding in an induced-fit configuration.

2.12.2 The PatchDock web server: Input, Output, and results

As the crystal structures of the ACA1_ proteins reported in our studies have not been resolved yet, therefore for the docking calculations we used the PDB ID of templates that were generated for *Acanthamoeba* proteins during homology modeling in the SWISS-MODEL server and were used for input in the PatchDock Server. Similarly, for the drug a PDB-ID (or PubChem ID) of the chemical compound was submitted to the automated PatchDock server. The run time of PatchDock for two input proteins of average size (about 300 amino acids) is <10 min on a single 1.0 GHz PC processor under the Linux operating system. In the results, the geometric score, ACE, the interface area size, and the actual rigid transformation of the solution are shown [152-154]. The results of the ligand docking that turns up with a higher docking score and minimum ACE values were considered optimal for interacting residues that are predicted for ligand-protein binding [154]

3 Experimental Assays, immunostaining, ELISA, colorimetric analysis, FACS analysis and DNA staining.

3.1 Introduction:

As detailed above in chapter-1, the rationale behind targeting *Acanthamoeba* trophozoites and cysts were to exploit the Ca^{+2} ion dependency of this parasite. Our approach was to first identify selective drugs (Table-4) that are known to, directly and indirectly, affect the Ca^{+2} ion concentration or Ca^{+2} homeostasis in human cells (Figure-9) and to test them in assays performed *in vitro*. Though the biology of *Acanthamoeba* and related free-living amoeba (FLA) has been studied in detail in the past, the role of Ca^{+2} and regulatory mechanisms that maintain a physiological level of this vital ion in the intracellular space in *A. castellanii* has not been studied in depth. Also, though the basic physiological functions like motility, phagocytosis, the formation of phagolysosome, role of Ca^{+2} ion -bound CaM regulating metabolic processes all are presumed to be related to Ca^{+2} ion in *A. castellanii*, but the effector adaptor proteins were not been reported or studied with the intention of druggable targets in the past. Molecular targets that are shared between humans and *Acanthamoeba* spp. have been reported in the past [17, 79, 102], but have not been elucidated yet, also targeting L-type VGCC like proteins as has been reported for parasites like *Leishmania donovani* [155], but not in *A. castellanii*. Based on the rationale that human-like Ca^{+2} regulatory mechanisms exist in *A. castellanii* (Figure 9), there was a need to experimentally validate the presence of the Ca^{+2} ion related proteins like VGCCs, CaM, and GPCRs that are coupled with Ca^{+2} ion in *A. castellanii*. For example, it was aimed to test VGCC blocking drugs (Table-4) on the growth and viability of *A. castellanii* to provide evidence of the possible presence of human-like VGCCs in *A. castellanii* (Figure 10 black parallel bars). Additionally, intracellular imaging for Ca^{+2} by the use of Fura 2 AM staining was aimed to provide evidence for the disturbances in Ca^{+2} regulatory mechanisms exerted by the drugs tested in our studies. Likewise, the chelation of

Experimental Assays, immunostaining, ELISA, colorimetric analysis, FACS analysis and DNA staining.

extracellular Ca^{2+} by EDTA and Pirenoxine was hypothesized to clarify the dependency of *A. castellanii* on extracellular Ca^{2+} . It is known that human mAChR1 and mAChR3 muscarinic receptors are coupled with channels that mediate Ca^{2+} -influx [143], but these muscarinic GPCRs have not been reported in *A. castellanii*. Immunostaining for human-like mAChR (Figure 10, green ribbons) and the testing of known mAChR1 and mAChR3 receptors blockers, by the use of antagonists like procyclidine/prochlorperazine, was hypothesized to reflect the role of Ca^{2+} ion-regulating proteins coupled to G-proteins in *A. castellanii*.

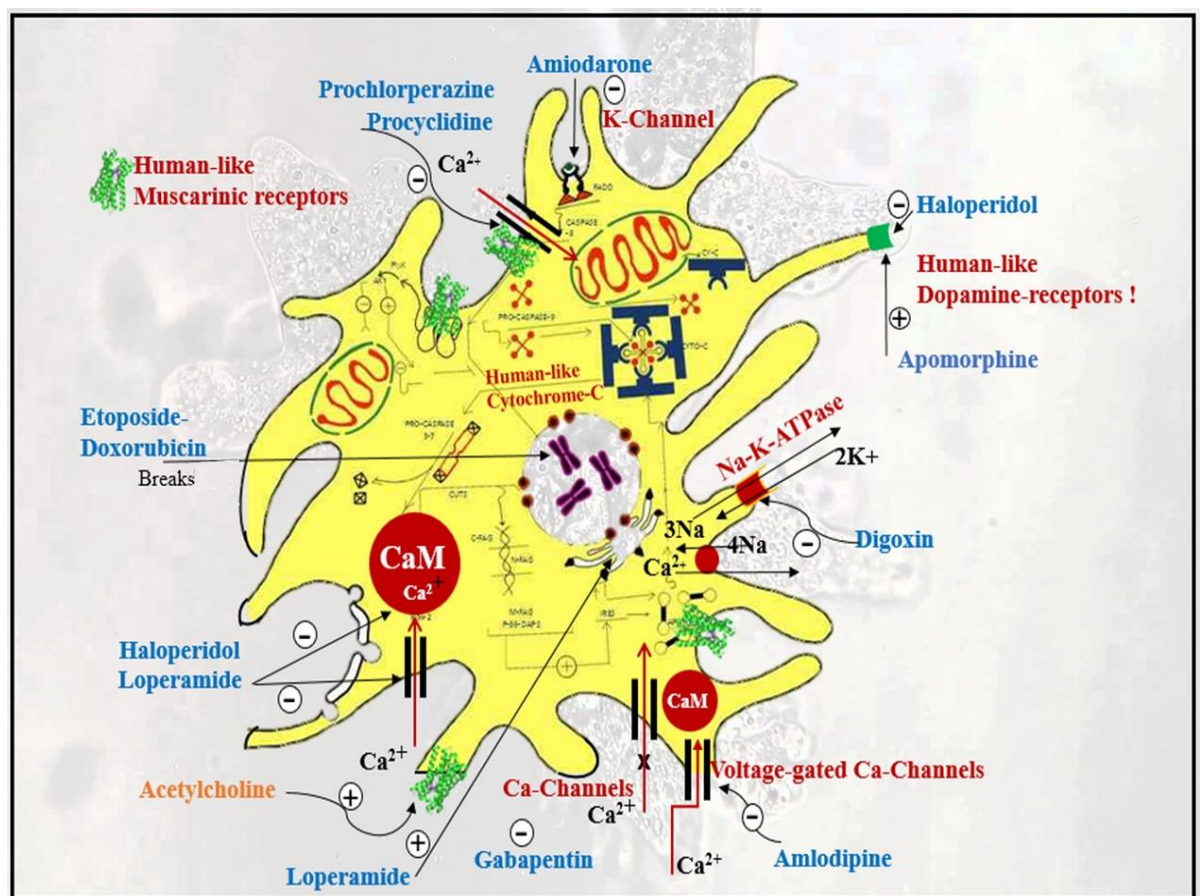


Figure 10. Molecular targets that were hypothesized in *A. castellanii*.

Drugs used in humans in (blue text) [■] non-infectious diseases that target Ca^{2+} channels and intracellular Ca^{2+} homeostasis regulating proteins were tested in trophozoite and cystic forms of *Acanthamoeba* spp. Human-like drug targets (red-text) [■] were hypothesized to be expressed and perform vital roles in *Acanthamoeba* spp. and related FLA. Stimulation or induction is shown with (+) and inhibition/antagonism is represented by (-) signs. Where a drug target in *Acanthamoeba* trophozoite was in doubt a (!) sign is used.

As an ionic form of Ca^{2+} is needed for vital functions of this cation in cell biology, drugs like acetazolamide that inhibit carbonic anhydrase and therefore the above-mentioned state of calcium, were expected to clue towards the cardinal role of Ca^{2+} in the growth and viability of *A. castellanii*. The effects of loperamide were compared with doxorubicin and etoposide in inducing apoptosis by causing dysregulation of Ca^{2+} homeostasis. Cytosolic proteins like calmodulin (CaM) which is cardinal Ca^{2+} homeostasis affecting protein (Figure 10, red circle) was considered as drug targets of the drugs loperamide, haloperidol, and prochlorperazine. Targets of the drugs that affect the Ca^{2+} homeostasis indirectly like digoxin and amiodarone (Figure 10) were hypothesized to affect the viability and growth of *A. castellanii*.

Results (below) of methods like testing the effects of VGCC agonist-antagonist on the growth and viability *A. castellanii*, Fura 2 AM staining intracellular calcium, immunostainings of mAChR1, ligand identification, LDH release, and establishing an apoptotic cell death were performed to explain the reasoning behind the selection of drugs (affecting Ca^{2+} homeostasis) (Table-4) and attaining the aim of the study (mentioned in chapter-1).

3.1.1 Materials and Methods overview

The source of the drugs, chemicals, dyes, antibodies, and calcium staining probe Fura 2 AM that were used in the experimental assays are detailed in chapter-2. Mostly, three independent experiments were performed in duplicates. For statistical analysis of the results, mostly, paired *t*-test, with one-tail distribution were done and at times when needed, one-way ANOVA with Dunnet's post-hoc was done and indicated in the legend. In all of the experiments that involved antibodies and fluorescent dyes, the manufacturer's instructions were followed.

3.2 Amoebistatic, Amoebicidal, and cysticidal drug assays

In assays, prochlorperazine, haloperidol, and digoxin showed inhibition of the proliferation and growth of *A. castellanii* trophozoites (Figure 11), at a dose of 25 µg per ml (Figure 12 A and [Baig AM, 2013, [[134]]]. Of the drugs tested in higher doses of 500 µg per ml amlodipine, loperamide, digoxin, and prochlorperazine showed amoebicidal effects in trophozoites of *Acanthamoeba castellanii* that were about 99% (Figure12-B) [Baig AM, 2013, [134]]. In later studies (cytotoxicity assays detailed below-Figure 27), we curtailed the doses to determine the minimal doses at which the drugs tested (Table-4) were capable of inducing amoebicidal effects in trophozoites of *A. castellanii*.

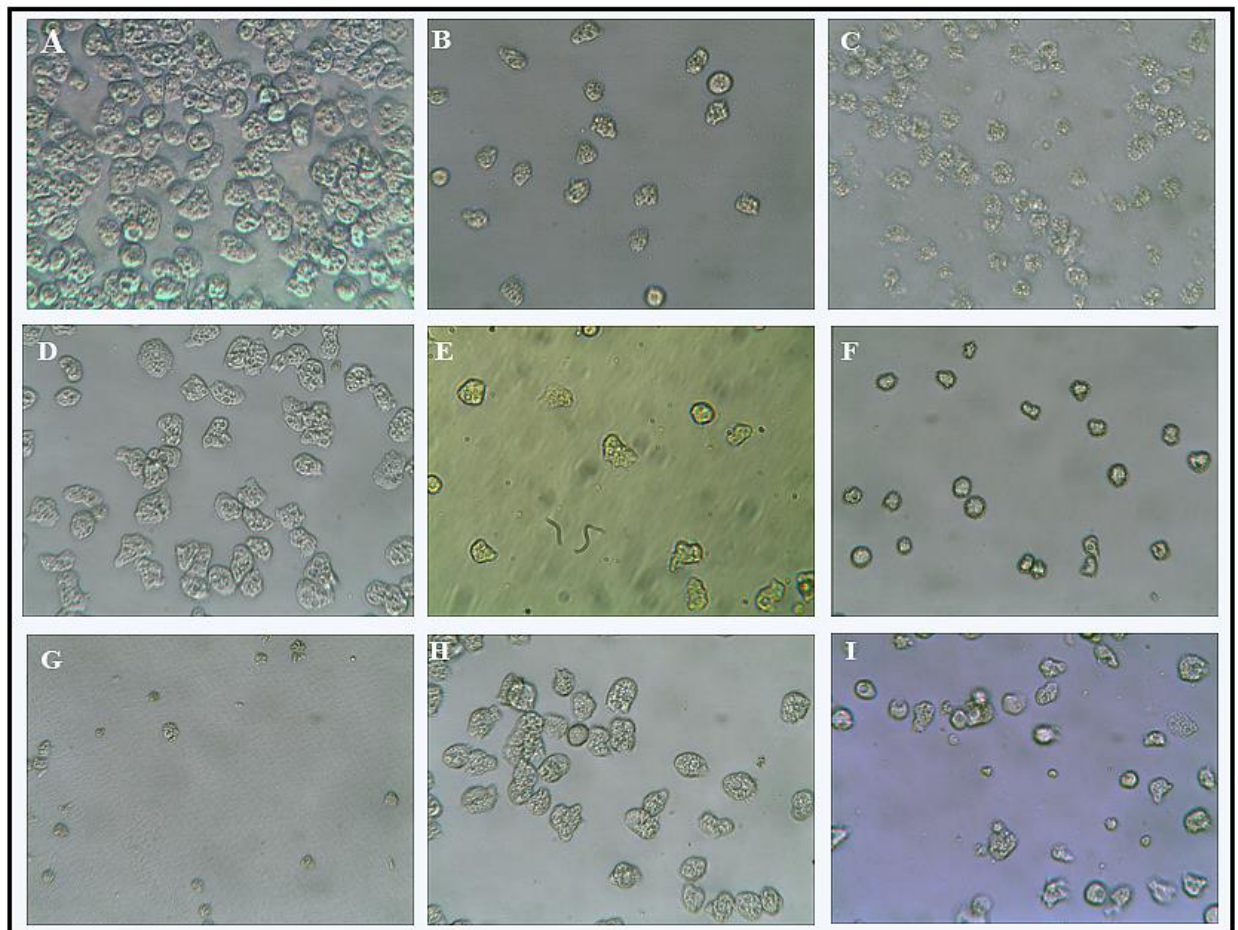


Figure 11. Effects of drugs tested in *Acanthamoeba* trophozoites.

FACS analysis and DNA staining.

Images (40x) of *Acanthamoeba* trophozoites (1×10^5) after 24h of exposure to different drugs. (A) *A. castellanii* trophozoites grown in growth medium PYG. Anti-muscarinic agents dicyclomine, procyclidine, and atropine (B, C, and D) showed anti-proliferative effects at doses of 90, 250, and 300 μ g per ml respectively. Amlodipine at 25 μ g per ml (E) and Loperamide at doses of 250 μ g per ml (F) exhibited amoebicidal effects. Digoxin (G) Haloperidol (H) and Prochlorperazine (I) in doses of 25 μ g per ml each showed amoebicidal effects. The results are representative of at least three independent experiments performed in duplicate. [Adapted from Baig AM 2013, [134]]

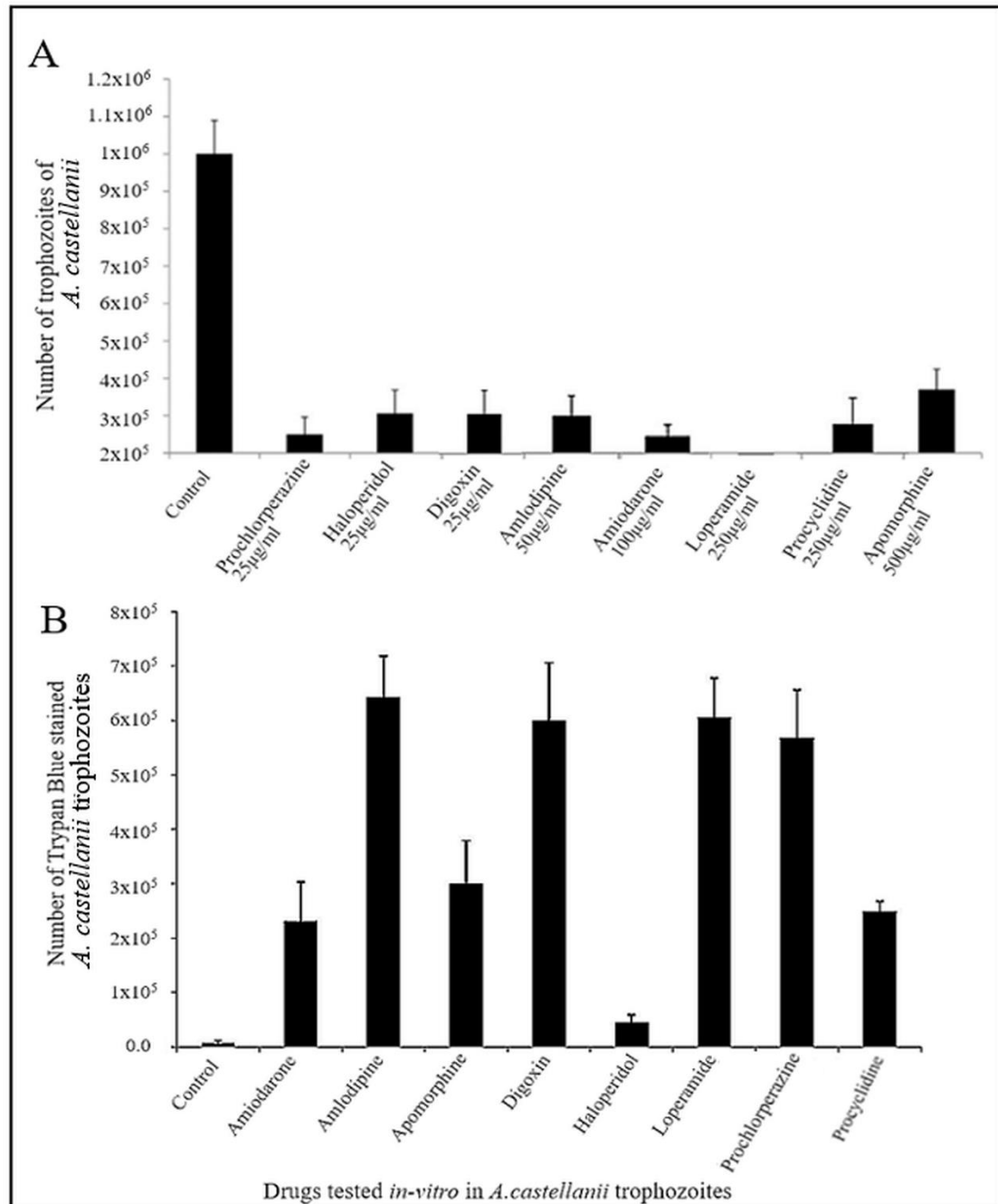


Figure 12. Results of drugs tested in vitro in trophozoites of *A. castellanii*

(A) *A. castellanii* (2×10^5 trophozoites) incubated with various concentrations of drugs in PYG medium at 30°C for 48 h. All drugs tested showed significant inhibition of *A. castellanii* growth at the indicated concentrations ($P < 0.01$; paired *t*-test; one-tail distribution). (B) Effects of tested drugs in *A. castellanii* trophozoites, the bars represent Trypan blue stained (dead) trophozoites. The results are representative of at least three independent experiments performed in duplicate. The data are presented as means and standard errors. [Adapted from Baig AM, 2013, [134]].

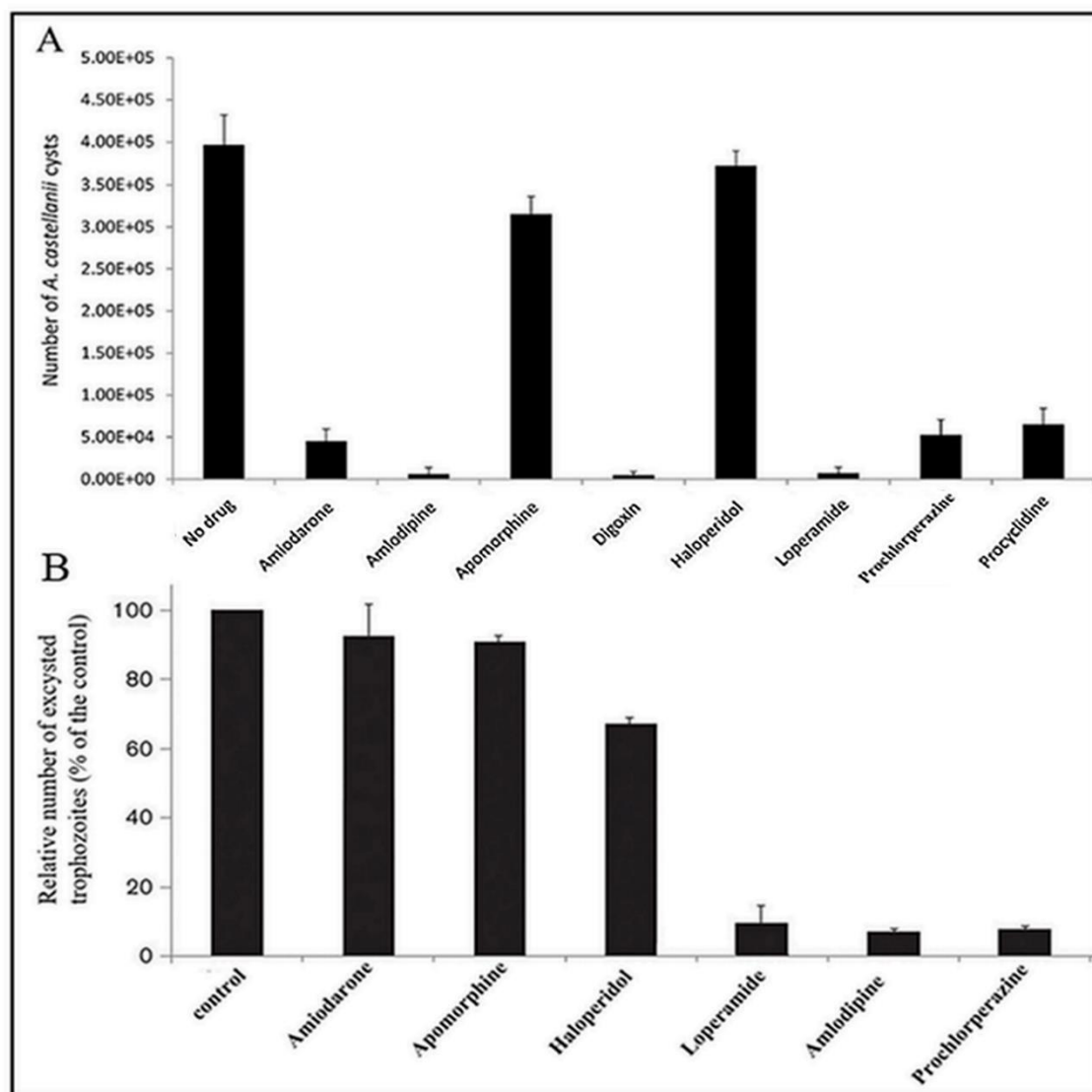


Figure 13. Effects of drugs against cysts: Encystation blockage and activity against cysts in *A. castellanii*.

(A) When tested for blocking encystation in *A. castellanii* all of the drugs except apomorphine and haloperidol prevented cyst formation (encystation). ($P < 0.01$; paired *t*-test; one-tail distribution). (B) As compared to controls (no-drugs), cysts treated with 250µg/ml of loperamide, 200µg/ml amlodipine, and 50µg/ml of prochlorperazine did not show encysted trophozoites to excyst in PYG for 2 weeks of incubation. For the rest of the drugs (250µg/ml) which included amiodarone, apomorphine, and haloperidol, the excystation of amoeba trophozoites was observed. The percentage of excysted amoebae in controls was considered as 100% and the effects of drugs are expressed as relative change. The results are representative of at least three independent experiments performed in duplicate. **[Adapted from Baig AM, 2013, [134]].**

Additionally, all the drugs except apomorphine and haloperidol prevented the process of encystation (Figure 13 A). Also, as compared to the control loperamide, amlodipine and prochlorperazine (Figure 13 B) showed to be effective against cysts of *A. castellanii* **[Baig AM, 2013, [134]]**, as the cysts exposed to these drugs failed to excyst till 2 weeks of incubation in growth medium PYG. The rest of the drugs which included amiodarone, apomorphine, and haloperidol were not seen to be effective against the cysts as amoeba trophozoites remerged in well plates and appeared motile and healthy **[Baig AM, 2013, [134]]**

3.3 Reproducibility and the effects of drug combinations in *A. castellanii* and related FLA.

As the drugs used exerted their inhibitory effects on diverse human cellular receptors and adapter proteins (Figure 10), it was tested if the results obtained previously **[Baig AM, 2013, [134]]** could be reproduced by experimentations of the drugs used alone and in combinations in *Acanthamoeba* and related FLA like *Balamuthia mandrillaris* **[Huma K, Baig AM, 2014, [135]]**. *Acanthamoeba castellanii* trophozoites were tested and showed susceptibility to a combination of 100 - 250 µM concentration of various drugs *in vitro* with drugs exhibiting drug synergism (Figure 14) **[Huma K, Baig AM, 2014, [135]]**. Drugs were also evaluated for their safety on human brain microvascular cells (HBMEC). Incubation of HBMEC with amoeba but without the drugs destroyed the human HBMEC but it was shown

FACS analysis and DNA staining.

that in the presence of the drugs, the amoebae were turned incapable of exerting their cytopathic effects on HBMEC. [Huma K, Baig AM, 2014, [135]].

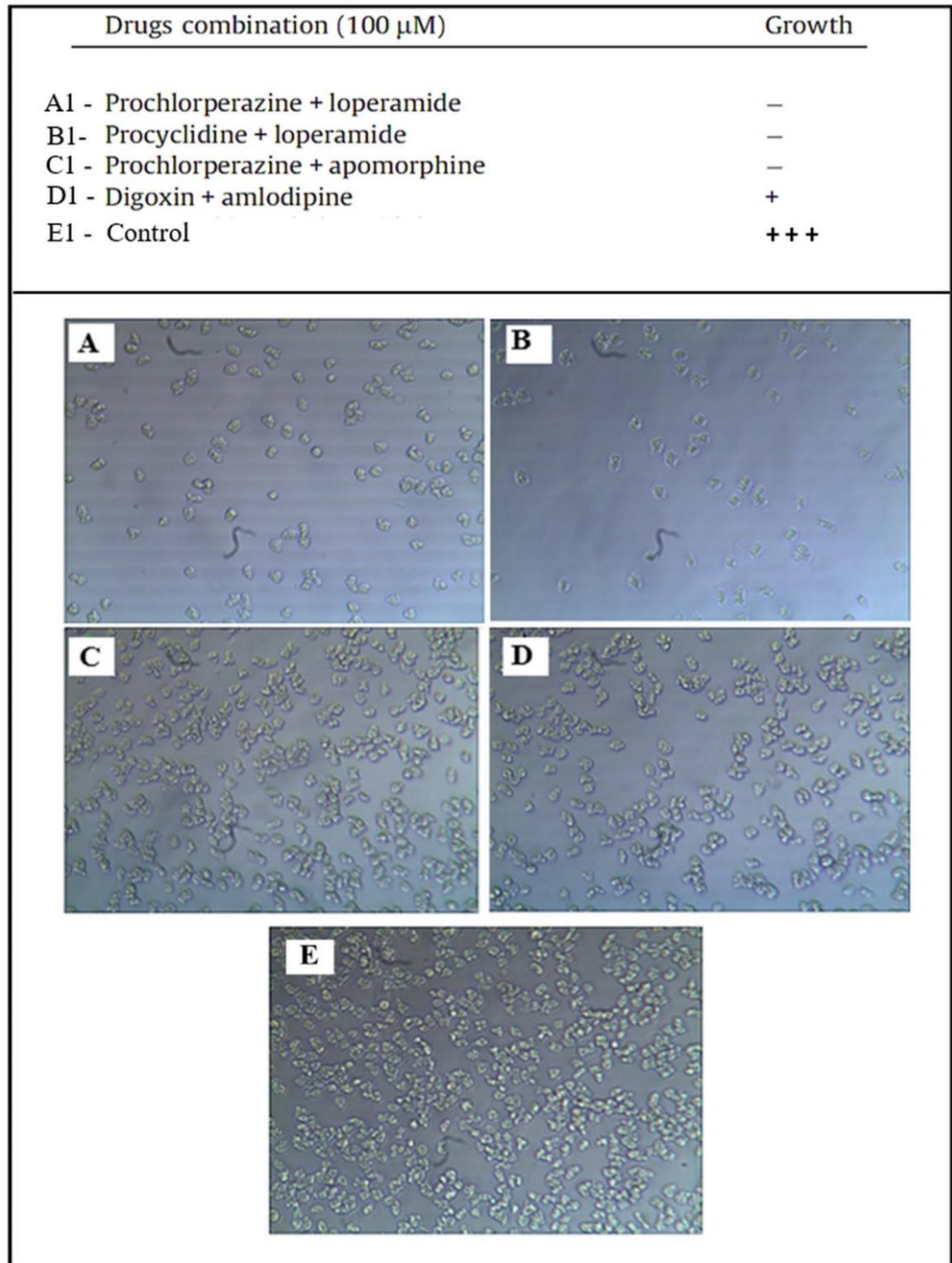


Figure 14. Effects of drugs used in combinations *A. castellanii* for 24h.

20x Images of the effects of combinations of different FDA approved drugs on the proliferation of (1×10^5) *A. castellanii* trophozoites. The sign (-) and (+) represent growth inhibition growth observed respectively. The combination of prochlorperazine + loperamide (A-A1), procyclidine + loperamide (B-B1), apomorphine + haloperidol (C-C1) in a dose of 100 μ M inhibited the growth of the trophozoites of *A. castellanii*. 250 μ M of digoxin + amlodipine also proved to be anti-proliferative for the trophozoites initially, as can be seen (D-D1), but growth continued after 48h (D1). Growth in the control (E) without any drugs was seen to be several folds of the initial seeding (E1). **[[Adapted from [Huma K, Baig AM, 2014, [135]].**

3.4 Drugs targeting Ca²⁺ signaling adapter proteins:

The drugs amlodipine, gabapentin and loperamide target various types of voltage-gated Ca²⁺ channel (VGCC) in humans (Table-4), with the latter drug also known to inhibit CaM. It was shown earlier that minimum inhibitory concentrations (MIC- 50% growth inhibition) needed to attain amoebistatic effects with VGCC blockers like amlodipine and prochlorperazine were as low as 50-25 μ g/ml respectively (Figure 13 A) as compared to the doses range between 250-500 μ g/ml needed for amoebicidal effects as reported previously **[Baig AM, 2013, [134]]**. To determine the minimum cytotoxic concentrations (MCC) needed to exert amoebicidal effects (~50%) for the VGCC blockers in particular and the rest of the drugs in general, further experiments were carried out. For amlodipine, it was shown that in the dose range of 40-50 μ g/ml, this drug can exert significant amoebicidal effects **[Baig AM, 2019d, [146]]** (Figure 15 A). For gabapentin, a related drug that blocks the alpha2/delta1 VGCC in humans showed to exert significant amoebicidal effects (P<0.001) in doses between 80-100 μ g/ml **[Baig AM, 2019d [146]]** (Figure 15 B). The effects of these VGCC blockers on the proliferation of *Acanthamoeba* trophozoites showed reduced trophozoites cell counts after 24h (Figure 15 A2, A3, and B2-B3)

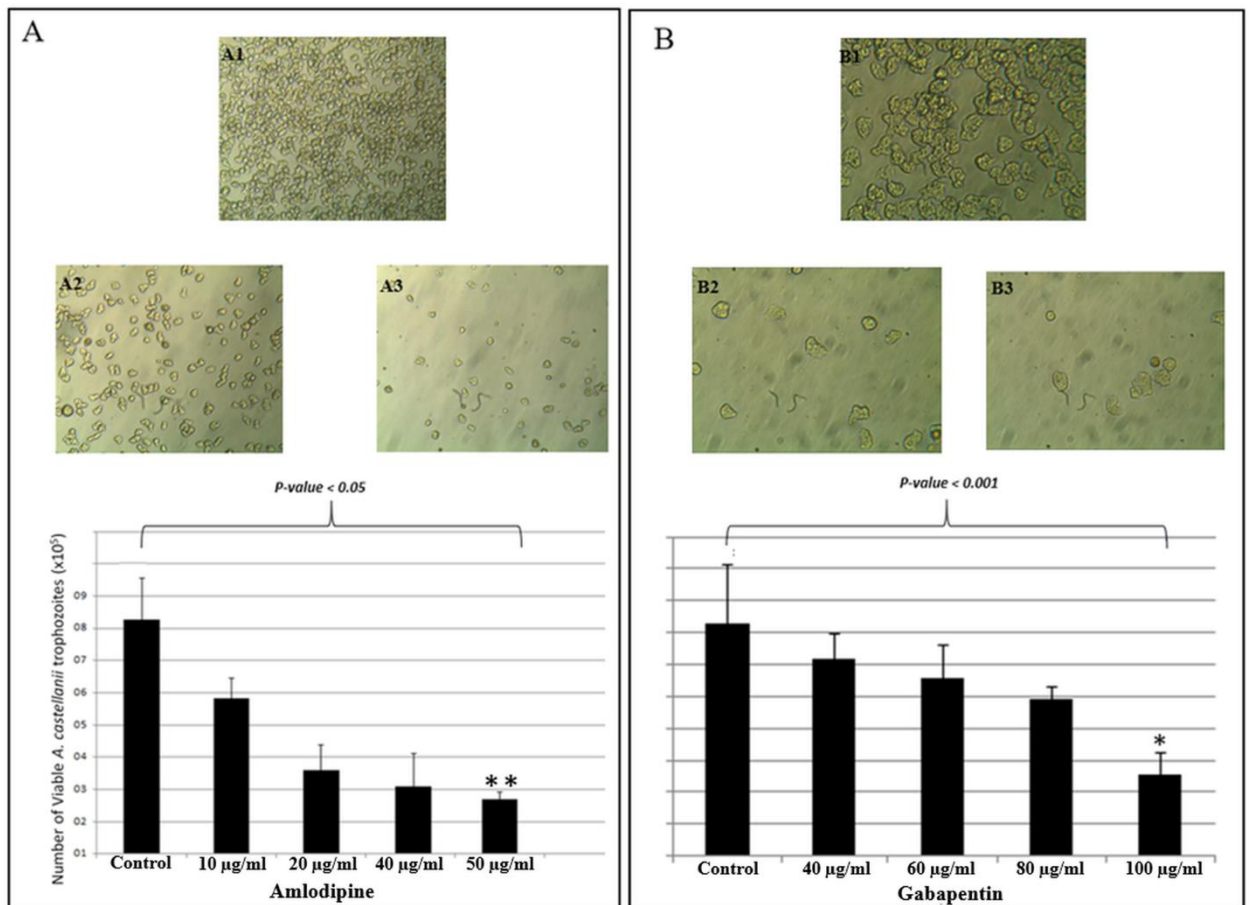


Figure 15. Amoebistatic effects of Amlodipine and Gabapentin in *A. castellanii* trophozoites.

Effects of minimum inhibitory concentration (MIC) of amlodipine (A) and gabapentin (B). (A1-B1). are controls of amlodipine and gabapentin respectively. Effects of 40 µg/ml and 50 µg/ml of amlodipine (** P < 0.05) (A2-A3) are shown (20x images). Effects of 80 µg/ml and 100 µg/ml of gabapentin (* P < 0.001) (B2-B3) respectively are shown (40x images). Histograms (A, B) show the MCC effects of amlodipine and gabapentin as compared to the controls. A paired student *t*-test; one-tail distribution was used. The results are representative of three independent experiments performed in duplicate. The data are presented as means and standard errors. [Adapted from Baig AM, 2019d [146]].

3.4.1 VGCC blocker exert apoptotic and amoebicidal effects

The known molecular targets of loperamide in humans are the P/Q type VGCC, opioid receptors, and CaM (Table-4). Amoebicidal and apoptotic effects in differential doses of loperamide were reported in our studies [Baig AM, 2017d [141]] in *A. castellanii* where loperamide possibly acted by affecting CaM and human-like VGCCs [Baig AM, 2019d [146]] in a dose range of 100-150 µg/ml. It was shown that loperamide exerts minimum cytotoxic concentration MCC (~50%) at 150 µg/ml (Figure 16 A and D). Also, loperamide (80 µg/ml) when combined with the haloperidol (30 µg/ml) proved to reduce the proliferation of trophozoites of *A. castellanii*. (Figure 16 A) as compared to the control. Our studies show that in addition to amlodipine, gabapentin [Baig AM, 2019d [146]] (Figure 15), and loperamide [Baig AM, 2017d [141]] (Figure 16), other VGCC blockers like verapamil and nifedipine also exert significant amoebicidal effects in a dose range of 50-100 µg/ml (Figure 17 and 28).

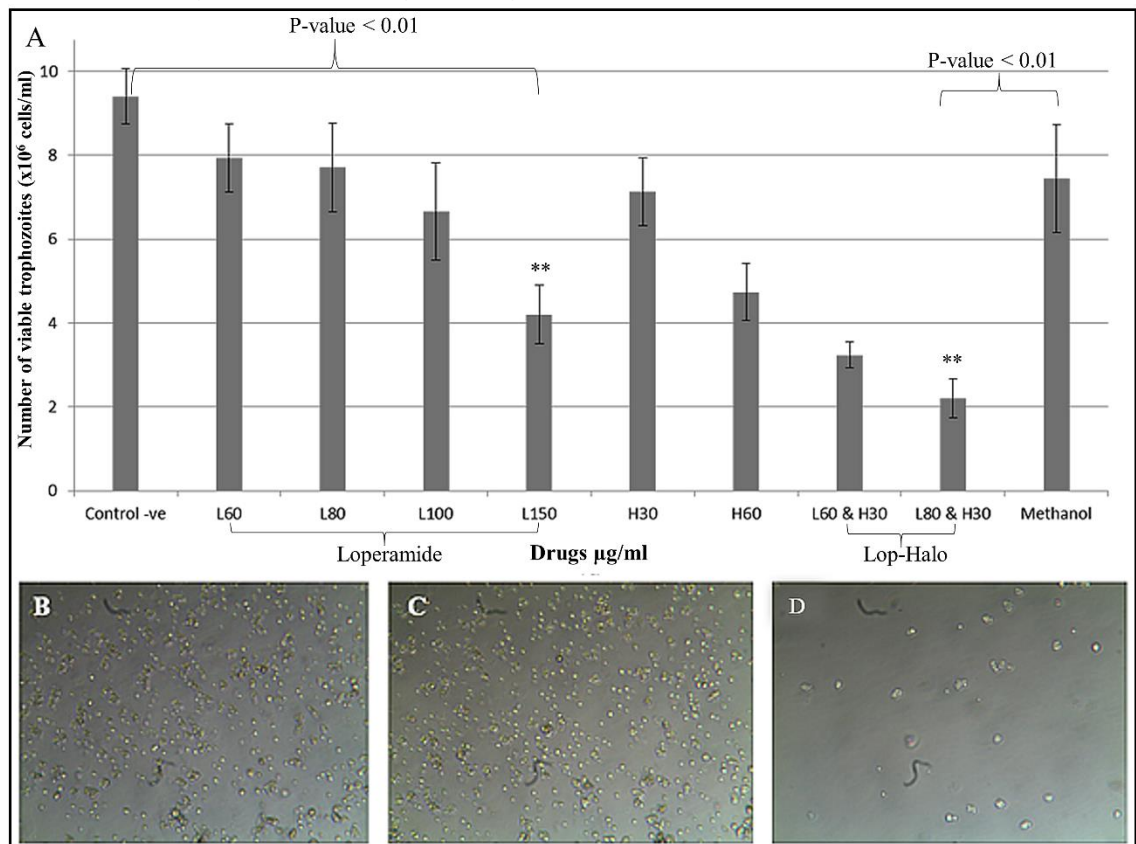


Figure 16. Effects of different doses of loperamide in *A. castellanii* trophozoites.

The minimal cytotoxic concentrations (MCC) of loperamide were observed at 150 $\mu\text{g/ml}$ in the histogram (A-lane-5, and D) and control (20x Image B). At 100 $\mu\text{g/ml}$ loperamide (A-lane-4, and C) did not exert significant amoebicidal effects. Also shown in the histogram are the effects of loperamide with haloperidol in different concentrations in (1×10^5) *A. castellanii* trophozoites. Loperamide 80 $\mu\text{g/ml}$ + haloperidol 30 $\mu\text{g/ml}$ showed significant growth inhibition (last 3 columns- A) as compared to the solvent control. (** $P < 0.01$ paired *t*-test; one-tail distribution). One-way ANOVA and Dunnet's comparison test (post hoc test) were done for Lop-Halo assays. The results are representative of at least three independent experiments performed in duplicate. The data are presented as means and standard errors. [Adapted from Baig AM, 2017d [141]].

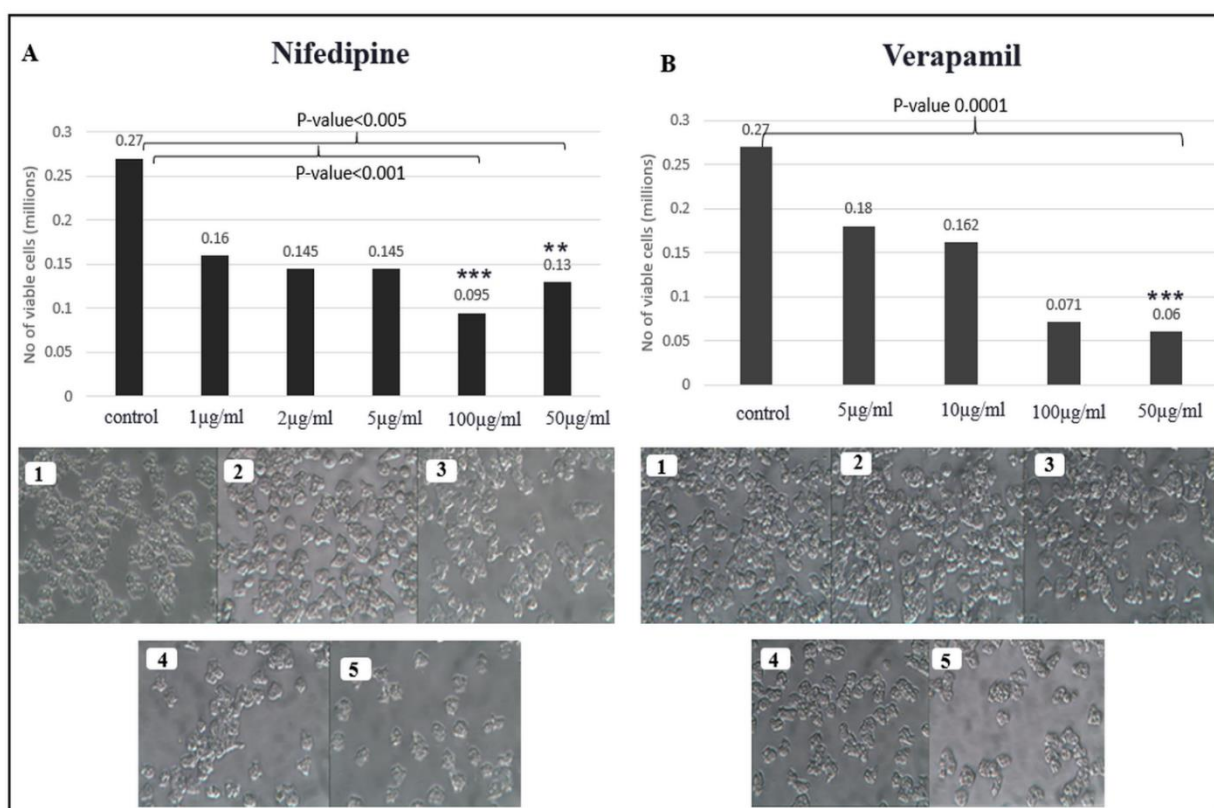


Figure 17. Effects of different doses of nifedipine and verapamil in *A. castellanii*

(A) Nifedipine: showed significant antiproliferative effects in dose ranges of 100 and 500 $\mu\text{g/ml}$ (** $P < 0.005$ and *** $P < 0.001$ respectively - paired student *t*-test; one-tail distribution) (A: lane-5 and 6 respectively; Images A4-A5) as compared to controls. Doses of 1-2-5 $\mu\text{g/ml}$ (A lane-2, 3, and 4) did not show significant

antiproliferative effects. (B) **Verapamil**: showed significant antiproliferative effects in doses range of 100 and 50 μ g/ml (***) $P < 0.0001$ - paired student *t*-test; one-tail distribution) (B: lane-4 and 5; Images B4 B5 respectively) as compared to control. Doses of 5 and 10 μ g/ml (B-lane-2 and 3) did not show significant antiproliferative effects. The results are representative of at least three independent experiments performed in duplicate on 0.15×10^6 cells after 24h. The data are presented as means and standard errors. [Adapted from Baig AM, 2019d j [156]].

3.5 Fura-2 AM staining of trophozoites treated with VGCC blockers

Drugs used in studies were aimed to bring Ca^{2+} depletion and disrupt the Ca^{2+} homeostasis in the cytosol (detailed in chapter-1). Amlodipine, loperamide, gabapentin, nifedipine, and verapamil that belong to the VGCC class of drugs were used to deplete the intracellular Ca^{2+} inhibiting their influx via VGCC. Prochlorperazine, procyclidine, and other related drugs are known to antagonize receptors that are coupled with calcium channels [143], and therefore were also expected to lower the intracellular Ca^{2+} as assumed previously [Baig AM, 2013 [134]]. Our experiments showed that the neuroleptic drugs that are antagonists of biogenic amine receptors [143] coupled with calcium channels like promethazine also proved to be amoebistatic and amoebicidal in doses in a range of 31.25 – 125 μ g/ml respectively [Baig AM, 2019h [157], (Figure 27) and presumably acted via affecting the intracellular Ca^{2+} ion concentrations.

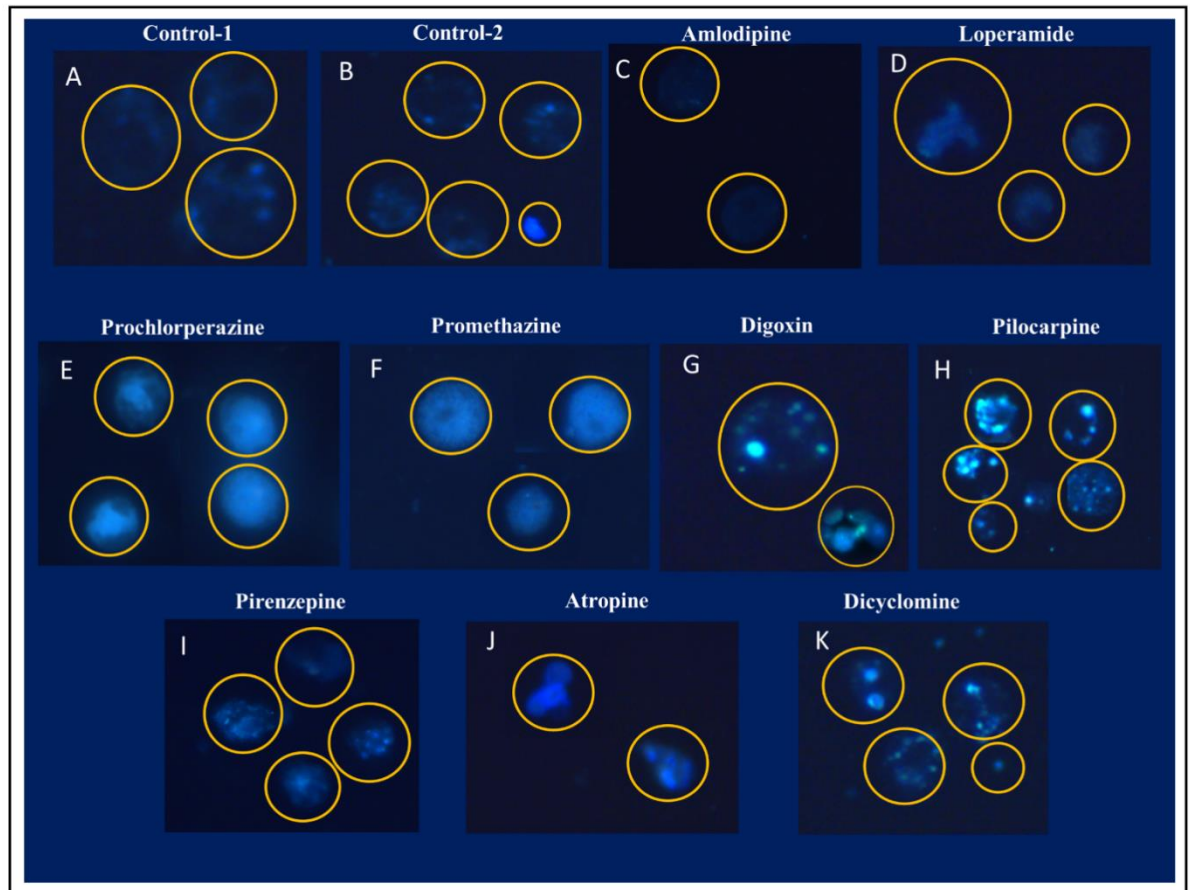


Figure 18. Fura-2AM staining in *Acanthamoeba* trophozoites.

A. castellanii trophozoites demonstrated Ca^{2+} dysregulation caused by drugs blocking VGCC and muscarinic receptors. The Fura-2AM staining was compared with controls in PYG (A) and PBS (B) without drugs [[Adapted from Baig AM, 2019i, [157]] +Unpublished data].

The fluctuations in Ca^{2+} ions after exposure to various drugs used in our assays (Table-4) was established by the use of Fura-2 AM staining (method details in chapter-2), which was compared with the amoeba in the controls (PYG) (Figure 18-A) and PBS (Figure 18-B) without drugs. Notable in the Fura-2 AM staining was the depletion of intracellular Ca^{2+} ions induced by VGCC blockers (Figure 18 C, D). Enhanced Fura-2 AM staining with pilocarpine (Figure 18 H), dicyclomine, and digoxin (Figure 18 K, G) was seen. Diffuse homogenous

FACS analysis and DNA staining.

staining with Fura-2AM was seen with prochlorperazine, promethazine, and atropine (Figure 18 labeled with names).

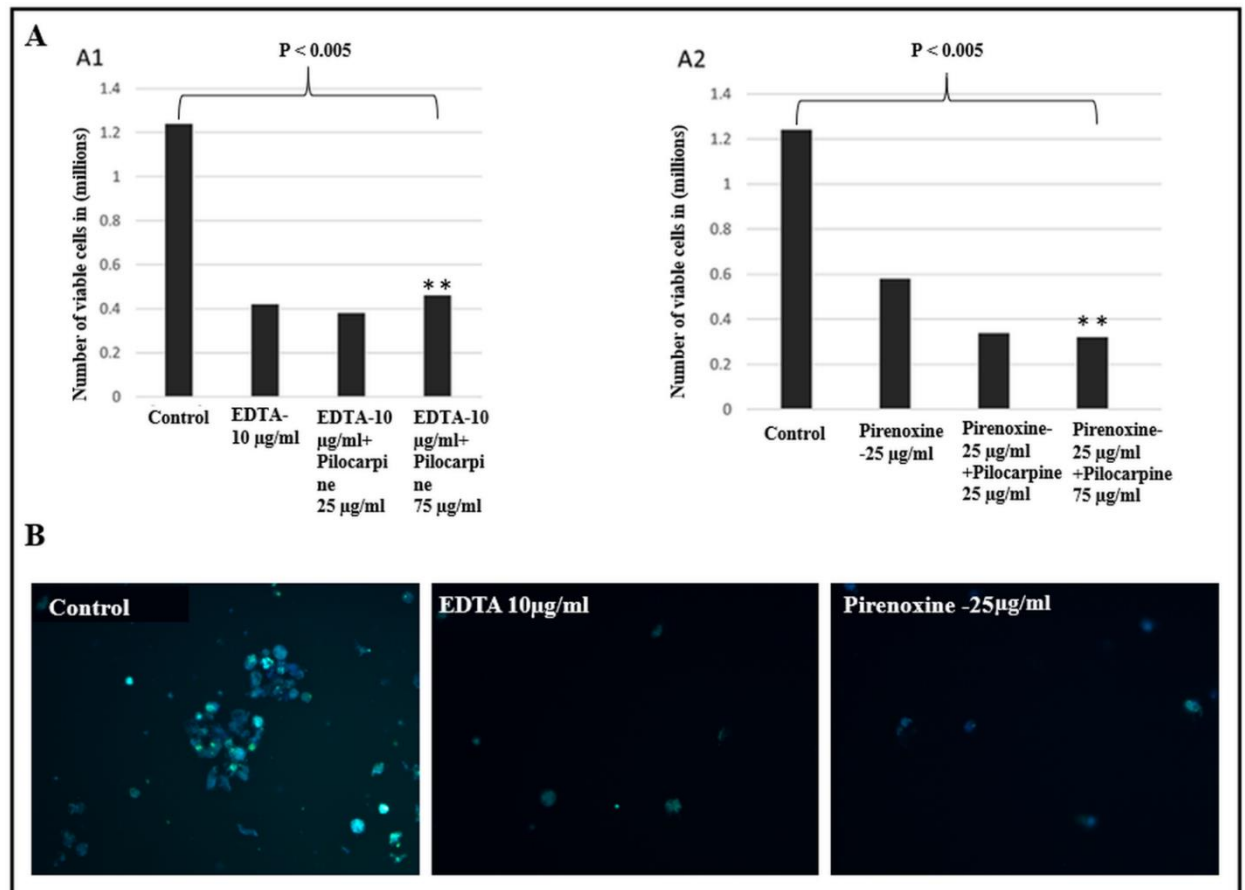


Figure 19. *A. castellanii* with Ca²⁺ chelating agents stained with Fura-2AM

(A1) Effects of EDTA 10µg/ml with and without pilocarpine. (A2) Pirenoxine dissolved in the solvent in a dose of 25 µg/ml with and without pilocarpine. (**P< 0.005: paired t-test; one-tail distribution) (B) Fura-2 AM staining in control without any drug in PYG medium, with EDTA10µg/ml and Pirenoxine 25µg/ml (left to right) showed reduced staining with Ca²⁺ chelating agents. Pilocarpine (Ca²⁺ influx inducing agent) failed to rescue the trophozoites. The results are representative of at least three independent experiments performed in duplicate. [Adapted from Baig AM, 2019i, [158]]

3.5.1 Ca^{2+} depletion caused by Ca^{2+} ion chelators EDTA and pirenoxine in *A. castellanii*

To show the dependency of *A. castellanii* on extra-cellular Ca^{2+} in other experiments, we tested the effects of Ethylenediaminetetraacetic acid (EDTA) and pirenoxine that are known to chelate the extra-cellular Ca^{2+} . Both drugs reduced the growth and proliferation of *Acanthamoeba castellanii*. [Baig AM, 2019i [158]] (Figure 19).

3.6 Effects of Drugs targeting human-like ion channels and proteins

A. castellanii trophozoites showed susceptibility to amiodarone which targets K-channel (KCN) and VGCC alpha-2/delta-1 protein in human cells. Amoebicidal and amoebistatic effects were observed with amiodarone in a dose range of 40-80 $\mu\text{g/ml}$ respectively (Figure 20, A and E-F, and Figure 27) [Baig AM, 2017e, [142]].

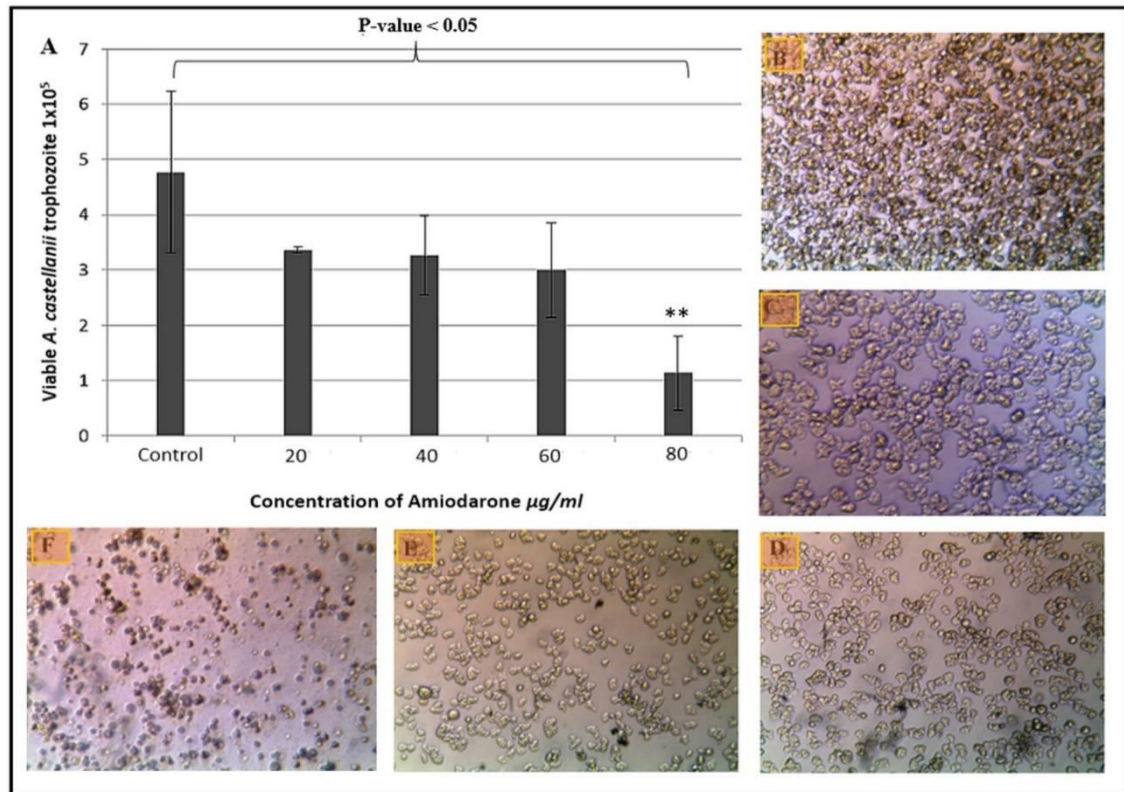


Figure 20. Amoebistatic and amoebicidal effects of amiodarone.

(A) Histogram showing a reduction in the number of viable trophozoites at a dose of 80µg/ml of amiodarone in 2.5×10^5 cells and 20x images were taken after a period of 24hrs. (B) -ve control, (C) 20µg/ml, (D) 40µg/ml, (E) 60µg/ml and (F) 80µg/ml of amiodarone. Note the dark staining trophozoites (F), confirmed for cytotoxic effects on staining with Trypan blue. (** P-value <0.05 paired *t*-test; one-tail distribution). The results are representative of at least three independent experiments performed in duplicate. The data are presented as means and standard errors. **[Adapted from Baig AM, 2017e, [142]].**

Acanthamoeba trophozoites were hypothesized to express human-like water and pH regulating adapter proteins (details below) like proton pumps, aquaporin (AQP), and carbonic anhydrase. The latter two are known targets of amlodipine, acetazolamide (AZM), and brinzolamide (BRZ). The trophozoites assumed rounded morphology and reduced growth and proliferation was observed. At 80 and 100 µg/ml, the drugs showed more profound effects than lower doses. (Figure 21 and Figure 27) **[Baig AM, 2018d, [147]].** BRZ also showed similar effects (data not shown). The latter two drugs are already used in the eye for the treatment of glaucoma [159] in the form of topical eye drops, therefore, they could be repurposed after clinical trials in humans with AK.

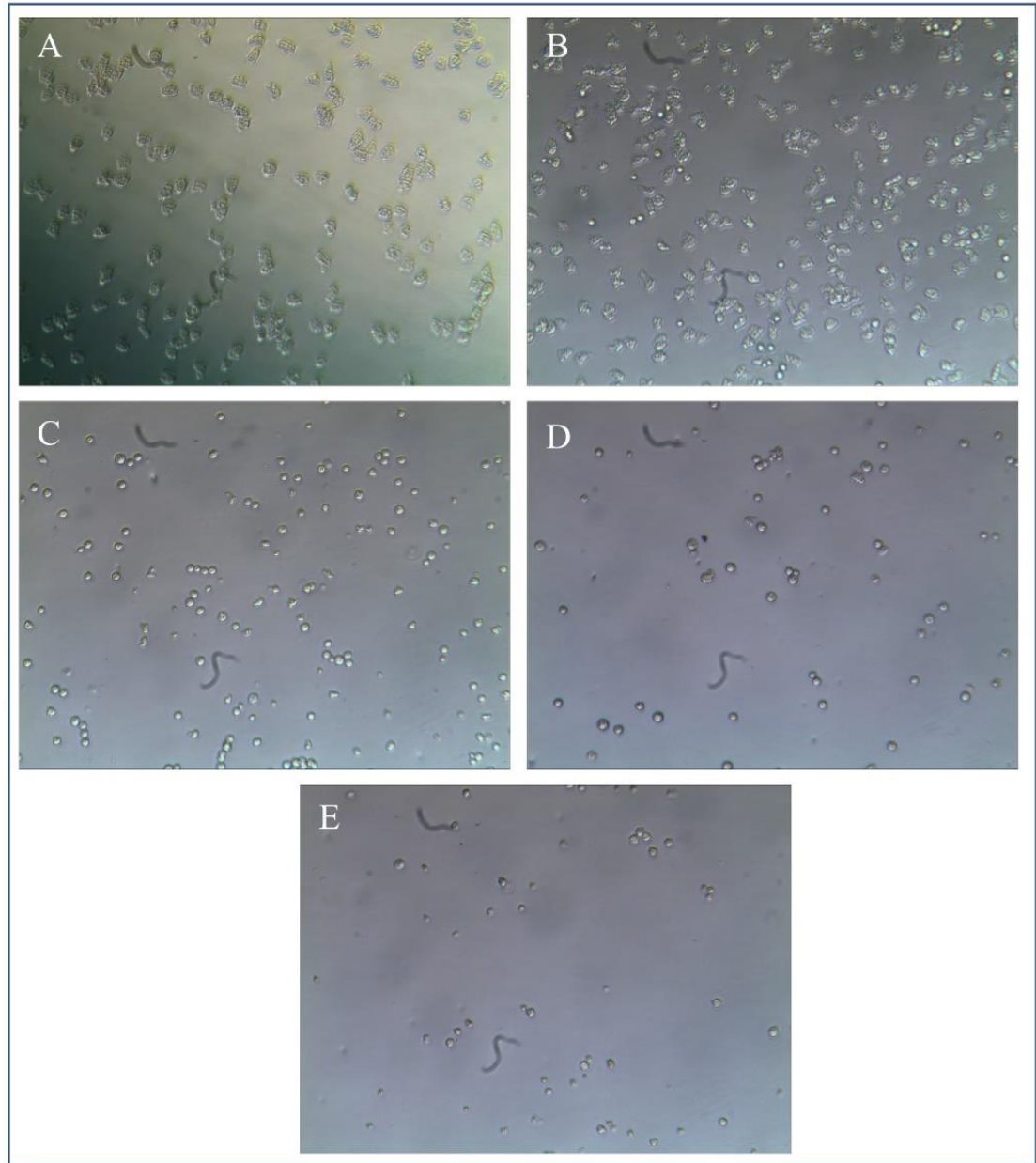


Figure 21. Effects of carbonic anhydrase inhibitor on *Acanthamoeba castellanii*.

(A) Control without AZM. Images (B, C, D, E) show the effects of 20-60-80 and 100µg/ml of acetazolamide respectively after 24h in trophozoites of *Acanthamoeba castellanii*. The trophozoites assumed a rounded morphology and showed reduced growth and proliferation. Concentrations of 80 and 100 µg/ml had more profound effects than lower doses (D, E). Data are representative of at least three independent experiments performed in duplicate [Adapted from Baig AM, 2018d, [147]].

3.7 The first evidence of a cholinergic ligand and druggable human-like muscarinic receptor (mAChR) like protein in *Acanthamoeba* spp.

3.7.1 Anti-human mAChR1 Antibody showed Immunostaining in *A. castellanii* trophozoites.

It was previously hypothesized that that *Acanthamoeba* trophozoites express human-like muscarinic receptors (Figure 10, green ribbons) that bind agonists like pilocarpine and ACh and are antagonized by muscarinic receptor antagonists [Baig AM, 2013 [134]]. In follow-up studies, we provided the evidence of a human mAChR like receptor [Baig AM, 2017a, [149]], with immunostaining using anti-human mAChR1 antibody that showed positive staining in *A. castellanii* trophozoites (Figure 22).

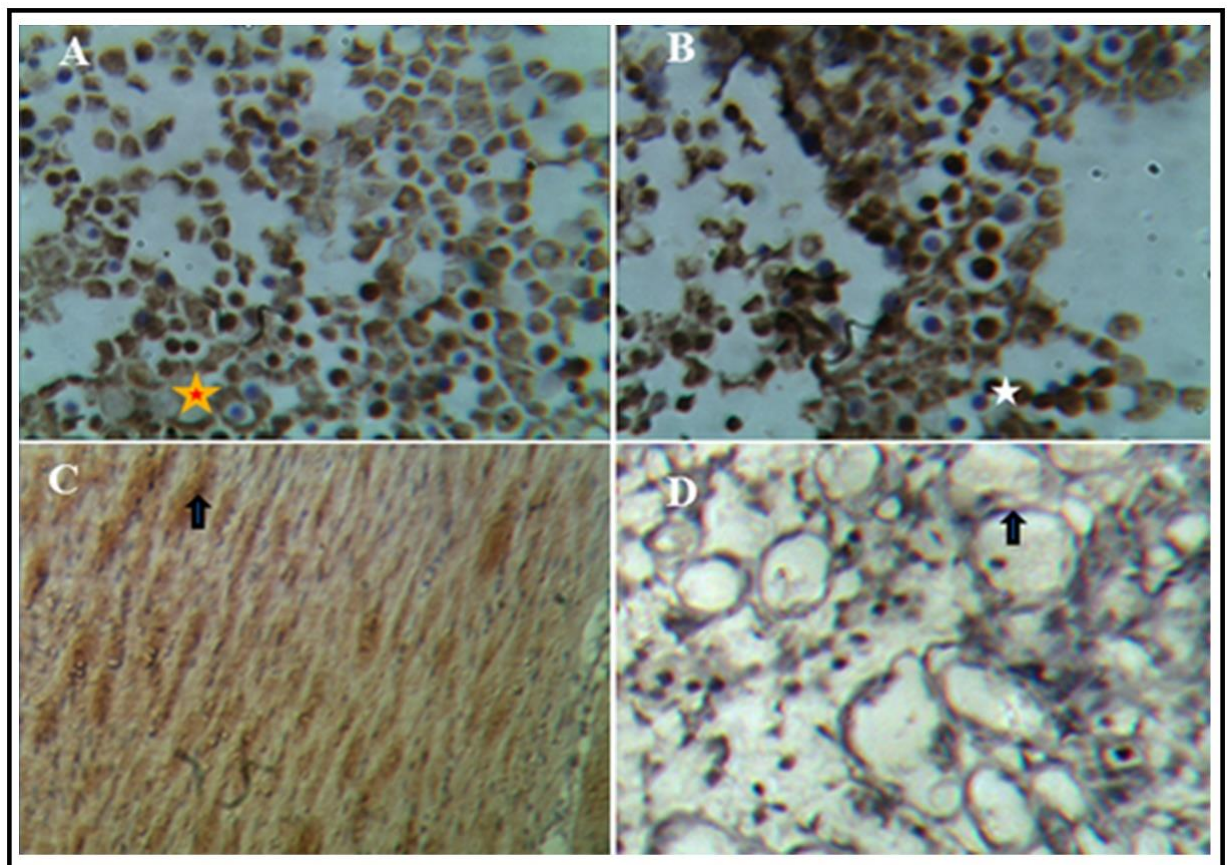


Figure 22. Immunostaining with anti-human mAChR1 antibody.

FACS analysis and DNA staining.

- (A) *Acanthamoeba* trophozoites, star showing positive staining of *A. castellanii* trophozoites (10x).
- (B) Cytoplasmic staining of *A. castellanii* trophozoites (white-star) (20x).
- (C) Smooth muscle cells showing staining (20x -positive control).
- (D) Fat cells showing an absence of staining (20x -negative control) **[Adapted from Baig AM, 2017a, [149]]**

3.7.2 Validation of the presence of ligand Acetylcholine in *Acanthamoeba castellanii* trophozoites.

A complete cascade of enzymes (detailed below) needed for ACh synthesis and the presence of the ligand ACh that exerts a possible growth promoting autocrine and paracrine effects in *A. castellanii* was reported **[Baig AM, 2018a,[160]]**. Colorimetric assay for ACh detection in the trophozoites was used (Figure 23) to demonstrate the presence of ACh in lysates of trophozoites of *A. castellanii*.

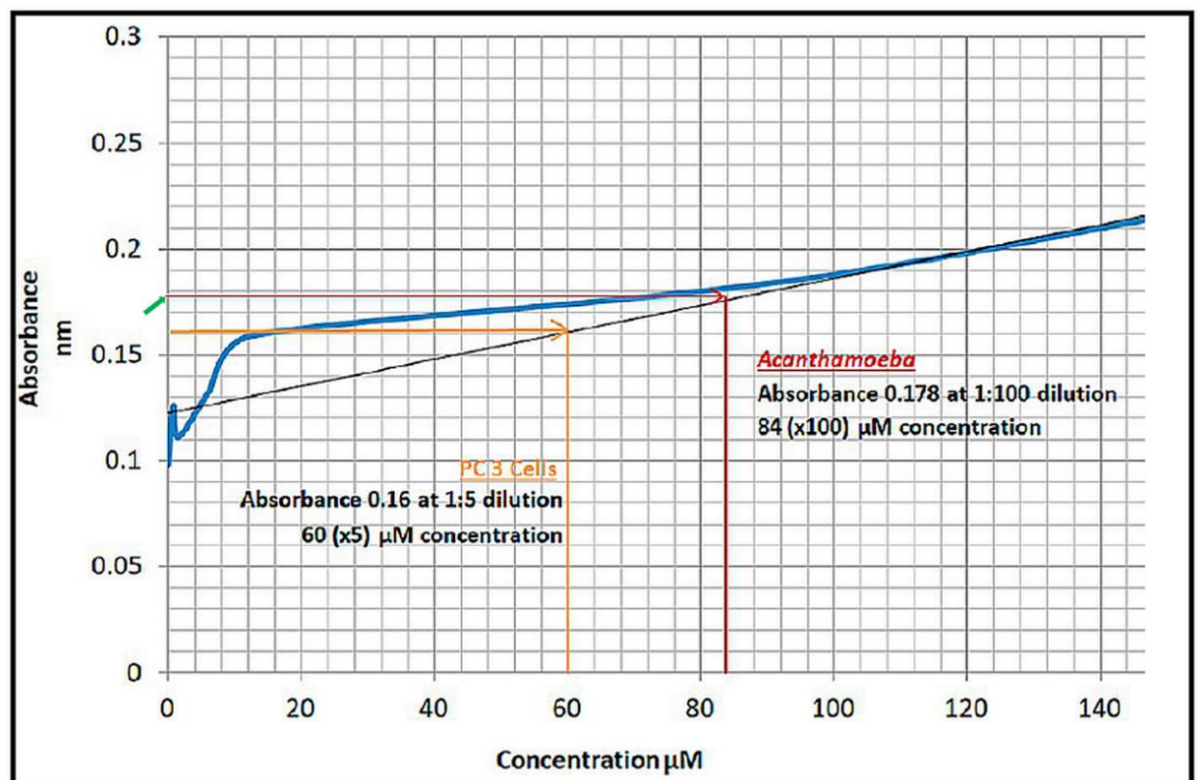


Figure 23. Colorimetric assay for acetylcholine (ACh) detection

The absorbance of trophozoite samples was tested and plotted against a standard curve. ACh was present at a concentration of 8.4 μM when the *Acanthamoeba* lysate was diluted 100 times. The red line (green arrow on the y-axis) represents absorbance and the corresponding concentration, while the orange line shows the presence of ACh in prostate cancer PC-3 cells as a positive control. The blue line represents the standard curve. The results are representative of at least three independent experiments performed in duplicates. [Adapted from [Baig AM, 2018a,[160]]]

3.7.3 mAChR antagonists exert amoebicidal effects in

***Acanthamoeba castellanii* trophozoites.**

Assays performed with 90 $\mu\text{g/ml}$ of dicyclomine and 100 $\mu\text{g/ml}$ of pirenzepine (Figure 24, Images, and histogram) showed significant amoebicidal effects [Baig AM, 2017a, [149]]. Taken together the growth assays, antagonist effects, immunostaining positivity for mAChR1 like protein, and virtual isolation of ACh in lysates of *A. castellanii* were the first reported [Baig AM, 2018a,[160]] evidence of the existence of a druggable cholinergic system.

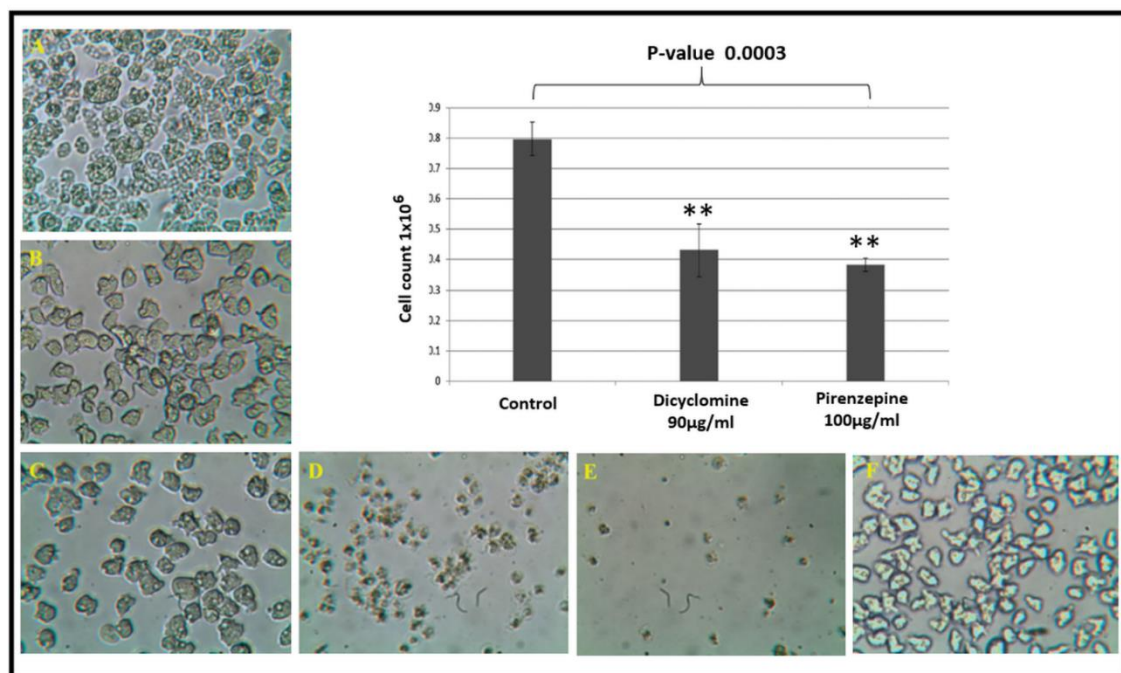


Figure 24. mAChR antagonists affect the growth and viability of *Acanthamoeba* trophozoites

(A) Solvent control in PYG.(B-C) Effects of 150 µg/ml and 200 µg/ml of pirenzepine respectively at the 12th h. (D-E) Effects of 150 µg/ml and 200 µg/ml of pirenzepine respectively at the 24th h. (F). Solvent (methanol) control at the 24th h. The histogram shows the effects of 90 µg/ml of dicyclomine and 100 µg/ml of pirenzepine in *A. castellanii* trophozoites (0.5×10^6) incubated with these mAChR1 antagonists. Experiments were performed in duplicates. One-way ANOVA showed a P-value of 0.0003. Dunnet's comparison test revealed a P-value < 0.01 for control vs dicyclomine 90 µg/mL and a P-value < 0.01 for control vs pirenzepine 100 µg/ml. 20x images of *Acanthamoeba* trophozoites. The results are representative of at least three independent experiments performed in duplicate. The data are presented as means and standard errors. [Adapted from Baig AM, 2017a, [149]].

3.7.4 Agonist effects clue towards human-like receptors and VGCC in *A. castellanii*

One important way to elucidate that the amoebistatic effects of the drugs tested (Table-4) occurred at the molecular level of human-like receptors and ion-channels was to observe if the agonists of these proteins can show growth-promoting and proliferative effects. Both ACh (Figure 25 C and second column D) and its indirect agonist physostigmine (Figure 25 E) caused growth and proliferation of trophozoites.

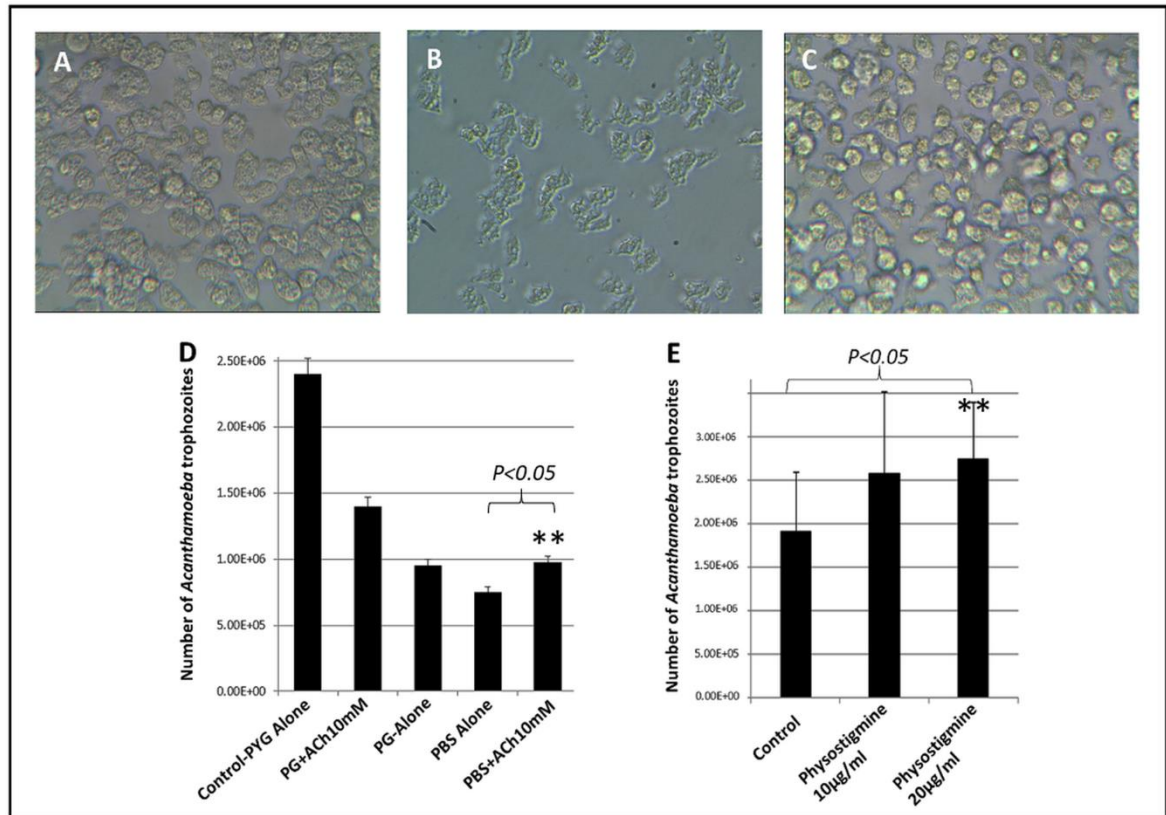


Figure 25. Effects of mAChR agonist in *Acanthamoeba* trophozoites.

Effects of agonists of cholinergic receptors in *Acanthamoeba* trophozoites 1×10^6 after 24h showed that as compared to control PYG medium (40x) (A) the proliferation of trophozoites continued without signs of encystation in PBS with ACh (B and the fifth in column-D). The proliferation of *Acanthamoeba trophozoites* continued with ACh despite the depletion of yeast in the growth medium (C and the second column in D) with peptone and glucose (PG) alone. Indirectly acting cholinergic agonist Physostigmine also showed proliferative effects in *Acanthamoeba* trophozoites as compared to controls (E). (** P-value < 0.05 , paired *t*-test; one-tail distribution). The results are representative of at least three independent experiments performed in duplicate. The data are presented as means and standard errors. **[[Adapted from Baig AM, 2017a [149] and Baig AM, 2018 a, [160]].**

Due to the unavailability of direct agonists of VGCC to antagonize VGCC blockers at their binding sites, we tested an indirect agonist Potassium chloride (KCL) instead (normally used in experiments involving tissue baths to open VGCCs), to alter the transmembrane potential in cells, to open unbound VGCC like proteins in *A. castellanii*.

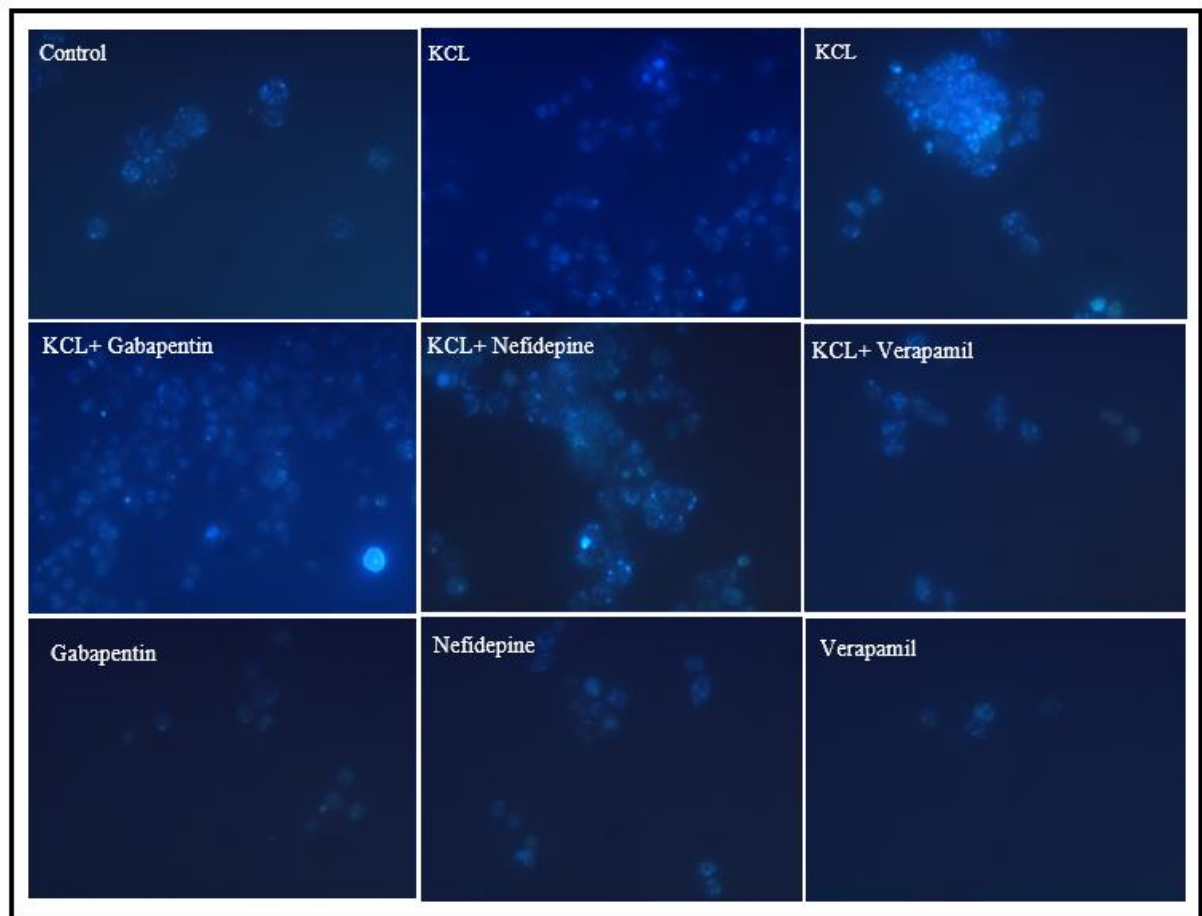


Figure 26. Effects of KCL and VGCC blocking drugs on Fura-2 AM staining in *Acanthamoeba* trophozoites.

Top row: Control shows Fura-2 AM staining in trophozoite compared to KCL in a dose of 20mM showed slightly enhanced staining with KCL alone (last two images).

Middle row: KCL, when tested with 100 µg/ml of the VGCC blocking drugs showed to oppose the effects of gabapentin and nifedipine (bright staining), but not verapamil.

Bottom row: Effects of VGCC blockers alone in a dose of 100 µg/ ml each for comparison. [Unpublished Data and partly adapted from Baig AM, 2019d j [156]-Methodology described in chapter-2, page #46]

**Experimental Assays, immunostaining, ELISA, colorimetric analysis,
FACS analysis and DNA staining.**

This experiment showed that KCL like in human cells can open VGCC (Figure 26-top row) and oppose the effects of drugs like nifedipine and gabapentin but could not effectively oppose the effects of verapamil (Figure 26 middle-row).

3.8 Elucidation of cell death mechanisms in *Acanthamoeba trophozoites* and cysts

3.8.1 Cytotoxic death in *Acanthamoeba trophozoites*

We used a combination of methods to demonstrate the cytotoxicity (amoebicidal effects) exerted by the drugs tested (Table-4) in *Acanthamoeba trophozoites*. Trypan blue staining (detailed above- Figure 13, 14, 16, 18, 21, 24), FACS analysis of the drug-treated cell, and staining with propidium iodide (PI) were a few of the various methods (detailed below in Figure 28) that were used to demonstrate the necrotic cell death in the trophozoites incubated in the *in vitro* assays. In almost all the cases the trophozoites presumed to be dead after exposure to the drugs were re-incubated in PYG to look for re-emergence of motile amoebal trophozoites. The latter was also done for the confirmation of cysticidal assays (Figure 13). Also, the trophozoites, considered to be dead, were tested by co-incubation with HBMEC to observe any cellular damage. The trophozoites were considered to be dead if only the mono-layers of HBMEC were seen to be intact [Huma K, Baig AM, 2014, [135]]. Additionally, to confirm the amoebicidal effects, LDH assays were also performed (Figure 27). Experiments were repeated several times to assure reproducibility. At times, a cluster of trophozoites that turned rounded in few hours and appeared to be dead (Figure 21), were observed for periods of 24h, and if the trophozoites regained their healthy states, it was reported [Baig AM, 2018d, [147]].

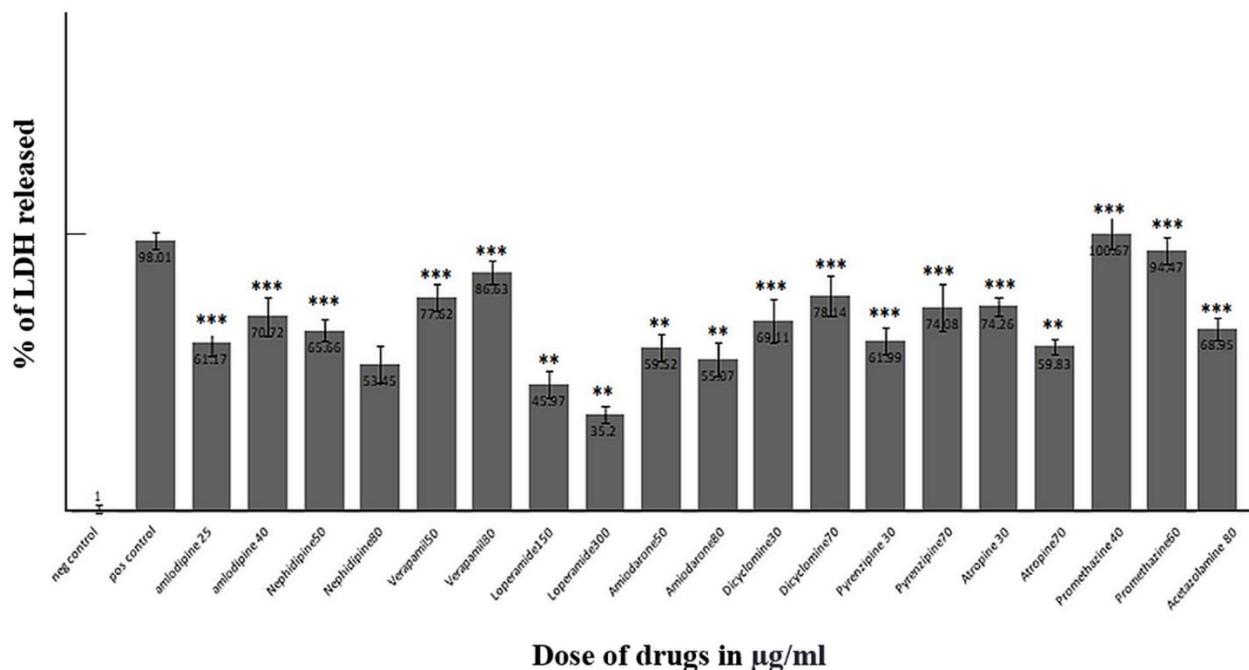


Figure 27. 1×10^6 *A. castellanii* trophozoites were incubated with and without drugs.

The supernatant was collected from 1×10^6 trophozoites/well and LDH concentration was measured in each sample by using the LDH assay kit. Results showed that LDH was released (y-axis) by exposure to all drugs in various concentrations (x-axis) in a dose-dependent manner. A paired student *t*-test with one-tail distribution was used, * $P < 0.05$, ** $P < 0.01$, *** $P < 0.001$. The results are representative of at least three independent experiments performed in duplicate. The data are presented as means and standard errors. [Unpublished data-methodology described in Chapter-2, Page # 43]

3.8.2 Programmed cell death: Apoptosis like features induced by drugs in *A. castellanii*

Some of the drugs tested in *A. castellanii* in the assays showed amoebicidal effects by possibly evoking a programmed cell death (PCD) like mechanism as indicated by morphological features akin to apoptosis (Figure 28, and 29). Expression of morphological features like formation and shedding of blebs on the cell surface in *A. castellanii* trophozoites was observed after exposure to low

**Experimental Assays, immunostaining, ELISA, colorimetric analysis,
FACS analysis and DNA staining.**

doses of loperamide (Figure 29, A) [Baig AM, 2017d [141]] and digoxin [Baig AM, 2016b [161]], which is akin to an apoptotic form of PCD [162, 163]. Similar features were also observed with known apoptotic drugs like doxorubicin and etoposide (control) (Figure 28, D) in *Acanthamoeba* trophozoites. Our studies reported a form of PCD that resembles eukaryotic apoptosis in *A. castellanii* [Baig AM 2017c [164]]. A few studies were done in the same year 2017 [155, 165] also provided evidence for PCD in *Acanthamoeba* spp., reinforcing the hypothesis that this unicellular eukaryote has the adaptor proteins that are required to cascade a PCD-like cell death. Our studies showed *Acanthamoeba* trophozoites after incubation with etoposide exhibited surface blebbing (a known feature of apoptotic bodies) (Figure 28, C) with phosphatidylserine staining Annexin-V [Baig AM 2017c [164]] and fragmented DNA staining (a known feature of cells undergoing apoptosis) with Acridine orange (Figure 28-A) [Baig AM, 2017d, [141]]. On flow cytometry, the trophozoites exposed to digoxin 40µg/ml with 7-Aminoactinomycin (7AAD), normally extruded by viable cells with intact cell membranes, was used instead of propidium iodide to measure cell death induced by digoxin. The trophozoites scattered first toward early and then late apoptotic zones (Figure 28-B, B2-B3 respectively). DNA laddering (a known feature of apoptotic cells) was also noted in trophozoites exposed to loperamide (data not shown) at a dose of 100 µg/ml [Baig AM 2017c [164]]. The evidence for the presence of adaptor proteins needed to execute the intrinsic pathway of apoptosis was identified in *A. castellanii*. (details in next chapter) and the evidence of apoptosis-like PCD was published [Baig AM, 2017c, [164]].

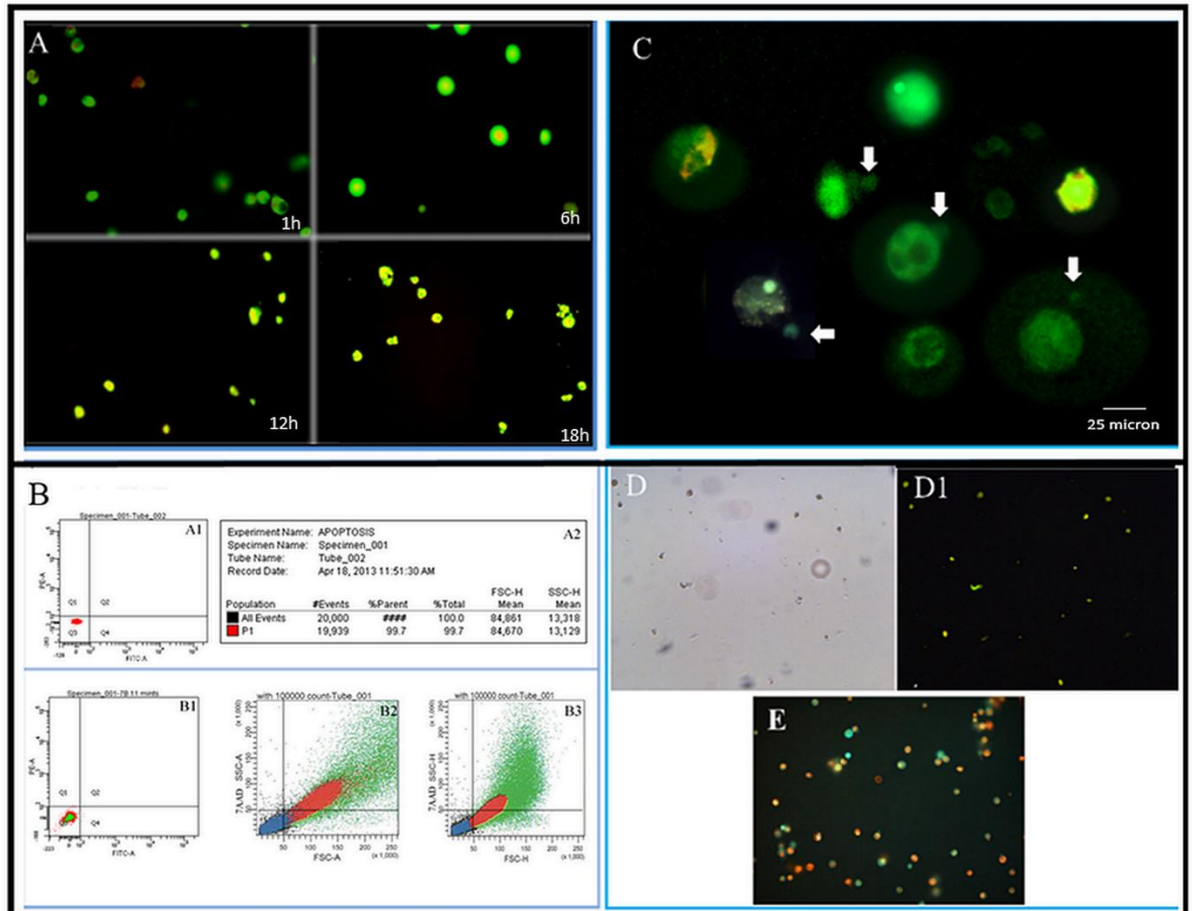


Figure 28. Programmed cell death in *Acanthamoeba* trophozoites.

(A) *Acanthamoeba* trophozoites after incubation with 100 µg/ml of loperamide, acridine orange (AO) staining shows a progressive increase (1h, 6h, 12h) in staining that maximized at 18h.

(B) FACS analysis showing the *A. castellanii* incubated with 40µg/ml of digoxin and 10µg/ml 7-Aminoactinomycin D (7-AAD). The cells (B1) started scattering towards early apoptotic- Q4- (B2) and towards the late apoptotic zone -Q2- (B3) at the 16th -18th hours after drug exposure.

(C) Annexin-V-FITC Conjugate (green). Red = propidium iodide (fluorescent DNA dye) (40x) images of *Acanthamoeba* trophozoites after incubation with etoposide at 18h. Note membrane blebbing (arrows), a known morphological finding of cells undergoing apoptotic.

(D-D1) Annexin V-FITC Conjugate (green). Red = propidium iodide (PI) 20x images of *Acanthamoeba* trophozoites under normal light (D) and *Acanthamoeba* trophozoites under a fluorescent microscope (D1) at 24h after incubation with doxorubicin. AO/PI staining with 250 µg/ml of loperamide show mostly necrotic trophozoites 12h after incubation (E). [Partly adapted from Baig AM, 2017c [164], and [Baig AM, 2016b [161]].

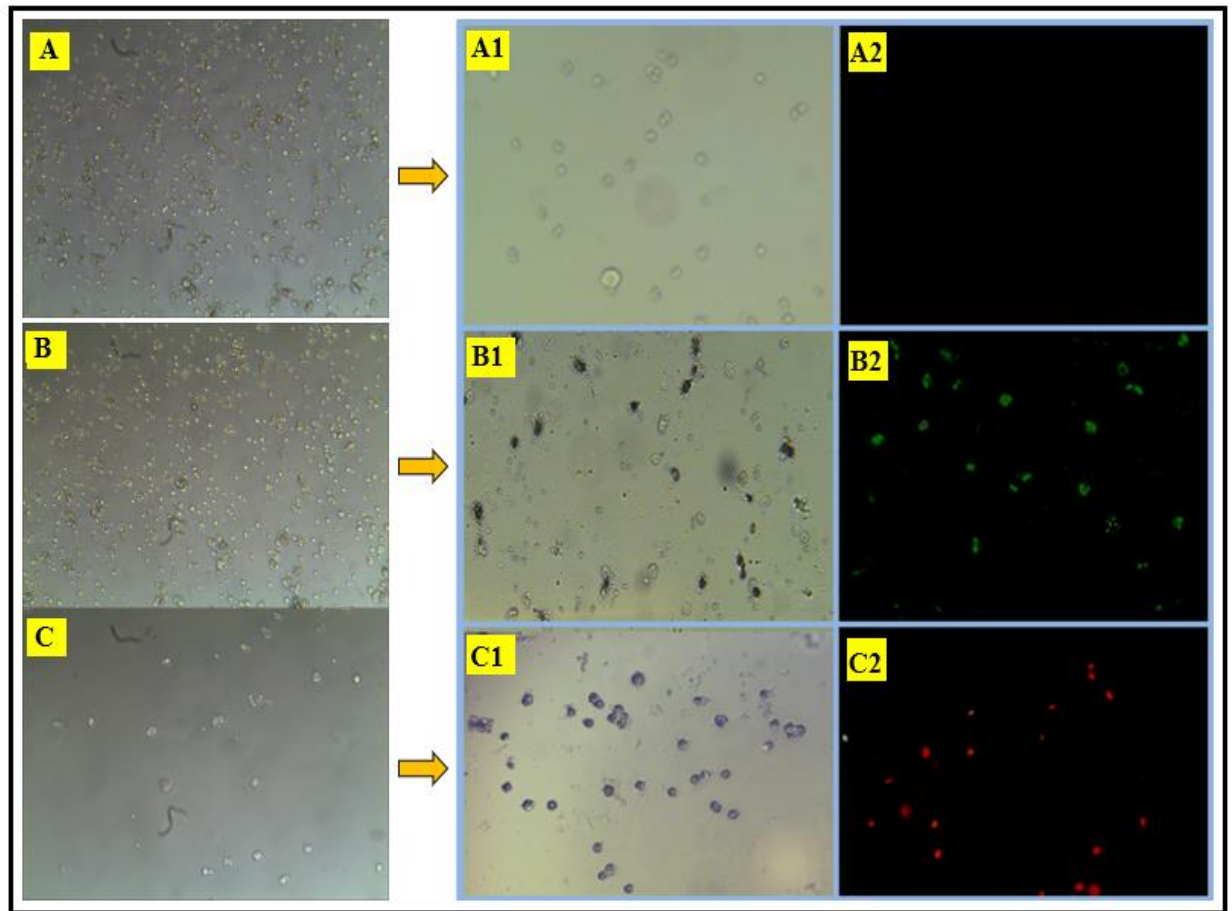


Figure 29. 20x Images of loperamide treated *A. castellanii* trophozoites:

(A) Solvent control in PYG (B) loperamide 100 $\mu\text{g/ml}$ (C) loperamide 250 $\mu\text{g/ml}$. (A1) *A. castellanii* was seen under normal light at 6h after loperamide 100 $\mu\text{g/ml}$.

(A2) Annexin V exposed trophozoites of *A. castellanii* seen under FITC at 6h after loperamide 100 $\mu\text{g/ml}$. No Annexin V fluorescence of the cell membranes seen.

(B1) *Acanthamoeba* trophozoites were seen at the 18th-hour loperamide under normal light. (B2) Annexin-V stained *Acanthamoeba* under FITC at 18th hour.

(C1) PI stained *Acanthamoeba* incubated with 250 $\mu\text{g/ml}$ of loperamide after 12 hours of drug exposure, under normal light.

(C2) Necrotic PI stained *A. castellanii* trophozoites incubated with 250 $\mu\text{g/ml}$ of loperamide after 12 hours. Green/Red filter excitation at 540/25nm and emission at 655/55nm maximum. [Adapted from Baig AM, 2017a [141]]

3.9 Summary of findings

Experiments done in *A. castellanii* trophozoites and cysts by drugs targeting Ca^{2+} homeostasis in humans (Table-4) showed amoebicidal, amoebistatic, and cysticidal effects. Repeatedly, the assays showed the drugs when used alone and in combinations were able to affect the growth and viability of *A. castellanii*. The VGCC targeting drugs in particular like amlodipine, nifedipine, verapamil, loperamide, amiodarone, and gabapentin directly affected the viability of the trophozoites of *A. castellanii*. Staining with Fura 2 AM showed the dysregulation in cytosolic Ca^{2+} induced by the drugs VGCC blocking drugs used in the experimental assays. The use of divalent cation chelating agents like EDTA and pirenixine, which restricts the uptake of Ca^{2+} ions, also proved to inhibit the growth and affect the viability of *A. castellanii*. The drugs that affect the intracellular pH by inhibiting the enzyme carbonic anhydrase and therefore the ionic state of calcium, like acetazolamide were also seen to exert dose-dependent amoebistatic and amoebicidal effects. Drugs that act as a cholinergic antagonist on muscarinic GPCRs known to be coupled with Ca^{2+} channels [143] also proved to be amoebistatic and amoebicidal *A. castellanii*. To validate that the effects of muscarinic GPCR antagonists like atropine, pirenzepine, and dicyclomine, immunostaining was done with anti-human mAChR1 antibody to show the expression of human-like mAChR1 receptor in *A. castellanii*. A cholinergic cascade and the presence of ACh were further documented in *A. castellanii*. To emphasize the rationale of the existence of human-like VGCC in *A. castellanii*, KCL was used to affect the transition of VGCC in *A. castellanii*. Finally, the mechanisms involved in cell death-like apoptosis and necrosis were shown. To show that trypan blue staining was due to cytotoxic effects of the drugs tested in our experiments, LDH release assays were done (Figure 27). Apoptosis was validated by Acridine orange and Annexin -V staining and experiments showing DNA laddering [Baig AM 2017c [164]]., a hallmark of apoptosis. Taken together we were able to show the significance and the validity

of the rationale of Ca²⁺ homeostasis affecting the growth and viability in *A. castellanii*, on which the studies were based.

3.9.1 Discussion

In the post-genomic era, the application of omics-based methodologies such as proteomics and transcriptomics has extended our understanding of parasite biology [2] and enabled the drug target prediction in general and in parasitic diseases with high mortality rates like malaria [167]. In the pre-genomic era *in vitro* testing of drugs in *Acanthamoeba* trophozoites and cysts that are prescribed in non-infectious conditions in humans can be traced back to 1970 and 1980s [98]. In 1984, the phenothiazine group of compounds like trifluoperazine dihydrochloride and chlorpromazine hydrochloride was shown to exhibit *in vitro* activity against the pathogenic free-living amoebae *N. fowleri*, *A. culbertsoni*, and *A. polyphaga*. Later again, the phenothiazines (chlorpromazine and trifluoperazine) were tested to show 70-90% of inhibition of *Acanthamoeba* growth by 5 and 10 µg/ml of the drugs [168, 169] with the uncertainty of the drug targets in *Acanthamoeba* spp. The molecular targets of the above-mentioned drugs were unclear. It was thought that either there was a sensitivity of amoebal calcium regulatory protein to the phenothiazine compounds or that the effects observed were due to the lipophilic action of the drugs on the amoeba plasma membrane [99, 168, 169]. A few plant products were also tested *in vitro* and three plants (*Ipomoea* sp., *Kaempferia galanga*, and *Cananga odorata*) were found to be cytotoxic for all three species of *Acanthamoeba* and an extract prepared from the plant *Gastrochilus panduratum* was lytic for *A. polyphaga* and growth-inhibitory for *A. castellanii* and *A. culbertsoni* [170, 171]. Miltefosine, an alkylphosphocholine was tested against *Acanthamoeba* spp and other parasites like *Leishmania* spp. and *Trypanosoma cruzi* and *Trypanosoma brucei* spp in 2003 [172] and again in 2009 [173]. Miltefosine is not a conventional antibiotic or anti-parasitic agent but exhibited anti-parasitic effects. Drugs having anti-malarial effects with unclear cellular targets like Artemether have also been shown to exert anti-amoebic effects against *Acanthamoeba* spp. [174]. The use

of atropine and analgesics in the form of eye drops had been reported to cure few cases of AK without any explanation of the molecular targets in *Acanthamoeba* spp. [175]. Other chemical compounds like caffeine and Maslinic acid are examples of other non-antimicrobial agents that have been tested and reports suggest they affect the growth and viability of *Acanthamoeba* by programmed cell death [176]. The drugs that are used to treat AK and GAE clinically in the past like fluconazole and sulphadizine shows that the cellular components unique to *Acanthamoeba* trophozoites were targeted to minimize adverse effects during the chemotherapy [16, 17, 36]. Given the drugs that are directed against molecular targets unique to *Acanthamoeba* spp. have not been able to minimize morbidity and mortality associated with AK and GAE respectively, as can be gauged by the morbidity seen in AK and the existing mortality observed in GAE. There is a need to introduce safer agents (Figure 10- blue-text) with the potential of repurposing, if possible. As evolutionarily humans share several proteins and enzymes with other unicellular eukaryotes [111, 177] we hypothesized the presence of homologs of diverse forms of protein in *Acanthamoeba* spp. as has been shown in the past [11, 169, 173]. Of the drugs tested in the past and experimented in our assays, are the neuroleptic agents belonging to the phenothiazine class drugs like prochlorperazine, chlorpromazine, and haloperidol which has a high margin of safety (therapeutic index) in humans (oral LD50 of 500 to 5000 mg/kg) [159]. This group of drugs, in particular, are important as they could be of value for human testing in *Acanthamoeba* infection and possibly repurposing them in AK and GAE. Recently our published study has shown that a drug-related to this class, promethazine exerts amoebistatic and amoebicidal effects in *Acanthamoeba* trophozoites in doses as low as 62.5-100 µg/ml. [Baig AM, 2019h, [157]].

Of the drugs tested initially in high doses (250-500 µg/ml), in subsequent studies and later by LDH release assays (Figure 27), it was shown that the selected drugs (Table-4) exhibited amoebicidal effects in *A. castellanii* trophozoites in the lower doses.

3.9.2 Summary

Drugs used in *in vitro* assays in *A. castellanii* have multiple known molecular targets in humans (Figure 10), but one feature that is common to most of them is that they directly or indirectly were seen to influence the Ca^{2+} ion concentration in *A. castellanii*. The selection of drugs (Table 4) that are already approved by drug regulating agencies and target the Ca^{2+} homeostatic pathways was made. The data presented in the experiments indicate distinct evidence of the Ca^{2+} ion homeostasis regulating VGCCs and proteins like CaM in *A. castellanii* as potential drug targets that can be exploited to obtain amoebicidal, amoebistatic, and cysticidal effects. Proteins expressed in form of receptors coupled with Ca^{2+} channels like mAChR are also important druggable targets as antagonizing them proved to be amoebicidal and amoebistatic in *A. castellanii*. Also, deprivation of extra-cellular Ca^{2+} ion by EDTA and pirenixine in our studies has proven to be amoebicidal in trophozoites of *A. castellanii*.

3.9.3 Aims Achieved:

The aims of our studies, as mentioned in chapter-1, that were achieved by the published experimental work in a series of papers are listed below:

1. Targeting the Ca^{2+} homeostasis in *Acanthamoeba* spp. by drugs already in use for non-infectious diseases produced amoebicidal, amoebistatic, and cysticidal effects in the trophozoite and cystic forms of *A. castellanii* respectively.
2. Drugs that are known Ca^{2+} blockers in humans and directly inhibit the VGCC in human cells proved to be amoebistatic, amoebicidal, and cysticidal in *A. castellanii* trophozoites in a dose-dependent manner.

**Experimental Assays, immunostaining, ELISA, colorimetric analysis,
FACS analysis and DNA staining.**

3. Immunostaining in *A. castellanii* showed that it expresses human-like muscarinic receptors and VGCC in the trophozoite forms, which when antagonized, by FDA approved antagonistic drugs of these proteins exhibited amoebicidal and amoebistatic effects.
4. Drugs that are known to target Ca^{+2} homeostasis indirectly in humans induced dose-dependent necrotic and apoptotic forms of cell death in *A. castellanii*.

4 Identification of drug targets: Bioinformatic computational tools and drug docking predictions

4.1 Introduction:

The identification of molecular drug targets in a microbe involves a diverse range of methodologies as detailed in the chapter-1. The use of bioinformatics computational tools in druggable targets have played a fundamental role in the repurposing of drugs and novel target discovery in microbes [102, 103]. As the knowledge of the molecular basis of biological systems evolves, the tools for storing and analyzing the data on molecular targets have amplified as well. The methodologies include a ligand-based and a structure-based approach (Figure-7). With the availability of diverse compound databases, this cost-effective structure-based or ligand-based strategy has significantly increased the efficiency of drug discovery and provide promising avenues to conquer life-threatening diseases. In the last decades, three-dimensional structures for over 50,000 proteins have been deposited in the Protein Data Bank (PDB) [178]. Concerning antiparasitic drugs, various well-established protein targets have had their structures solved, either by X-ray crystallography or NMR methods. Additionally, knowledge obtained from the parasite genome databases has been modeled using experimentally determined structures as templates [109-111]. The structural information of proteins obtained from these genome database repositories has opened the avenue to engage screening projects, to determine protein targets in specific parasites like *A. castellanii*. The availability of information on the genome, transcriptome, and proteome of *A. castellanii* available in online databases enabled the next step in our studies, which was to identify the drug targets hypothesized in *A. castellanii* (aims detailed in the chapter-1). The prediction and exploration of the molecular targets of drugs used in *A. castellanii* trophozoites were based on the prior knowledge of the molecular targets [101, 159] of the drugs in humans

Identification of drug targets: Bioinformatic computational tools and drug docking predictions

(Table-5) that had shown *in vitro* amoebistatic, amoebicidal and cysticidal effects in *A. castellani* (as detailed in chapter-3). Genomic, proteomic, and transcriptome information coupled with the use of bioinformatics computational tools can be an enormous source to investigate the expression of molecular drug targets. Bioinformatics encompasses a diverse range of computational tools to facilitate sequence alignment and homology modeling (Figure-7), database design and data mining, macromolecular geometry, construction of the phylogenetic tree, protein function prediction, gene discovery, and expression data clustering [144]. The methodological approach and tools used in drug target discovery in our studies are detailed in length in the methodology section (chapter-2) which was designed to achieve the aims like a)- Identification of a primitive protein homolog (by BLASTp) of the molecular target of the drugs tested in experimental assays. b)- Build template-based models of the *Acanthamoeba* protein identified as a drug target homolog in BLASTp searches and spot amino acid sequence similarities in the ligand-binding pockets between model and template developed for *Acanthamoeba* proteins, c)- Predict the docking of the drugs tested in experiments on to the templates developed for *A. castellanii* proteins. As based on the evolutionary distance that exists between human and *Acanthamoeba* spp., the proteins encoded in *Acanthamoeba* were expected to have differences in chain length and amino acids sequences (except for the ligand/drug binding orthosteric sites), a ligand-based homology modeling to determine amino acid similarity in the orthosteric ligand/drug binding site was considered to be cardinal to explain the drug effects seen in the *in vitro* tests (detailed below).

Identification of drug targets: Bioinformatic computational tools and drug docking predictions

Table 5: Published papers on human-like receptors and proteins targeted *in vitro* by drugs in *Acanthamoeba* trophozoites and cysts.
[++++: 80-95%, +++ 60- 75%, ++, 50-55%]

Drugs	Target receptors and proteins in Humans	Approval status	Effects in <i>Acanthamoeba</i>	Year of Publication
<ul style="list-style-type: none"> • Amlodipine 	VGCCs, CA,	FDA approved	Amoebicidal ++++	Baig AM, 2013 (Targets hypothesized)
<ul style="list-style-type: none"> • Loperamide 	TPC1, CaM, Opioid receptors	FDA approved	Amoebicidal++ (cysticidal ++ loperamide-amlodipine)	Baig AM, 2017a
<ul style="list-style-type: none"> • Gabapentin 	VGCC: alpha2/delta1		Amoebicidal+++	Baig AM, 2019b
<ul style="list-style-type: none"> • Chlorpromazine 	Multiple GPCRs	FDA approved	Amoebicidal +++	Schuster, F - 1984 (targets not reported)
<ul style="list-style-type: none"> • Procyclidine • Prochlorperazine • Haloperidol • Atropine 	<div style="border-left: 1px solid black; border-right: 1px solid black; padding: 5px; margin-left: 20px;"> mAChRs, mAChRs, CaM, alpha-adrenergic, D2, mAChRs, </div>		Amoebicidal+++	Baig AM, 2013-14
			/ (cysticidal ++ prochlorperazine)	Baig AM, 2017b
				Baig AM, 2019
<ul style="list-style-type: none"> • Digoxin 	Na-K ATPase,	FDA approved	Amoebicidal +++	Baig AM, 2016
<ul style="list-style-type: none"> • Promethazine 	mAChRs, 5HTalpha-adrenergic, D2, CaM, histaminergic	FDA approved	Amoebicidal +++	Baig AM, 2019
<ul style="list-style-type: none"> • Amiodarone 	K- channel, Na-channel, ergosterol synthase	FDA approved	Amoebicidal ++	Baig AM, 2017d

Identification of drug targets: Bioinformatic computational tools and drug docking predictions

<ul style="list-style-type: none"> • Apomorphine 	D2-agonist 5HT-antagonist	FDA approved	Amoebistatic ++	Baig AM, 2013
<ul style="list-style-type: none"> • Nifedipine • Verapamil • Diltiazem 	VGCCs, L-type, N-type, and P/Q -type	FDA approved	Amoebicidal +++ Cysticidal +	Baig AM, 2019j
<ul style="list-style-type: none"> • EDTA • Pirenoxine 	Ca ²⁺ Ions – chelators	FDA approved	Amoebistatic +++/Amoebicidal ++	Baig AM 2019i
<ul style="list-style-type: none"> • Acetazolamide 	Carbonic anhydrase and AQP inhibitor	FDA approved	Amoebistatic++	Baig AM, <i>et al.</i> 2019b
<ul style="list-style-type: none"> • Etoposide, Doxorubicin 	Intrinsic apoptosis adaptor proteins like cytochrome-c	FDA approved	Programmed cell death: Apoptosis	Baig AM, 2017e

4.2 Materials and Methods

The bioinformatics computational tools that were used in the published studies to identify potentially druggable targets in *A. castellanii* include a combination of methodologies (detailed in Chapter-2, section-2) to provide the evidence of possible drug targets in *A. castellanii*. The sequence of known molecular drug targets in humans of the drugs tested in *A. castellanii* (Table-5- 2nd column) were downloaded from National Center for Biotechnology Information (NCBI) [138] and UniProt [143]. The sequence of these proteins was searched for a homolog (evolutionarily related protein) in the *A. castellani* genome by selecting *Acanthamoeba* as the target organism using the BLASTp tool. Sequence similarity estimations were aimed to establish the possibility for sequence homology that has possibly existed during eukaryotic evolution. For the search of molecular drug targets in *Acanthamoeba castellanii*, proteins in *Acanthamoeba* spp. that had attributes (protein family, GPCR, and Ca²⁺

Identification of drug targets: Bioinformatic computational tools and drug docking predictions

binding attributes) similar to human drug targets were selected and investigated for sequence similarities, ligand binding prediction, homology modeling, and drug docking predictions. The *A. castellanii* genome sequences databases that are freely available at The NCBI [138], UniProt [143], EBI Europe [179], DDBJ japan [180], AmoebaDB.org [181] were accessed to retrieve the genomics, transcriptomics, and proteomics data of *Acanthamoeba* trophozoites. Proteins with transcript identities ACA1_xxxxxx (x denotes a six-digit unique identity) were downloaded from the AmoebaDB.org database for comparison with similar proteins in humans. Homology modeling was performed for *Acanthamoeba* protein that was found to be homologs of human proteins drug targets for determining unique attributes of amino acid sequence and orientation in the drug binding pockets between the proteins compared. Rectangular cladograms and circular (sunbursts) trees using NJ method were constructed to show the distribution of the protein drug targets in the eukaryotic time-line. Finally, molecular modeling softwares was used to predict the docking of the drugs (Table-5) on the templates developed for the *Acanthamoeba* proteins.

4.3 The Transcriptome of *Acanthamoeba castellanii* trophozoites.

4.3.1 Evidence of mRNA encoding drug target proteins in *Acanthamoeba* spp.

ACA1_167020, ACA1_092610, and ACA1_270170 are *Acanthamoeba* proteins with attributes of calcium ion-channel, ion-transport and evolutionarily belong to the family from which human VGCC has possibly evolved [Baig AM, 2017d [141]] were reported to be possible drug targets of loperamide, amlodipine, gabapentin [Baig AM, 2019d, [146]], [Baig AM, 2017h, [141]]. The percentages of mRNA encoding these proteins were retrieved from AmoebaDB.org (Fig 32-top row). This was done to analyze the active expression and ranking of expression for this

Identification of drug targets: Bioinformatic computational tools and drug docking predictions

gene compared to all other genes expressed in *A. castellanii*. mRNA encoding the ACA1_167020 and ACA1_092610 showed around 75% and 65% expression while ACA1_270170 exhibited below 50% of mRNA expression [Baig AM, 2019d, [146]], (Figure 32 -left to right: top row). *Acanthamoeba* ACA1_366720 is a putative CaM and like human CaM is composed of 149 amino acids. This protein and its orthologs in *A. castellanii* like ACA1_280720 were hypothesized to be the target of drugs like loperamide [Baig AM, 2017d [141]], prochlorperazine [Baig AM, 2013, [134]] and promethazine [Baig AM, 2019h [181]]. The mRNA encoding ACA1_280720 and ACA1_366720 showed above 85% and 65% of the mRNA encoding these proteins in the transcriptomic database of *Acanthamoeba castellanii* trophozoites [175] (Figure 32, 4th from the left in the top row).

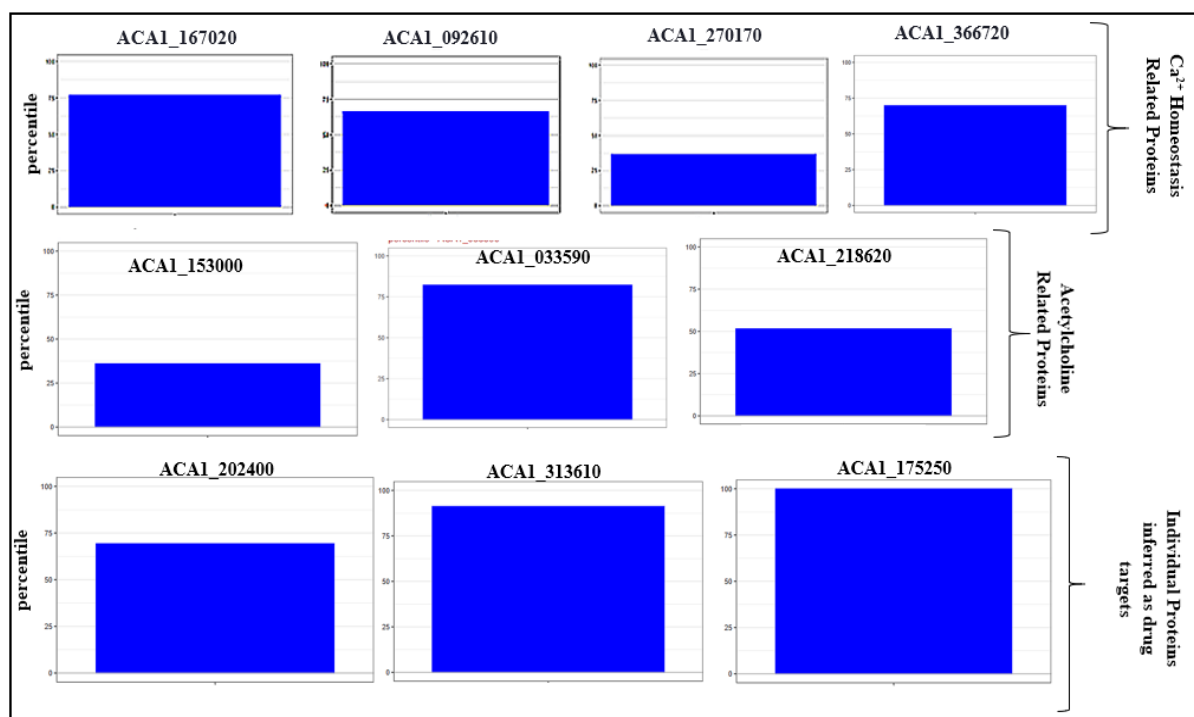


Figure 30. Transcriptomics of human-like proteins that were hypothesized as drug targets in *Acanthamoeba* trophozoites.

Identification of drug targets: Bioinformatic computational tools and drug docking predictions

The percentile graph shows the ranking of expression for genes of *Acanthamoeba* proteins that are related to Ca²⁺ homeostasis (top-row), cholinergic receptor and pathways (middle-row), and targets indirectly affecting Ca²⁺ ions (bottom row) compared to all other genes expressed in *A. castellanii*. [Adapted from Baig AM, 2019d [182]].

4.4 Induction of CaM gene expression in *A. castellanii*

Reverse transcription-polymerase chain reaction (RT-PCR) with Real-time polymerase chain reaction (qPCR) were done for measuring mRNA encodings and cloning CaM from human cells, we thought it would be exciting to test the same in *Acanthamoeba* spp. by using primers prepared against human CaM nucleotides in WBCs and prostate cancer cells. We surprisingly found that the primers prepared to synthesize cDNA of CaM from human WBCs and human cancer cell nucleotides (mRNA) of (PC-3, DU145 cells) were also able to induce the synthesis of the CaM in *Acanthamoeba castellanii* T4 genotype (Figure 31). The similarities of *Acanthamoeba castellanii* mRNA against the forward and reverse primers are shown (Figure 31 A) and detailed in the methodology section (chapter-2). With a total of 13 and 11 identical positions in the forward primer and reverse primer respectively, the cDNA formed was able to induce the synthesis of CaM in *A. castellanii* (Figure 31 B1-B2) and fold difference in CaM expression in the target gene was normalized to β -actin relative to the expression at time zero (Figure 33 B2). A near-identical sequence similarity (85.3%) between human CALM-1 (NP_008819.1) and *Acanthamoeba* putative CaM (ACA1_366720)

Identification of drug targets: Bioinformatic computational tools and drug docking predictions

yellow star-B2) alone and along with Trifluoperazine (TFP) are shown that binds CALM 1 (green lines, without stars). Fold difference in CaM expression in the target gene was normalized to β -actin relative to the expression at time zero. PCR cycles performed with ambient airflow to maintain temperature and relative fluorescent units (RFU) are shown (B2) [Unpublished data Method described in Chapter-2 Page # 51]

4.5 mRNA encoding human-like cholinergic enzymes and mAChR like proteins

The *Acanthamoeba castellanii* hypothetical protein (GenBank ID: ACA1_153000: Uniprot-ID; L8HIA6) was hypothesized to be a human acetylcholine binding mAChR1-like protein, a target of drugs like muscarinic antagonists [Baig AM, 2017a, [149]]. The expression of mRNA encoding this protein (Figure 30, the first histogram in 2nd row) and human-like choline acetyltransferase and cholinesterase (Figure 30, last two histograms in 2nd row) that are involved in acetylcholine (ACh) synthesis were also retrieved [Baig AM, 2018 a, [160]] (Figure 30, 2nd row).

4.6 mRNA encoding K-channels, Na-K ATPase, and cytochrome -C

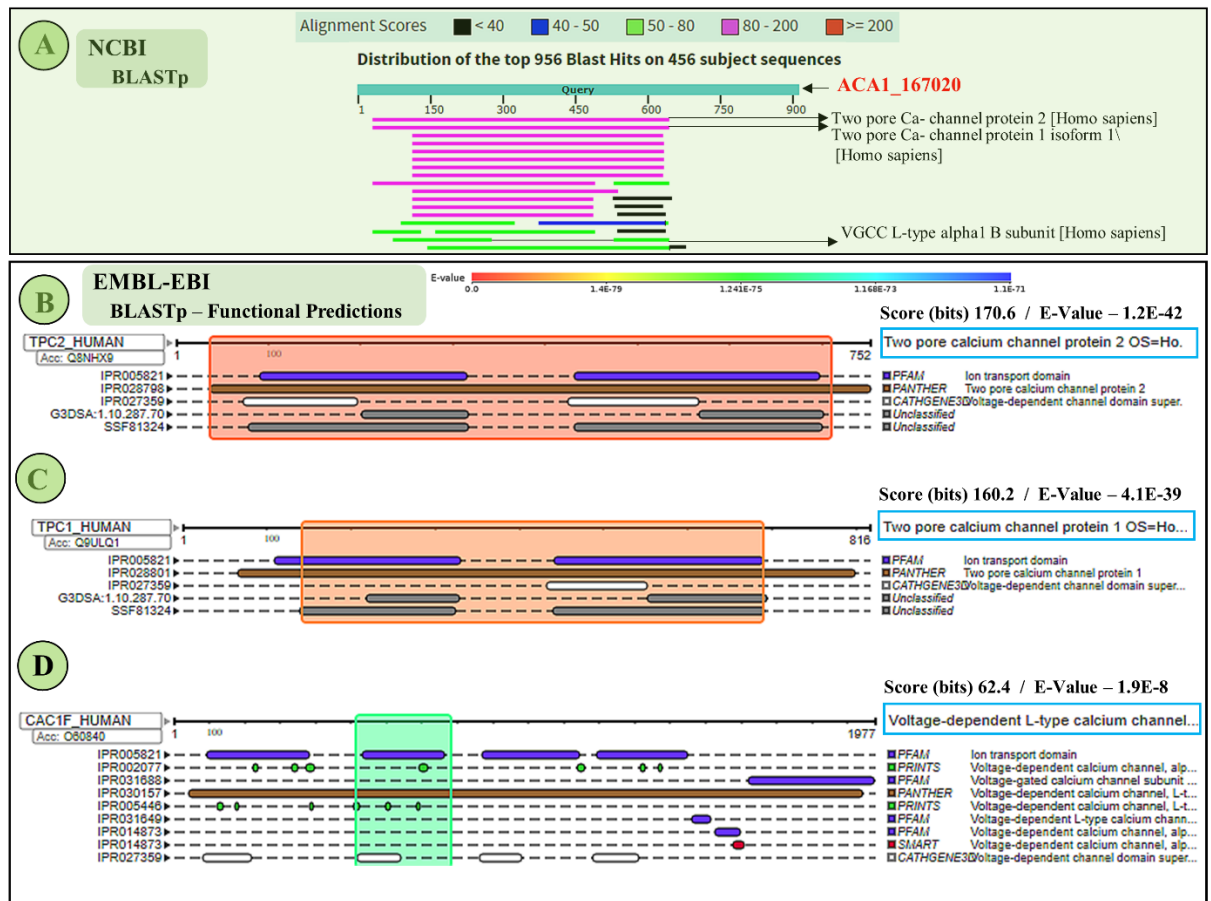
In our studies done *in vitro*, *Acanthamoeba castellanii* trophozoites exhibited susceptibility to drugs like amiodarone [Baig AM, 2017e [142]] (targets human K-channels-Irk), digoxin [Baig AM, 2016b [161]] (inhibits Na-K-ATPase), and intrinsic apoptosis-inducing drugs (inducing cytochrome-c release) like doxorubicin and loperamide [Baig AM, 2017 [141, 161]]. The mRNA encoding the above proteins in *Acanthamoeba castellanii* (Figure 30-bottom row) were retrieved from AmoebaDB.org to estimate their expression levels.

Identification of drug targets: Bioinformatic computational tools and drug docking predictions

4.7 BLASTp results and phylogenetics of human-like drug targets in *A. castellanii*.

4.7.1 Identification of Human-like VGCC and CaM in *Acanthamoeba castellanii*.

The target proteins inhibited by loperamide, amlodipine, nifedipine, verapamil, and gabapentin include diverse types of human VGCCs (Table 5). The protein sequence of human VGCCs like two-pore (TPC), human-L-type1.1/, alpha-2/delta1, and 1.2, P/Q type 2.1 were searched (detailed in chapter-2) for proteins with sequence similarities in *Acanthamoeba* genome databases to identify VGCCs like targets in *A. castellanii*. The



Identification of drug targets: Bioinformatic computational tools and drug docking predictions

BLASTp search showed *Acanthamoeba* ACA1_092610, ACA1_270170, and ACA1_167020 to have sequence similarities with human VGCCs. The

Figure 32. BLASTp results of *Acanthamoeba* protein ACA1_167020.

(A) The alignment scores of ACA1_167020 by BLASTp search in NCBI. (B-D) BLASTp results show functional annotation, sequence identification, and homologs (highlighted blue boxes -right panel) with scores, and e-values (shown above the highlighted boxes). BLASTp results show human TPC1, TPC2, and CAC1F VGCC as homologs of *Acanthamoeba* ACA1_167020 [Adapted from Baig AM, 2017d [141]]

BLASTp results showed its sequence similarities with human TPC-1, TPC-2, and VGCC of L-type (Figure 32). The protein sequence alignment scores of ACA1_167020 BLASTp in NCBI and EMBL-EBI BLASTp results against five to nine databases are shown (Figure 32 B-D). The ACA1_167020 gene showed two conserved domains for Ion-trans family protein (Figure 33 A) and its evolutionary associations with human VGCCs as shown in the phylogenetic tree and the sunburst developed by MSA in NCBI and Pfam database (Figure 33 B, C).

Identification of drug targets: Bioinformatic computational tools and drug docking predictions

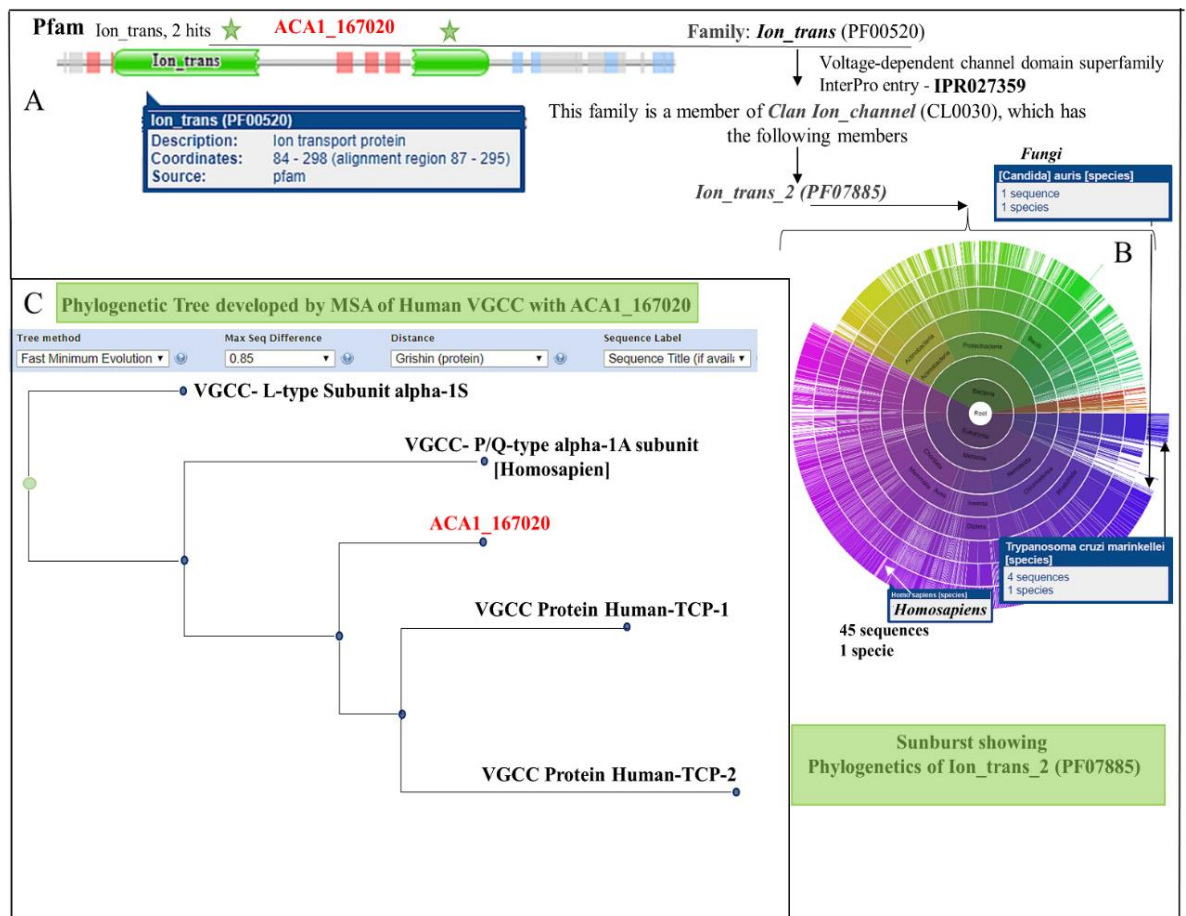


Figure 33. Highlights of the Ion-trans domain in the ACA1_167020 gene and its phylogenetics.

(A) The ACA1_167020 gene has two Ion_trans domains (green stars-A). (B) The VGCC superfamily in the Pfam database (using NJ method) showed Ion_trans_2 as a member of the Clan Ion channel (CL0030) from which the VGCCs are derived and are shown to be distributed across prokaryotes (right panel: green color in sunburst), fungi, unicellular eukaryotes and humans (purple color in sunburst with a white arrowhead at the margin). (C) Phylogenetic neighbor-joining (NJ) method (left-panel) showed the two-pore channel (TPC1 and TPC-2) type human VGCC and ACA1_167020 to share a common ancestor (3rd internal node from the left). [Adapted from Baig AM, 2017d [141]].

The *Acanthamoeba* protein ACA1_092610 is an EF-hand domain-containing protein with a calcium-binding domain [181]. The sequence of this protein on a BLASTp search showed similarities of these proteins

Identification of drug targets: Bioinformatic computational tools and drug docking predictions

with human diverse types of human VGCCs (Figure 34). The protein sequence alignment scores of ACA1_092610 BLASTp in NCBI (Figure 34 A) and EMBL-EBI automated servers (Figure 34 B-D)

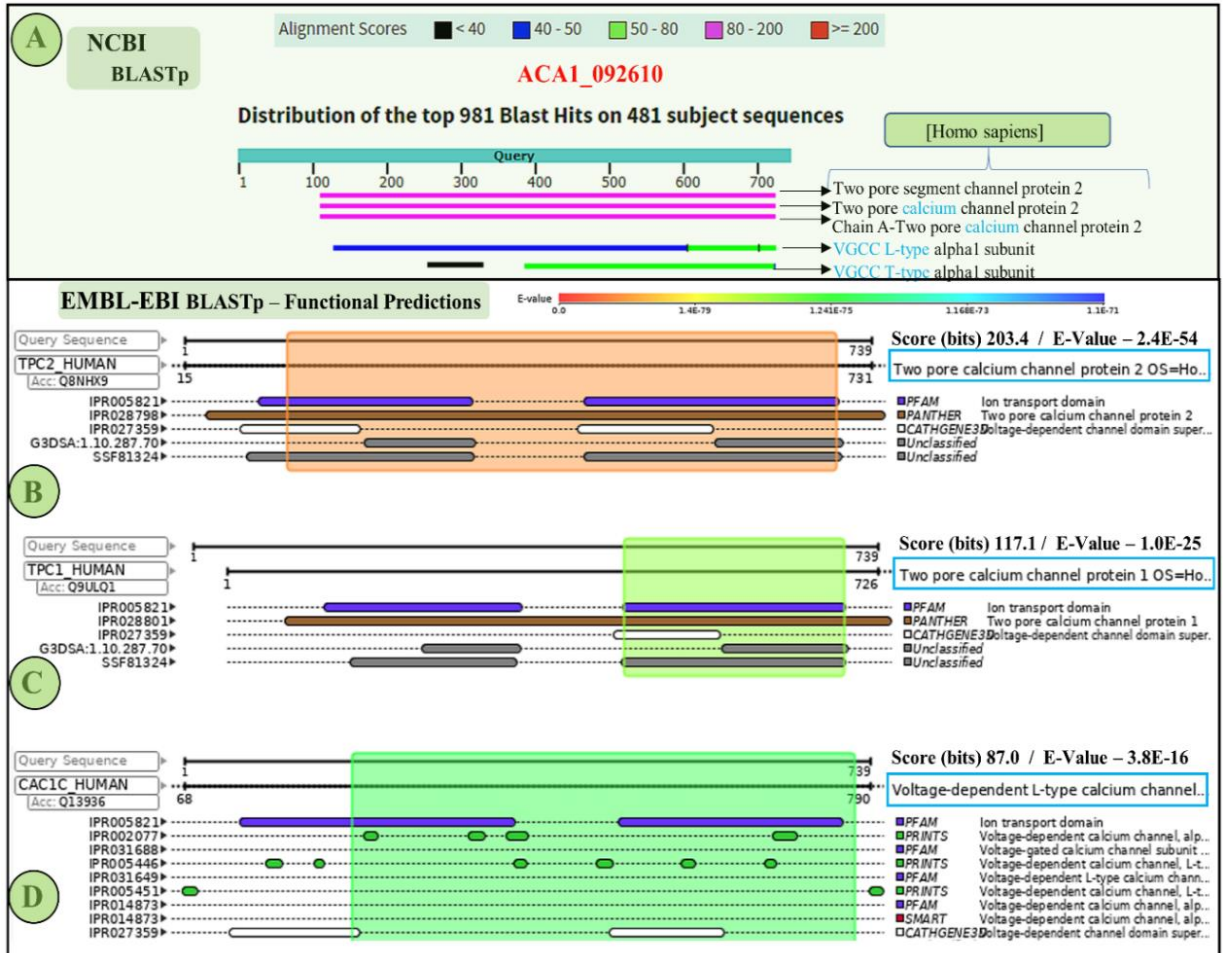
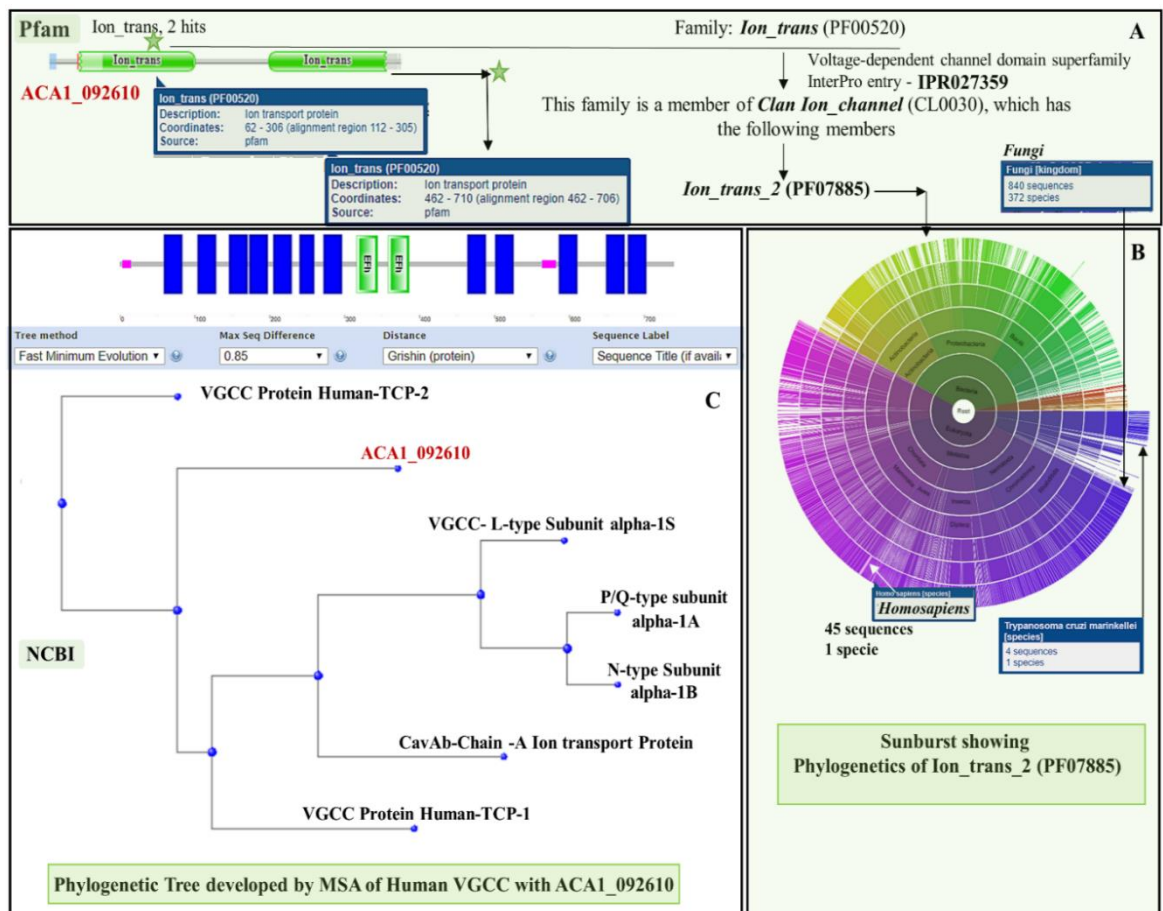


Figure 34. BLASTp results of ACA1_092610

(A) The alignment scores of *Acanthamoeba* protein ACA1_092610 by BLASTp search. (B-D) BLASTp results (rows with colored bars) show sequence identification, functional annotation, and homologs (highlighted blue boxes - the right panel) with scores, and e-values (shown above the highlighted blue boxes). BLASTp generated human TPC1, TPC2, and L-type human VGCC as homologs of *Acanthamoeba* protein ACA1_092610 [Adapted from Baig AM, [141, 146]]

Identification of drug targets: Bioinformatic computational tools and drug docking predictions

against five to nine databases to find regions of sequence similarity generated functional and evolutionary features resembling human VGCCs. ACA1_092610 the sequence showed human-like VGCCs like family domains with significant scores and e-values in BLASTp results (Figure 34 B, C, D). The ACA1_092610 gene showed two conserved domains for Ion-trans family protein (Figure 35 A-top panel) and its evolutionary associations and attributes like human VGCCs as shown in the phylogenetic tree and sunburst developed by MSA in NCBI and Pfam database (Figure 35 B, C). Ion-trans-2 family protein and the VGCC derived from this family are distributed across species as shown in sunbursts generated in the Pfam database (Figure 35 right panel).



Identification of drug targets: Bioinformatic computational tools and drug docking predictions

Figure 35. Evolutionary distribution of the lon-trans 2 domain in ACA1_092610.

(A) The ACA1_092610 gene has two lon_trans domains (green stars). (B) The evolutionary origins of a VGCC superfamily developed in the Pfam database (using JN-method), showed lon_trans_2 as a member of the Clan lon channel (CL0030) from which VGCCs are derived and reported to be distributed across prokaryotes (right panel: green color in sunburst), fungi, early uncharacterized eukaryotes and humans (purple color in sunburst with a white arrowhead at the margin). (C) The rooted rectangular cladogram server (left-panel) shows protein ACA1_092610 to share a common ancestor with various types of known human VGCCs (second internal node from the left). Phylogenetic neighbor-joining (NJ) method showed rooted rectangular cladogram showing the origins and distribution of human two-pore VGCC -2 (TPC-2) and *Acanthamoeba* VGCC-like protein ACA1_092610 can be traced back to a common ancestor (node at the extreme left) [Adapted from Baig AM, 2017, 2019 [141, 146]]

Another *Acanthamoeba* protein, ACA1_270170 on the BLASTp search showed a similarity of this protein with alpha-2/delta1 VGCCs (Figure 36-bottom). The BLASTp results (Figure 36 A, C, rows) by fetching data from five to nine linked databases to show the functional and evolutionary clues towards its structure and function which resembles human VGCC. ACA1_270170 sequence showed human-like alpha-2/delta-1 VGCCs domain (Figure 36 C). The ACA1_270170 gene showed conserved domains for alpha-2/delta-1 (Figure 36-purple segment with annotation) and its distribution across species as shown in the sunburst (circular tree format) developed in the Pfam database server (Figure 36 C). Pairwise alignment of the ACA1_270170 protein sequence with human alpha-2/delta-1 showed identical Ca-binding sites (Figure 36 A-small black arrows) in both protein sequences.

Identification of drug targets: Bioinformatic computational tools and drug docking predictions

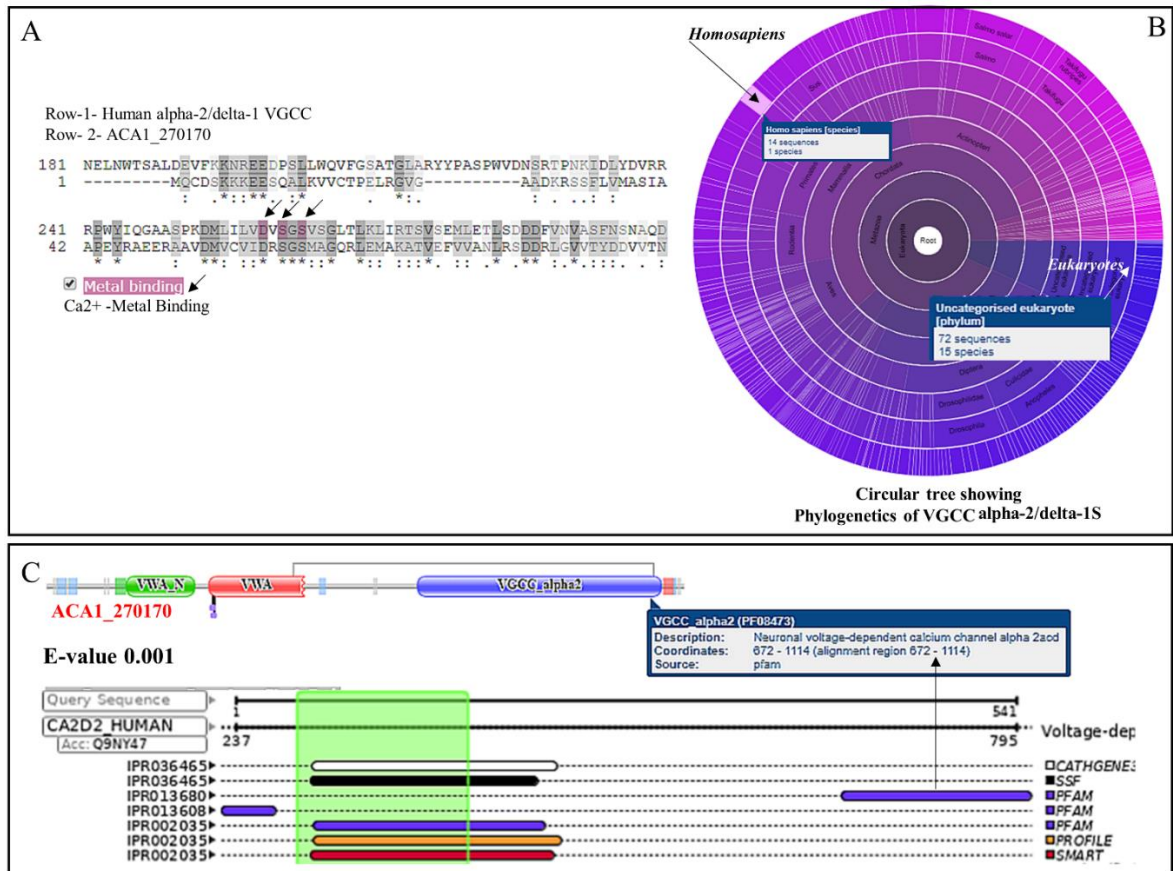


Figure 36. BLASTp results and distribution of VGCC alpha2/delta1 across species.

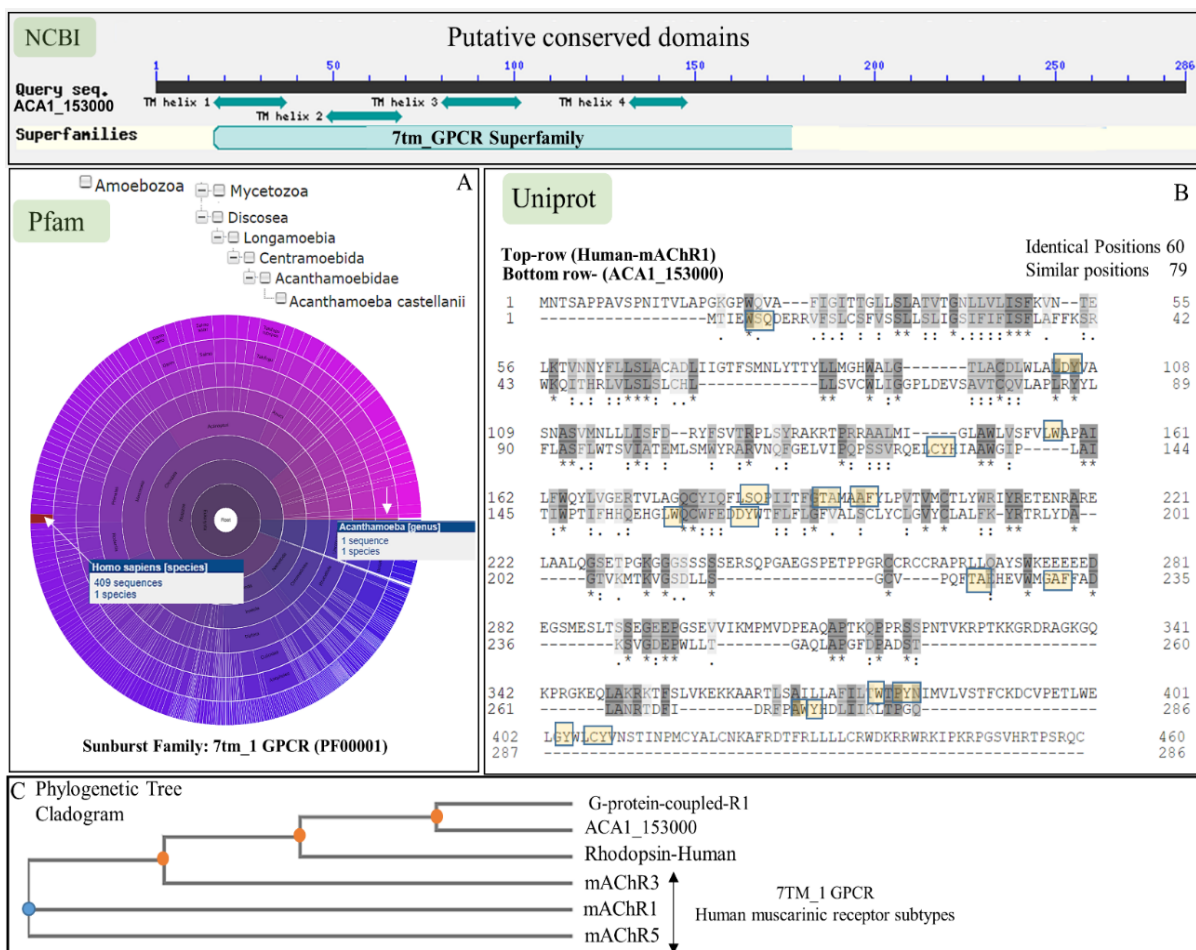
(A) Sequence alignment showing identical amino acids in calcium-binding residues between human alpha2/delta1 VGCC and ACA1_270170. (B) The Pfam automated server using an NJ method, shows a circular tree (sunburst) showing the distribution of alpha2/delta1 protein family across species from unicellular eukaryotes (white arrow) to humans (black arrow) (C) BLASTp results showed functional annotation of VGCC alpha-2 with an e-value of 0.001 for ACA1_270170 [Adapted from Baig AM, 2019d [146]].

Acanthamoeba protein ACA1_366720 is a putative CaM in *Acanthamoeba* spp. Phylogenetics and BLASTp results of CaM showed this EF- Hand 7 protein to be evolutionarily conserved across species (Figure 37 B) and a sequence identity of 85.3% with human CaM

Identification of drug targets: Bioinformatic computational tools and drug docking predictions

4.7.2 Identification of cholinergic ligand-receptor organizations in *Acanthamoeba castellanii*.

The *Acanthamoeba* protein ACA1_153000 like a human- muscarinic receptors mAChR showed putative conserved domain of 7tm_GPCR superfamily (Figure 38, NCBI-top) and in the Pfam database (Figure 38 A), circular tree developed clued towards its evolutionary links to the Rhodopsin family (a family to which mAChR belongs) (Figure 38-A) and 7tm_1 GPCR. MSA of ACA1_153000 with mAChRs, human GPCR-1/3, and Rhodopsin receptor with the development of a phylogenetic tree showed its evolutionary links with the 7tm_1 GPCR family (Figure 38 C).



Identification of drug targets: Bioinformatic computational tools and drug docking predictions

Figure 38. BLASTp results, sequence alignments, and Phylogenetic of ACA1_153000.

Acanthamoeba ACA_153000 gene has conserved domains for 7tm_GPCR superfamily protein as shown in data retrieved from NCBI BLASTp (top panel) and shown in a circular tree (sunburst) (A). 69 identical positions were shown on Clustal Omega sequence alignment of human mAChR1 and ACA_153000 (B). A rectangular cladogram generated showed the common ancestral origin of human mAChR3 and ACA1_153000 (first orange internal node from the left) (C). MSA using Clustal Omega in Uniprot automated server and phylogenetic tree using the NJ method showed *Acanthamoeba castellanii* has a single sequence (ACA_153000) of 7tm_GPCR family that like human mAChRs and Rhodopsin can be traced back to a common node [Adapted from Baig AM, 2017a [149]].

On sequence alignment, ACA1_15300 protein with human mAChR1(Figure 38 B), 69 identical positions were seen, but the sequence identity percentage was low.

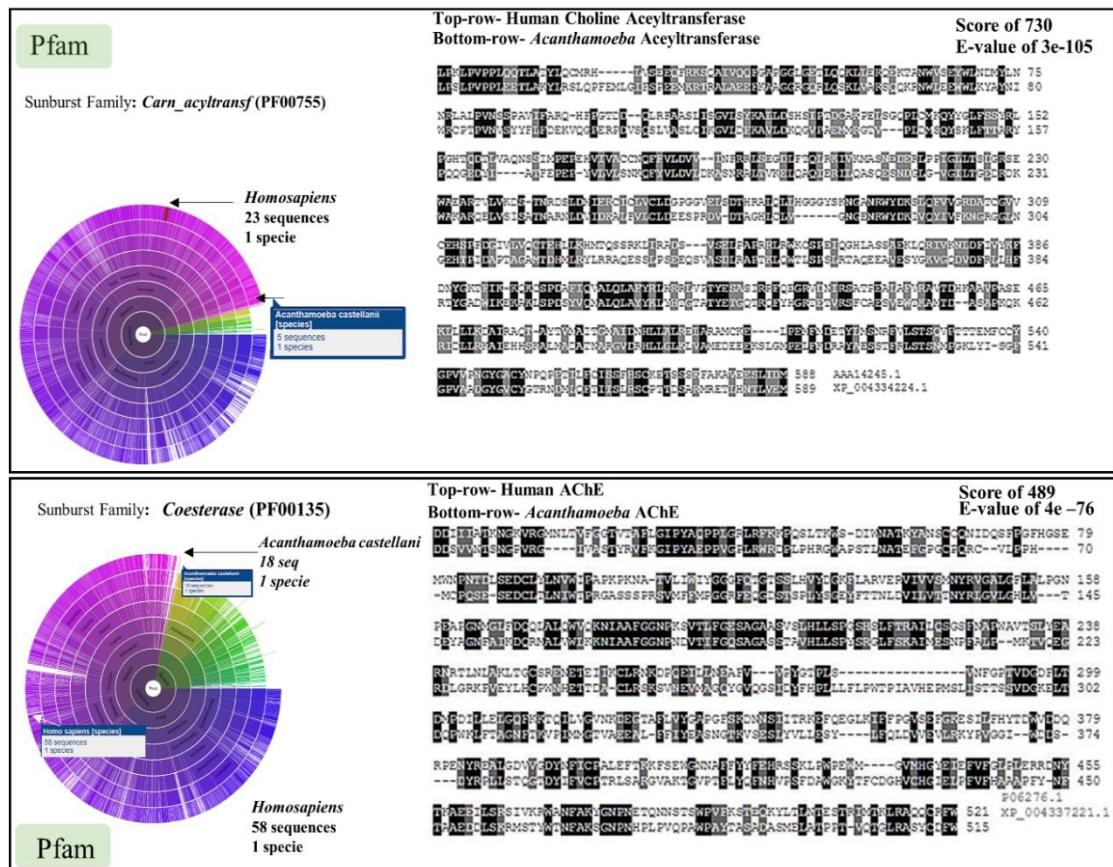


Figure 39. Sequence alignments of human and *Acanthamoeba* enzymes.

Acanthamoeba and human choline-carnitine acetyltransferase (top-panel) and cholinesterase (bottom-panel) were compared by sequence alignments using Clustal Omega in Uniprot automated server showed them to be homologs. The distribution of the enzymes across species is shown in Pfam using the neighbor- NJ method generated circular trees (left side both panel). Note the significant BLASTp scores and e-values for the enzymes acetyltransferases (top-panel) and cholinesterases (bottom-panel). **[Adapted from Baig AM, 2018a [160]].**

Two cardinal human enzymes cholinesterase and cholinesterase have homologs in *Acanthamoeba* spp. BLASTp results for human choline acetyltransferase and cholinesterase showed a homolog for each enzyme in *Acanthamoeba castellanii* with significant score and e-values (Figure 39-top-right both panels). Phylogenetic sunburst developed for the choline acetyltransferases (Figure 39-top panel) and cholinesterases protein family (Figure 39-bottom panel) distribution across species.

Identification of drug targets: Bioinformatic computational tools and drug docking predictions

(A) MSA between human lanosterol synthase, ACA1_108830 cycloartenol synthase, and lanosterol synthase of *T.cruzi* showed identical active and binding sites (top-panel). (B) A rectangular cladogram shows the evolutionary origins of ACA1_108830 cycloartenol synthase, human and *T.cruzi* lanosterol synthase (blue nodes and branches). (C) BLASTp identified ACA108830 and human lanosterol synthase to be homologs (bottom panel) **[Adapted from Baig AM, 2017e[142]]**

As Amiodarone has been shown previously to target lanosterol synthase in *Trypanosoma cruzi* [183], it was hypothesized that the presence of a similar enzyme in *Acanthamoeba* spp. could have contributed to the amoebicidal effects reported in our studies. BLASTp results showed a lanosterol synthase-like protein both in *Acanthamoeba* (ACA1_108830) and the human genome (accession # P48449). MSA of the enzyme from three species showed the proteins exhibit similar binding and active sites (Figure 41, top-panel green-red highlights). The phylogenetic tree using the NJ method constructed by the NCBI automated server showed an evolutionary distribution of lanosterol synthase across species (Figure 41 middle panel). BLASTp showed ACA1_108830 to be near identical to human and *T.cruzi* enzymes (Figure 41-bottom panel).

Digoxin is a drug that is known to target Na-K ATPase in human cells. BLASTp search for the presence of a homolog protein in *Acanthamoeba* spp. fetched ACA1_313610 as a match for human Na-K ATPase with 30% sequence identities, higher scores, and an e-value of 1e-120. (Figure 42 A). The human gene for Na-K ATPase has a cation ATPase domain (Figure 42, A-green circle). BLASTp results of *Acanthamoeba* ACA1_313610 showed human Na-K ATPase as a match with a score of 1012 and an e-value of 1e-120. A circular tree showing the distribution of the cation ATPase domain of human Na-K ATPase showed its origins in prokaryotes (Figure.42 C-green), humans, and *Acanthamoeba* spp (Figure 42 C – inserts with arrows)

Identification of drug targets: Bioinformatic computational tools and drug docking predictions

inhibitory effects in trophozoites of *Acanthamoeba* spp. and a homolog of this human enzyme was searched in the *Acanthamoeba* database. Our results show an amoebal carbonic hydratase on MSA with diverse CA expressed in human cells has in a common proton acceptor site (Figure 43- A-red arrow). Phylogenetic tree as rectangular cladogram (Figure 43- C) and sunburst (Figure 43-B) of *Carb_anhydrase* family across species show the encoding of this protein in humans and early unicellular eukaryotes like *Acanthamoeba* spp.

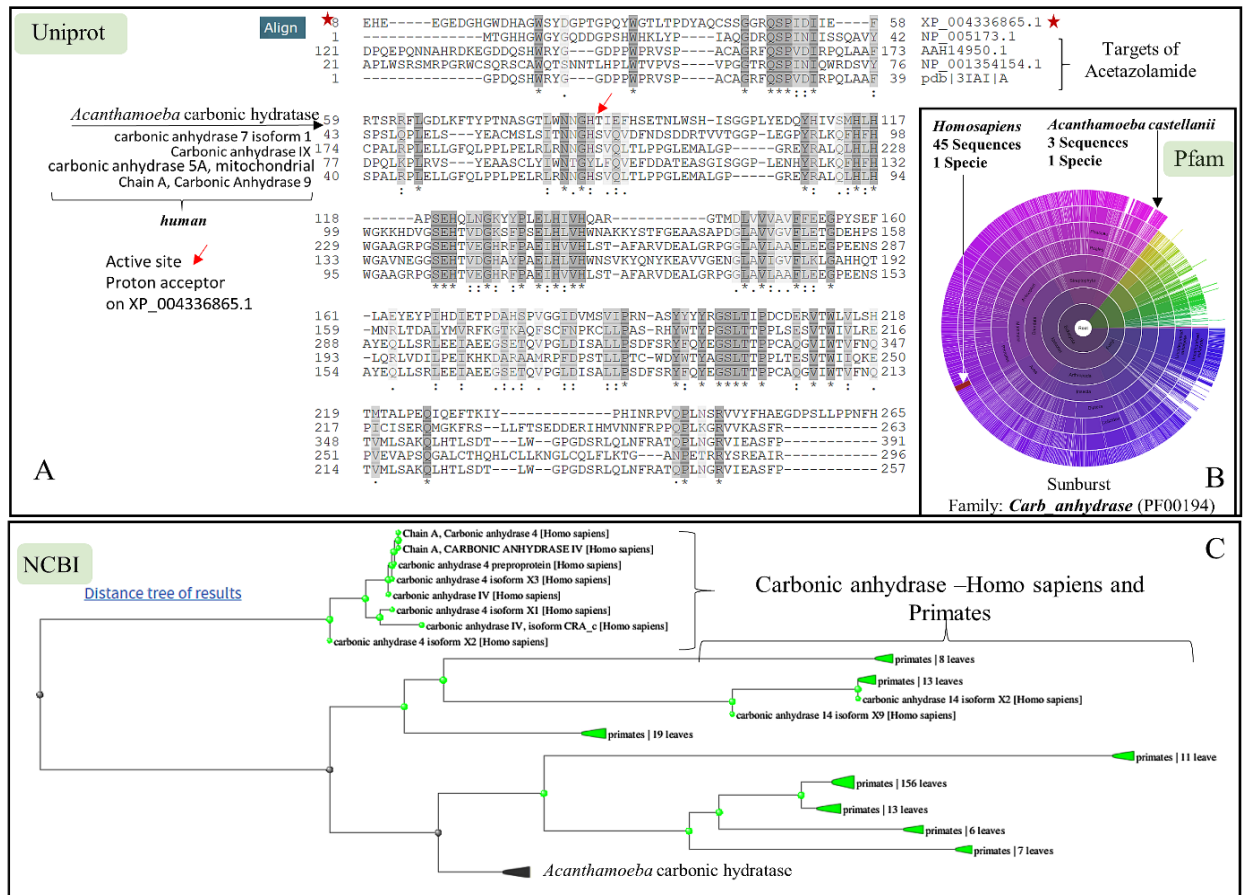


Figure 43. MSA of *Acanthamoeba* carbonic hydratase and its evolutionary origins.

(A) *Acanthamoeba* carbonic hydratase on MSA with diverse carbonic anhydrases expressed in humans showed a common proton acceptor site (A). circular tree sunburst (B) and rooted rectangular cladogram (C) of the *Carb_anhydrase* family across species constructed using the NJ method show its expression in humans (B-white arrow). [Adapted from Baig AM, 2018d [147]].

Identification of drug targets: Bioinformatic computational tools and drug docking predictions

4.8 Homology Modeling :

Homology modeling for *Acanthamoeba* proteins that were hypothesized as drug targets were expected to clarify the effects of the drugs that were observed and confirm the finding of the BLASTp results and functional prediction made for the ACA1 proteins as mentioned in the previous section (above).

4.8.1 Human-like VGCC and CaM in *Acanthamoeba castellanii*

The automated SWISS-MODEL web server homology modeling tool was used for the construction of template-based models for ACA1_167020 as detailed in chapter 2. Template-based models of human VGCC L-type (Figure 44-A) and model of human TPC-1(Figure 44-B) were retrieved that showed identical ligand binding amino acid residues between the model and template.

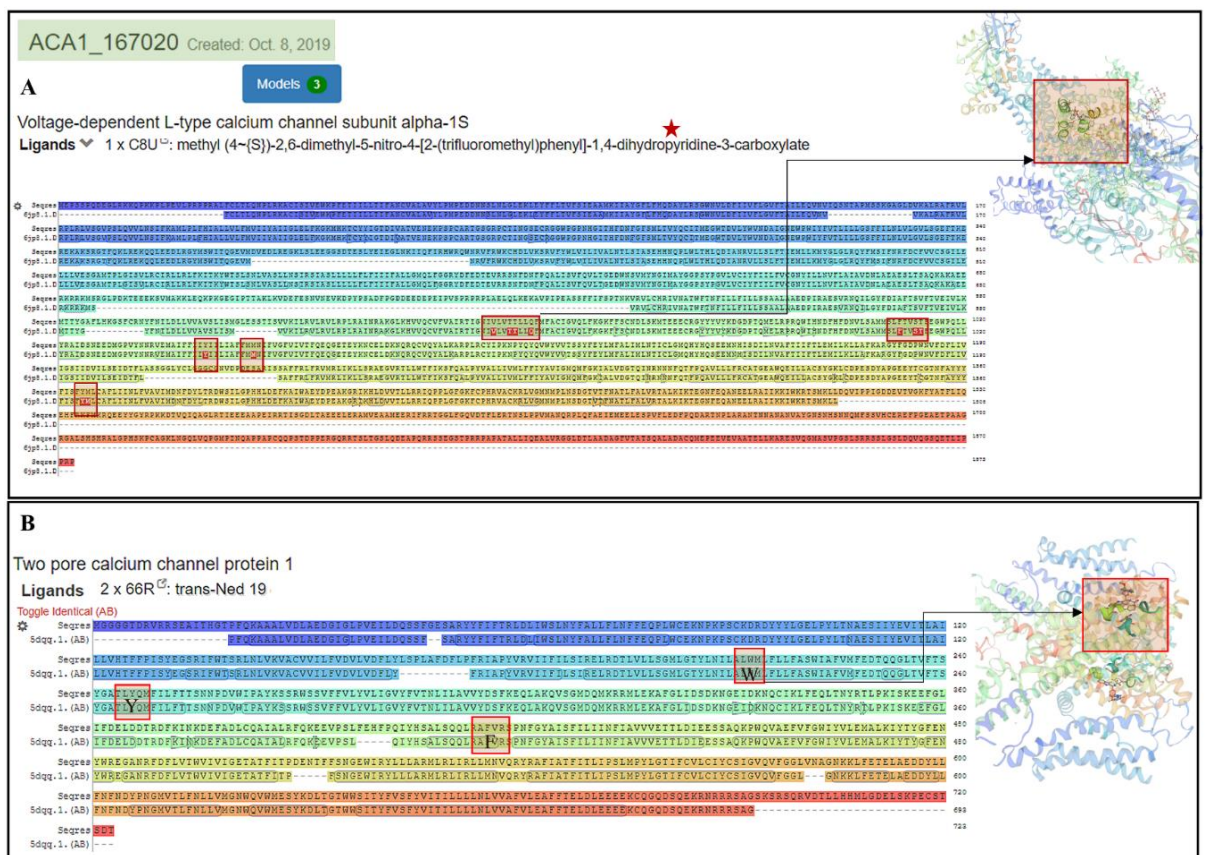


**Figure 45. Models developed for *Acanthamoeba* protein
ACA1_092610.**

(A-B) Three models of TPC1, TPC2, and L-type VGCC developed for ACA1_092610 in the SWISS-MODEL automated server using templates 5dqq.1A, 5jp8.1 D, and 6nq0.1 A respectively. The sequence identities and coverage of model-template amino acids are shown. (B) Model-template alignment for human TPC-2 (colored rows -B) show identical amino acid residues (encircled in the rows) for ligand (EUJ) binding between a template for ACA1_092610 (bottom row) and the model (top-row). A binding site for EUJ in the model is shown in a rainbow (C) which corresponds to the amino acid residues enclosed in a rectangle in colored rows. **[Adapted from Baig AM, 2017d, 2019d [141, 146]].**

Acanthamoeba protein ACA1_270170 on homology modeling developed a template (6jp5.1C)-based model (Figure 46- model in ribbons at the left) of human VGCC 1.1. The alpha-2/delta1 is a component of the human L-type VGCC 1.1 (highlighted in the next two ribboned models within rectangles). Sequence alignments show identical NAG (Figure 46 pink circles) and Ca²⁺ ion binding sites (Figure 46 grey circles) in the template and model.

Identification of drug targets: Bioinformatic computational tools and drug docking predictions

CaM retrieved is shown (Figure 47-top right ribbon). The model and template showed identical ligand (Ca^{2+}) binding amino acid residues (Figure 47 pink rectangles – bottom rows) which are also shown in the transparent model (Figure 47 top-right).

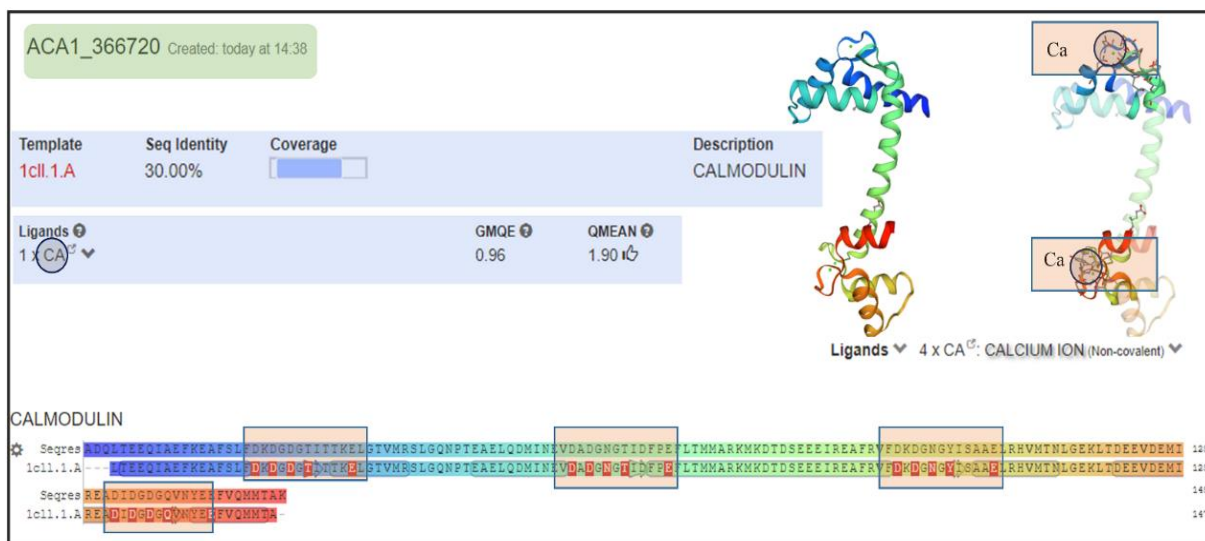


Figure 47. Homology modeling of ACA1_366720 a putative CaM in *A. castellanii*

The homology modeling for the ACA1_366720 developed template (1c1l.1.A)-based model of human CaM. This model was developed with 30% sequence identities. The model (top colored row) and template (bottom colored row) show identical ligand (Ca^{2+}) binding amino acid residues (highlighted in the boxed area). [Adapted from Baig AM, 2017d [141]]

4.8.2 Evidence of human-like muscarinic receptor and cholinergic enzymes in *A. castellanii*.

We had shown earlier that like human mAChR1 the ACA1_153000 has a 7tm conserved domain and had a phylogenetic relation to mAChRs (Figure 38). On homology modeling, ACA1_153000 developed a template-(5cxv.1) based model (Figure 50- full-colored ribbon A1) of human mAChR1 with ACh orthosteric antagonist Triotropium (OHK) bound to (Figure 48- A2-transparent model at right) it. Both the template and the

Identification of drug targets: Bioinformatic computational tools and drug docking predictions

model show identical amino acid residues (Figure 48-highlighted amino acid residues in rows) that engage tiotropium shown in the model (Figure 48 A3).

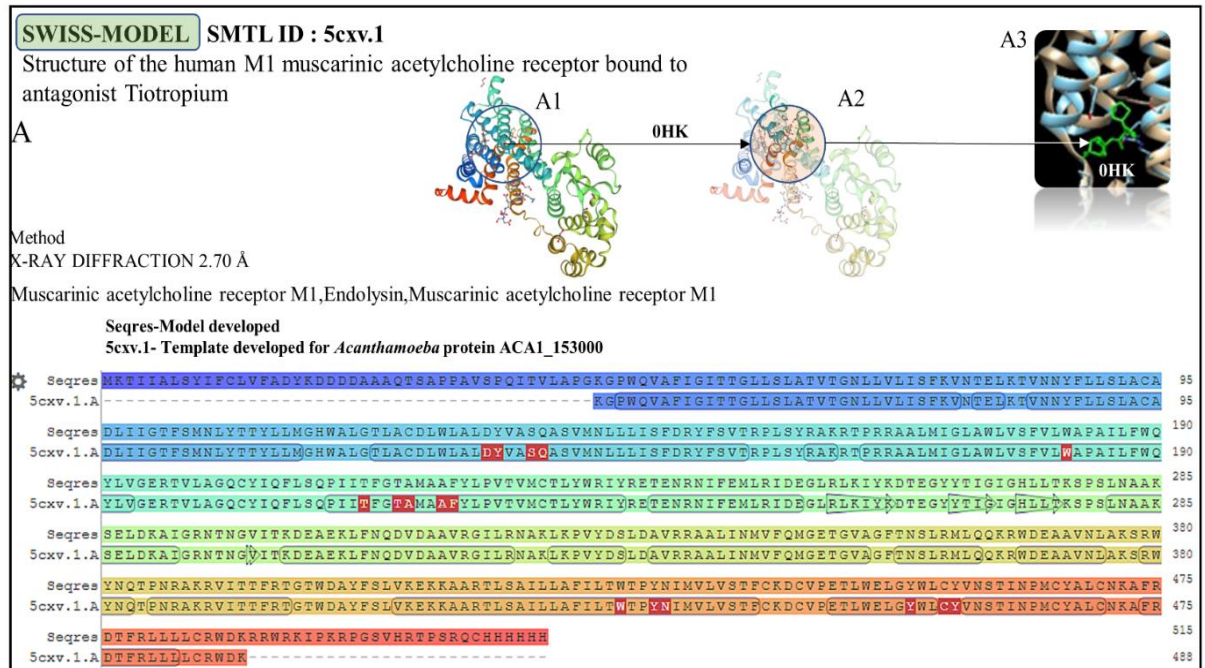


Figure 48. Homology modeling of *Acanthamoeba* protein ACA1_153000.

(A) Template-based model for ACA1_153000 constructed in the SWISS-MODEL server. The template 5cxv.1 (A) was selected to build the model of human-mAChR1 (A1-A2). The model (top colored row of the aligned sequence) and template (bottom colored row of the aligned sequence) showed identical amino acid residues (highlighted in rows) that engage an antagonist Tiotropium (OHK). The model of human mAChR1 is shown where ACh binds as an orthosteric agonist and Tiotropium OHK as an antagonist (A3). [Adapted from Baig AM, 2017a [149]]

Identification of drug targets: Bioinformatic computational tools and drug docking predictions

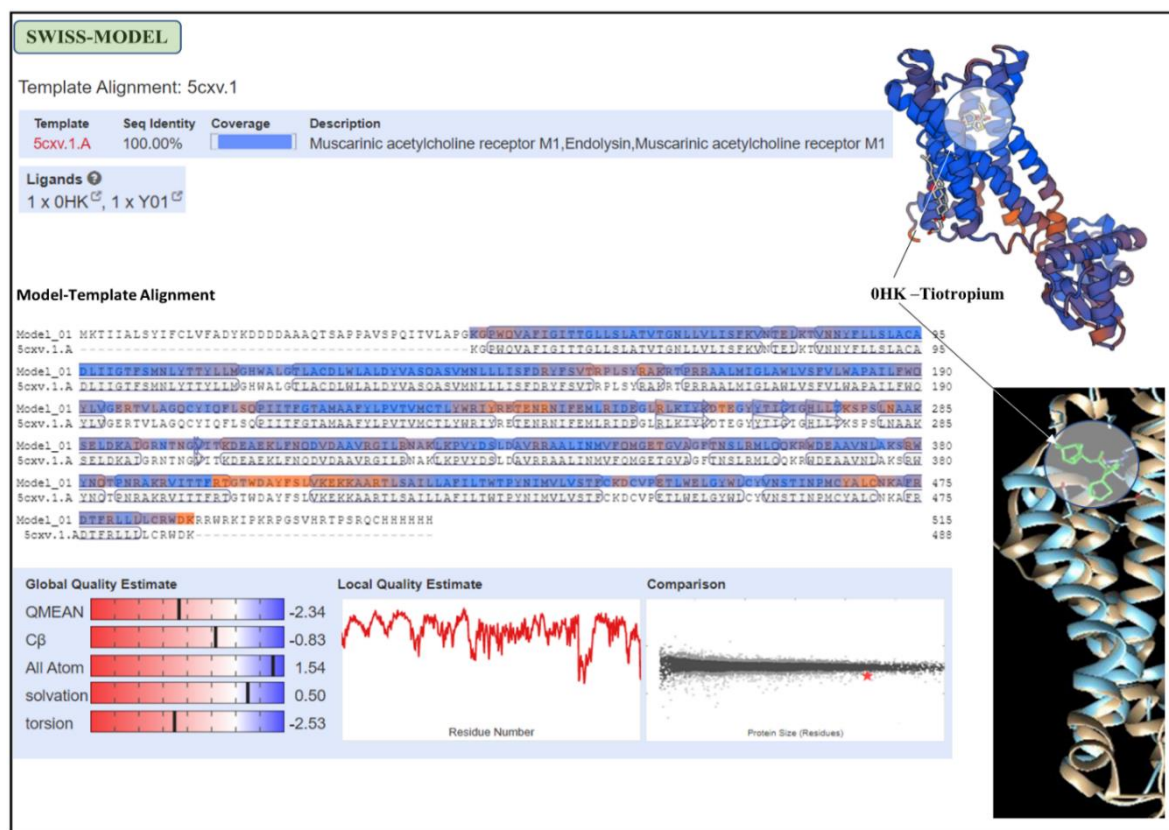


Figure 49. Alignment of the Model and template developed for ACA1_15300 hypothetical protein.

The amino acid residues between the model (human mAChR1) and the template generated for ACA1_153000 showed 100% sequence identities. The OHK- Tiotropium docking is shown (top-right). The model-template alignment is shown in colored rows. The global and local quality estimates with comparison are shown (bottom panel), model template ribbon overlap with docked tiotropium is shown on the left side. [Adapted from Baig AM, 2017a [149]].

The human mAChR1(model) and template 5cxv.1(for amoebal protein ACA1_153000) on sequence alignment (Figure 49-middle panel) showed identical amino acid residues needed for drug docking. The QMEAN, local quality estimate, and comparison are shown (Figure 49 bottom panel). A template model overlap (Figure 49-right panel) shows the similarity between the proteins human mAChR1 and the template 5cxv.1 in the drug tiotropium docking site.

Identification of drug targets: Bioinformatic computational tools and drug docking predictions

the model and template for ligand binding as also shown in the model (B2) [Adapted from Baig AM, 2018a, [160]]

4.8.3 Human-like K-Channels in *Acanthamoeba castellanii*

The homology modeling of ACA1_202400 developed a template (4kfm.1)-based model of G-Protein activated human inward rectifier K-channel (Figure 51-A). The model (Figure 51 A-top row of the colored sequence) template (Figure 51 A-bottom row of the colored sequence) showed identical amino acid residues engaged in binding 4 K ions (Figure 51 A1-A2-solid and transparent ribbon models). Also shown is the model (B1) template (B2) overlap (B3) that shows the degree of structural similarity between the model and template developed for ACA1_202400.

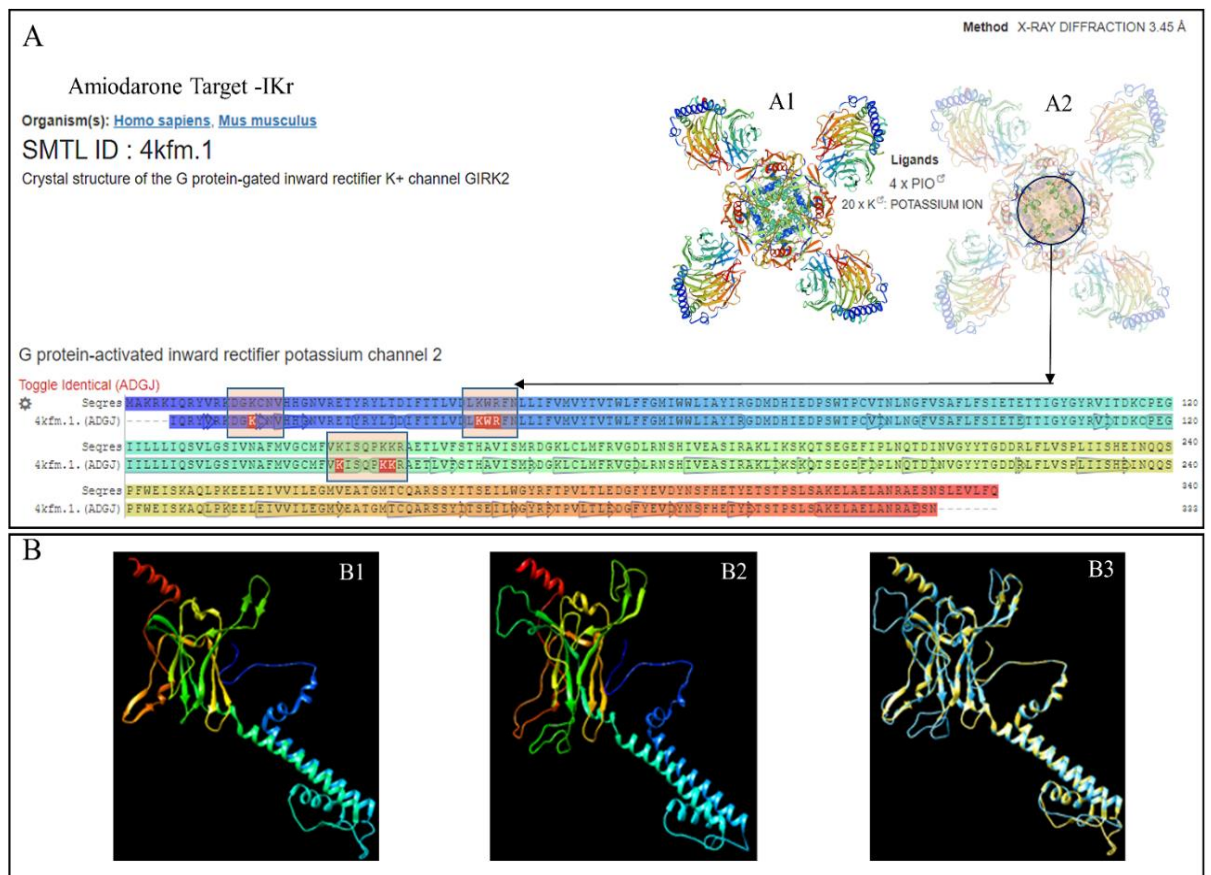


Figure 51. Homology modeling of *Acanthamoeba* ACA1_202400 K⁺ channel protein.

(A1) SWISS-MODEL homology modeling automated server developed a model of human G-protein gated inward rectifier K-channel protein for the *Acanthamoeba* ACA1_202400 K⁺ channel protein. Ligand binding residues (boxed in rows) showed identical amino acids between the model (A- top colored row) and template (A- bottom colored row) and identical position (arrows) in the model (A2 top-right). (B). Shown are a model (B1), template (B2), and their overlap (B3). [Adapted from Baig AM, 2017e [142]].

4.8.4 Human-like Na-K ATPase in *Acanthamoeba castellanii*

Of the ion-channels and protein pumps inhibited by drugs used *in vitro*, digoxin is known to inhibit human Na⁺-K⁺ ATPase [101, 159]. Homology modeling of ACA1_313610 developed a template (4xe5.1)-based model of mammalian Na⁺-K⁺ ATPase (Figure 52 A). Binding of digoxin and similar Na⁺-K⁺ ATPase inhibiting drugs bufalin and ouabain to the crystal structure of the mammalian Na⁺-K⁺ ATPase is shown (Figure 52, A1, A2, A3) with highlighted areas between model and template that bind digoxin and bufalin (Figure 52, B-orange boxes) as shown in the cutout segments (Figure 52- C).

Identification of drug targets: Bioinformatic computational tools and drug docking predictions

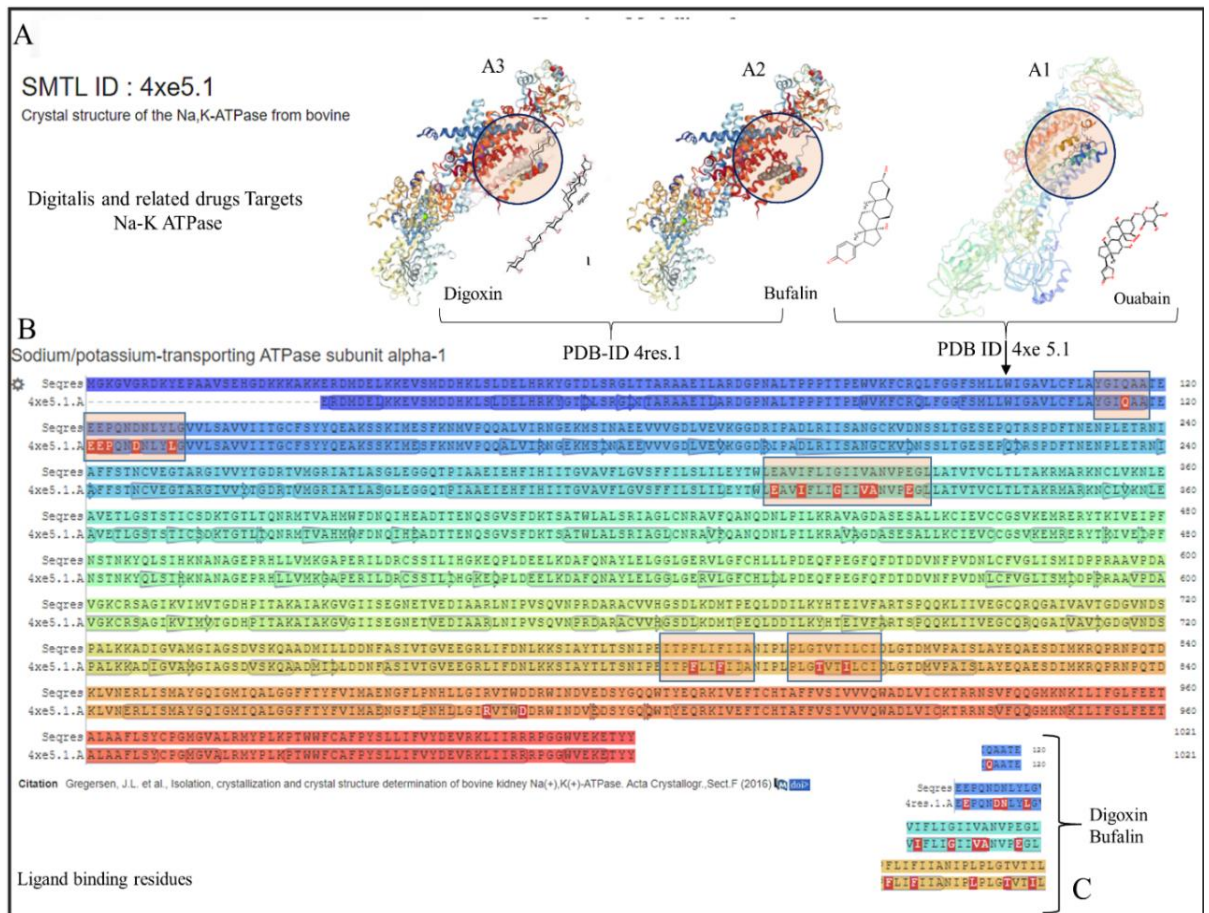


Figure 52. Homology modeling of *Acanthamoeba* protein ACA1_313610.

(A) Homology modeling of ACA1_313610 in the SWISS-MODEL automated web server developed a template (4xe5.1)-based model of mammalian (bovine) Na-K ATPase. The binding of drugs like digoxin, bufalin, and ouabain to the crystal structure of the mammalian Na⁺-K⁺ ATPase is shown (A1, A2, A3). (B) The highlighted areas between model and template that bind digoxin and bufalin (B-orange boxes in colored sequences) and cut out segments (C). [Adapted from Baig AM, 2016b [161]]

Identification of drug targets: Bioinformatic computational tools and drug docking predictions

4.8.5 Human-like Carbonic anhydrase and Aquaporins in *Acanthamoeba castellanii*

Homology modeling of amoebal ACA1_130470 which was found to be a homolog of human carbonic anhydrase was performed to study ligand binding attributes of the template for ACA1_130470 and model generated for this protein. A template (4X5S.1) -based model of carbonic anhydrase constructed in SWISS-MODEL server showed identical amino acid residues shown in sequences that engage the drug acetazolamide (Figure 53 A- highlighted and boxed in colored rows) and also highlighted in the models (Figure 53 A1 models on the right side).



**Figure 53. Homology modeling of *A. castellanii* carbonic anhydratase
and major intrinsic protein (MIP).**

(A) Amoebal carbonic anhydratase ACA1_130470 developed a template (4X5S.1) -based model of carbonic anhydrase that has identical amino acid residues (A- highlighted and boxed in between colored rows) that engage its inhibitor acetazolamide projected to model (A1). (B) *Acanthamoeba* major intrinsic protein on homology modeling developed a model (B1) of human AQP-1. The sequences of template and model are aligned (B-colored rows) with no ligand specified **[Adapted from Baig AM, 2018d [147]].**

Homology modeling on an *Acanthamoeba* major intrinsic protein (MIP) developed a template-based model of human Aquaporin-1 (AQP-1) (Figure 53 B1) with 32.86% sequence identities.

4.8.6 Human-like Cytochrome-c in *Acanthamoeba castellanii*

Programmed cell death that resembles apoptosis was hypothesized in *Acanthamoeba castellanii* that uses adapter proteins of intrinsic apoptotic pathways **[Baig AM 2017c, [164]]**. With homology modeling of *A. castellanii* ACA1_175250, a template with PDB ID 5exq.1 was used to develop the model of human cytochrome-C. On sequence alignment, the model showed identical amino acid residues with the template (Figure 54 bottom colored rows) that bind HEME as a ligand. The amino acid residues (highlighted in the boxed area) in the template that was developed, an identical area of ligand interaction in the model developed (Figure 54, top-right model with the encircled area) is shown.

Identification of drug targets: Bioinformatic computational tools and drug docking predictions

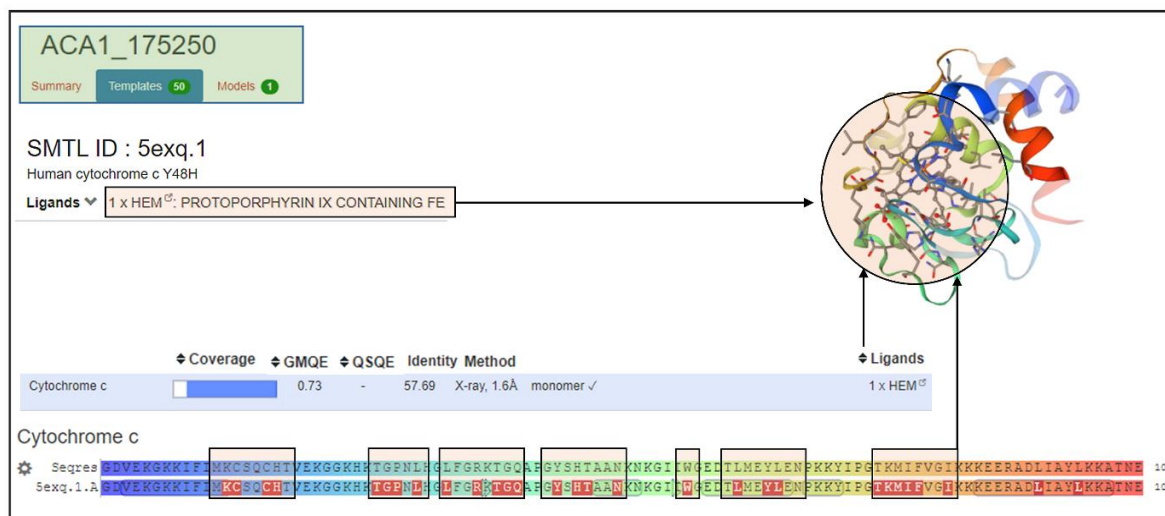


Figure 54. Homology modeling of *Acanthamoeba* ACA1_175250 cytochrome c, putative.

The SWISS-MODEL web server generated a template-based model of human cytochrome-c. The template with PDB ID 5exq.1 was used to develop the model of human cytochrome-c. The aligned sequences of the model (top row) with the template for ACA1_175250 (bottom row) showed identical amino acids residues (highlighted in the boxed area) that engage the ligand HEM (arrows pointed to the encircled areas in the model) [Adapted from Baig AM, 2017c [164]].

4.9 Results of Drug Docking Predictions:

4.9.1 Molecular Docking of Loperamide on templates generated for *A. castellanii* proteins

The drug docking prediction was performed to figure out if loperamide can dock on the hypothesized VGCCs in *Acanthamoeba* like protein ACA1_366720, ACA1_270170, and ACA1_167020. Loperamide showed induced-fit docking on the templates 3G43, 6NQ0, and 3BXK (Figure 55) which are PDB IDs for CaM, human TPC2, and P/Q type VGCC respectively. The scores, contact area, and atomic contact energy (ACE) for docking are also shown that clue towards the docking prediction of this drug to the templates developed for amoebal proteins.

Identification of drug targets: Bioinformatic computational tools and drug docking predictions

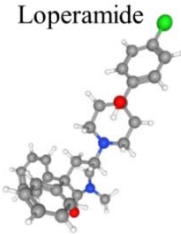
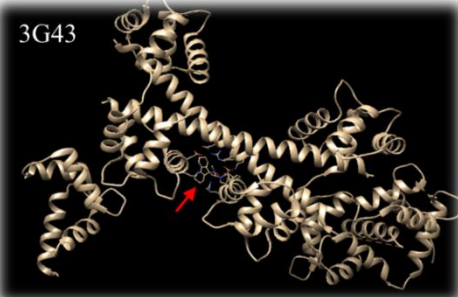
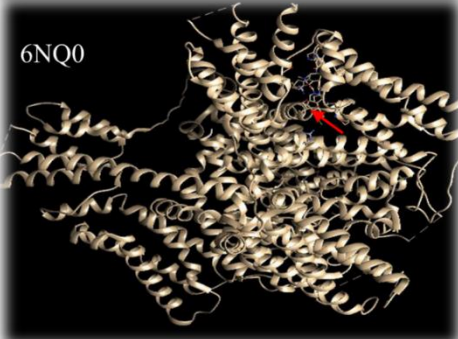
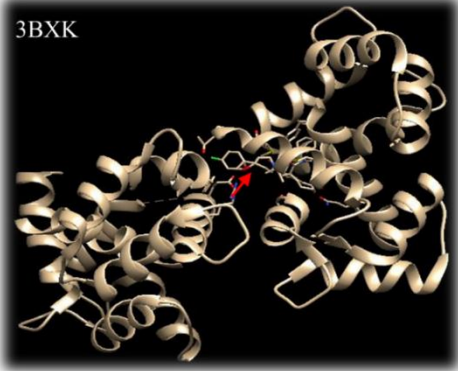
Molecular Docking		
Drug	Template build for <i>Acanthamoeba</i> proteins	Results
 Loperamide	Calmodulin-bound Cav1.2 3G43 	ACA1_366720 <ul style="list-style-type: none"> • Score: 6186 • Contact area: 770.40 • ACE: - 6.93
	Human TPCC2 ligand-bound 6NQ0 	ACA1_270170 <ul style="list-style-type: none"> • Score: 6432 • Contact area: 770.40 • ACE: - 5.33
	P/Q-type VGCC +CaM 3BXX 	ACA1_167020 <ul style="list-style-type: none"> • Score: 6338 • Contact area: 810.80 • ACE: - 191.10

Figure 55. Molecular docking of loperamide on the templates generated for *Acanthamoeba* proteins.

The PatchDock was used to dock loperamide on the SIWSS MODEL generated templates for ACA1_366720, ACA1_270170, and ACA1_167020. Loperamide is shown in an induced-fit configuration docked onto the templates. Scores, contact area, and ACE are shown under the result column. Scores were calculated based on atom-pairing frequencies and ACE values [Adapted from Baig AM, 2017d [141]]

4.9.2 Molecular docking of Amlodipine on templates generated for *Acanthamoeba* proteins.

Amlodipine is known to have multiple cellular drug targets in humans. PatchDock was used to dock amlodipine to templates developed for *Acanthamoeba* proteins as detailed above. Amlodipine showed docking on to the templates 5GJV, 3ML5, and 4FX5 (Figure 56). The scores, contact area, and ACE for docking are also shown that hint towards the probability of an induced-fit docking of this drug to the templates developed for amoebal proteins.

Identification of drug targets: Bioinformatic computational tools and drug docking predictions

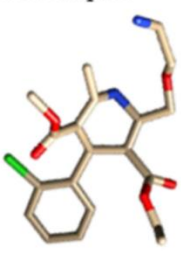
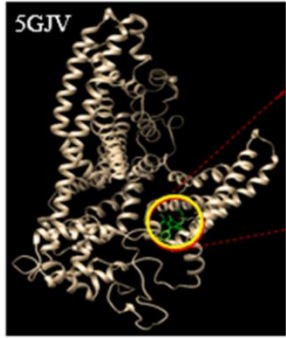
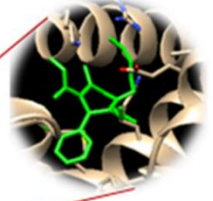
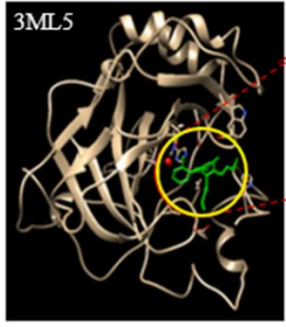
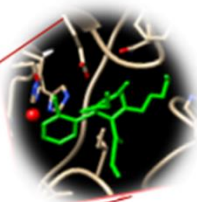
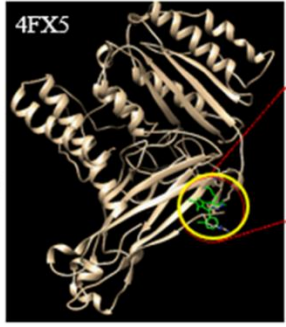
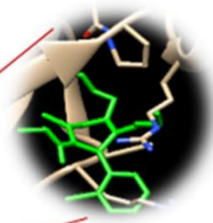
Molecular Docking		
Drug	Template build for <i>Acanthamoeba</i> proteins	Results
 Amlodipine	 5GJV ACAI_092610	 Score of 5490 Contact area:715 ACE -53.61
	 3ML5 ACAI_130470	 Score of 4510 Contact area:525.1 ACE -90.62
	 4FX5 ACAI_270170	 Score of 5584 Contact area:687 ACE -199.37

Figure 56. Molecular docking of amlodipine on templates generated for *Acanthamoeba* proteins.

The PatchDock was used to dock amlodipine on the SIWSS MODEL generated templates for ACA1_092610, ACA1_130470, and ACA1_270170. Amlodipine docked in an induced-fit configuration onto these templates. Scores, contact area, and ACE are shown under the result column. A four-digit score based on the ordered arrangement and atomic contact energy shows the docking probability of amlodipine on the templates [Adapted from Baig AM, 2019d [146]].

Identification of drug targets: Bioinformatic computational tools and drug docking predictions

4.9.3 Docking prediction of Atropine on templates generated for ACA1_153000

Template 5.cvx.1 was developed for *Acanthamoeba* protein ACA1_153000, The PatchDock predicted the docking of Atropine (an antimuscarinic agent that binds to human mAChRs) on the template 5cxv.1. A docking prediction of atropine on *Acanthamoeba* ACA1_153000 was obtained with a high score of 4762, a contact area of 556.80, and atomic contact energy (ACE) of -224.53 shows the induced-fit docking (Figure 57).

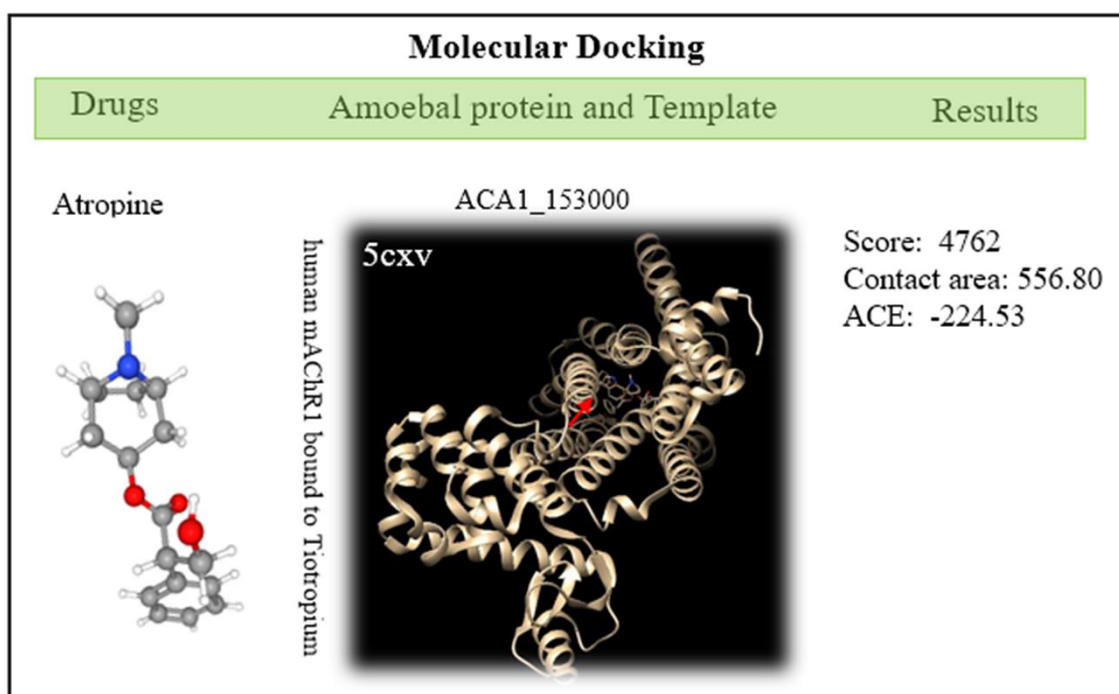


Figure 57. Molecular docking of atropine on a template for ACA1_153000.

The PatchDock was used to dock atropine on the SIWSS MODEL generated templates for ACA1_153000. Atropine (left-panel) docked onto the template 5cxv.1 (image with black background). Scores, contact area, and ACE are shown under the result column. A high, 4 digit score based on the geometric fit (contact area 556.80) and atomic contact energy (ACE -224.53) showed an induced-fit docking probability of atropine on the template 5cxv.1 [Adapted from Baig AM, 2017a [149]]

Identification of drug targets: Bioinformatic computational tools and drug docking predictions

4.9.4 Molecular docking prediction for Amiodarone on templates generated for *Acanthamoeba* proteins.

A VGCC like *Acanthamoeba* protein ACA1_092610, *Acanthamoeba* cycloartenol synthase (ACA1_108830), and KCN like ACA1_202400, showed docking prediction of amiodarone on the templates (Figure 58, in the center).

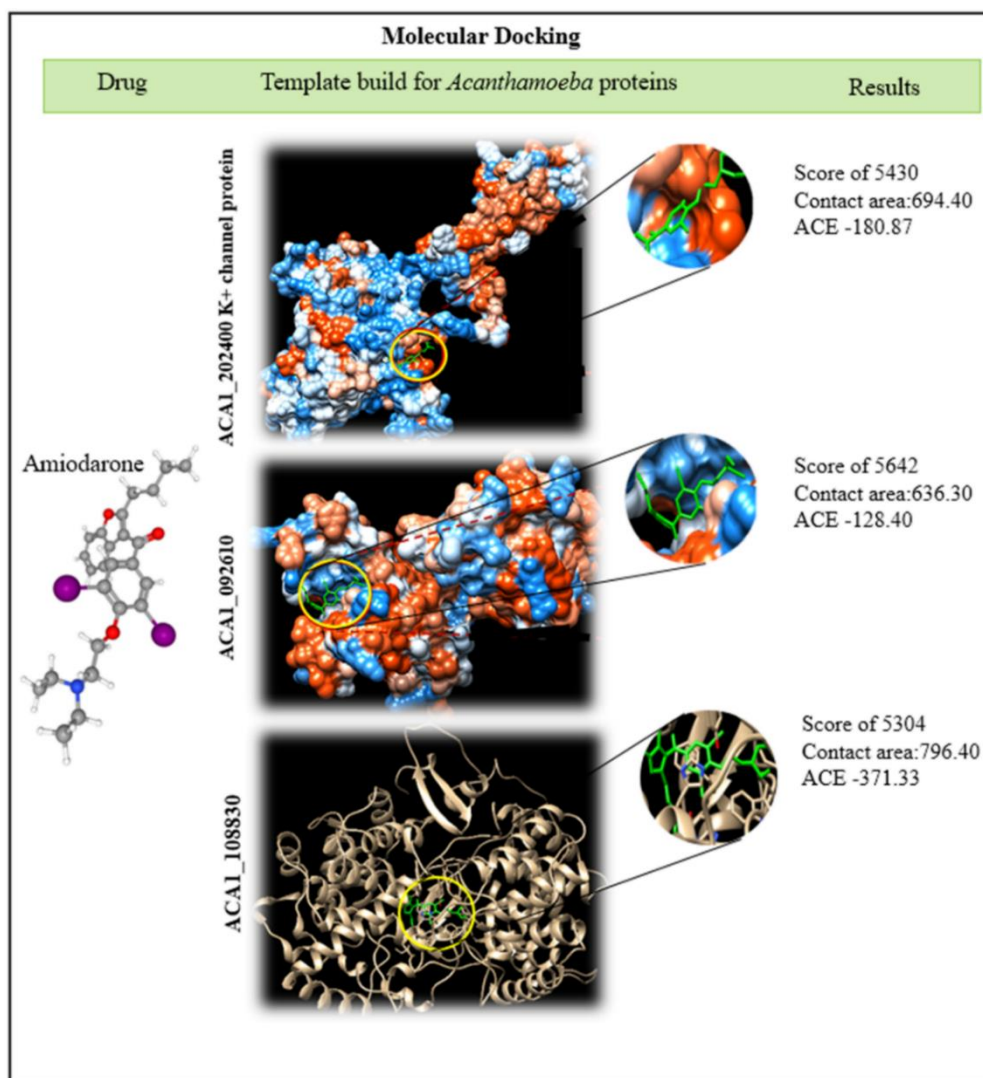


Figure 58. Molecular docking of amiodarone on template generated for *Acanthamoeba* proteins.

Identification of drug targets: Bioinformatic computational tools and drug docking predictions

Amiodarone (left panel) docked on the templates (images with black background) developed for ACA1_202400, ACA1_092610, and ACA1_108830. These proteins had developed models of KCN, L-type VGCC, and cycloartenol synthase on homology modeling. A high, four-digit score was generated for three dockings based on the geometric fit (contact areas) and ACE showed an induced-fit docking probability of amiodarone on the templates (areas of docking zoomed out, right side). The Scores, contact area, and ACE enabling the induced-fit configuration are shown under the result column. **[Adapted from Baig AM, 2017e [142]]**

4.9.5 Discussion

Application of computational tools like BLASTp, MSA, homology modeling, and molecular docking prediction of drugs on templates of the target proteins was used to provide a clue towards the mechanism of action of the drugs tested. In silico sketching or pre-screening of the compound, libraries may also be a beneficial approach for the identification of novel drug leads for parasitic infectious diseases. As mentioned previously, information that can be retrieved and manually curated from diverse online databases [99-101], can guide in drug selection. In the case of drug development strategy established on the reuse of existing licensed drugs for new medical indications, biological experiments conducted on a computer or via computer simulation are profited by pharmacological and clinical information available for approved drugs. A computational platform for drug discovery relies mostly on molecular docking, predicting the drug orientation within the binding site. This ligand-based technique has already been implemented for drug repurposing efforts. Computational drug repurposing is still waiting to see its first translational success with a compound reaching the market, but there is ample experimental evidence to support the feasibility of this approach. The need to discover novel antimicrobial drugs is expected to continue to grow the research community with ever-growing data stores

Identification of drug targets: Bioinformatic computational tools and drug docking predictions

and computational tools for analysis making it possible for scientists to identify likely candidate drugs for repurposing. For diverse parasites, in silico screening has played a significant role in drug target discovery as has happened with the discovery of inhibitors of *Entamoeba histolytica*, a protozoan intestinal parasite and the causative agent of human amoebiasis. As detailed previously, Debnath et al. [107] formulated auranofin, which has been in clinical use to treat rheumatoid arthritis for over 20 years for the treatment of human amoebiasis in 2012 that has gained an orphan-drug status. With the advances in computing bioinformatics computational tools, like BLASTp searches, homology modeling, and drug docking predictions, there have been developments in the identification of possible targets in pathogenic parasites by constructing an atomic-resolution model of the "target" protein from its amino acid sequence and an experimental three-dimensional structure protein design [27, 29]. Additionally, parasite genome databases are an enormous source of knowledge that can be used to investigate the protein expressions. The structural information of proteins obtained from these genome databases enables scientists to engage in screening projects that have helped in determining protein targets in specific parasites. In the case of drug target discovery in *Acanthamoeba* spp. there has been a paucity in the utilization of its available genomic, transcriptomic, and proteomic information [182]. Although recent studies have used the genome and transcriptome of *Acanthamoeba* spp. to elucidate drug targets in this protist pathogens [184-186], the use of homology modeling and drug docking prediction in the identification of molecular targets in *A. castellanii* needs to be fully employed to test new drug molecules for repurposing the drugs and chemicals already in use for non-infectious diseases. Ligand-based homology modeling as shown above in results can play a critical role in identifying evolutionarily related primitive molecular targets in parasites like *A. castellanii*. It has been shown that conserved regions for ligand docking in primitive proteins can be

Identification of drug targets: Bioinformatic computational tools and drug docking predictions

exploited to target *A. castellanii*. Molecular docking prediction of the receptor-ligand complexes has proved to be important for obtaining an induced-fit result in docking simulations.

4.9.6 Summary

The data presented here is the summary of studies performed for the identification of drug targets in *A. castellanii* with the use of bioinformatic computational tools. This study is attempted to provide an explanation for the effects of the drugs targeting Ca^{2+} homeostasis in *A. castellanii* (chapter-3) and validate the rationale of the Ca^{2+} dependency in *A. castellanii*, as detailed in chapter-1. The transcriptomic of trophozoites of *A. castellanii* showed the mRNA encoding diverse human-like proteins that were found to be homologs of human TPC, L-type, P/Q type, and alpha2/delta1 variants of VGCCs. Homology modeling with ligand binding attributes further confirmed the BLASTp findings (chapter-3) of the published data on VGCC like proteins in *A. castellanii*. Drug docking showed an induced-fit docking prediction of the drugs tested on the templates of the VGCCs and CaM like proteins reported in *A. castellanii*. Additionally, the template-based homology modeling (Figure 48, 49) was able to identify a possible human-like mAChR receptor in *A. castellanii* [Baig AM, 2017a [149]]. Also, a possible cholinergic cascade that synthesizes ACh was uncovered in the published studies, which can prove to be a potential drug target. Potential molecular targets of drugs like amiodarone, digoxin, and acetazolamide that affect the Ca^{2+} homeostasis were also uncovered by BLASTp, homology modeling, and drug docking predictions reported here and in the published papers. Overall, the results of the genomic, transcriptomics, bioinformatics computational tools coupled with drug docking prediction were able to attain the aims shown below as was aimed (chapter-1).

4.9.7 Aims Achieved:

1. Putative human-like two-pore (TPC), L-types VGCCs, CaM, G-protein coupled receptors (GPCRs), apoptosis regulating cytochrome-c and muscarinic receptor-like proteins coupled with Ca⁺² channels that are known targets of drugs tested in experimental assays, were identified in *A. castellanii*.
2. The evolutionary link between the human proteins that include the two-pore (TPC), L-types VGCCs, CaM, G-protein coupled receptors (GPCRs), apoptosis regulating cytochrome-c, and muscarinic receptor-like proteins with their homologs in *A. castellanii* were identified.
3. With drug docking predictions, evidence was shown for induced-fit docking of the drugs tested in *Acanthamoeba* spp. over the templates of the protein models developed for the trophozoite forms of *A. castellanii*

Evaluation of my contribution to the biology and drug target discovery in *Acanthamoeba* spp.

5 Evaluation of my contribution to the biology and drug target discovery in *Acanthamoeba* spp.

5.1 Contribution to the knowledge of drug targets in trophozoites and cysts of *A. castellanii*.

The published papers for the very first time have identified human-like proteins in *A. castellanii*. Evidence in support that the findings reported and its contribution to the knowledge in drug target discovery in *A. castellanii* can be gauged by the fact that previously *in vitro* assays with the drug belonging to the phenothiazine class were performed [98, 168, 175] but the receptors involved and their effects in dysregulation of Ca⁺² homeostasis was not known. Also, human-like VGCC proteins were for the very first time revealed in *A. castellanii* in the published work and they were proven to be viable drug targets by the results shown in *in vitro* effects of drugs (Chapter-3) like amlodipine, nifedipine, verapamil, and gabapentin. Similarly, the effects of the antagonism of a human muscarinic receptor mAChR like protein in *A. castellanii* (Chapter-3) are novel contributions made by the published work that implore to repurpose them in AK and GAE. Other examples of the contribution to the knowledge by the papers published between 2013-2019 include the discovery of a near-identical human-like cytochrome-c (59% -sequence identities and an e-value 0.0 on BLASTp results) involved in the intrinsic apoptosis pathway [Baig AM, 2017c [164]]., VGCCs, CaM, Na-K ATPase, and K-ion channels in *A. castellanii* (Table-5) reflect the contribution of the published work to the biology of *A. castellanii*.

5.1.1 Providing explanations to the cure of retrospective cases of *Acanthamoeba* keratitis.

After reporting the amoebicidal effects of anticholinergic drugs like procyclidine and atropine, it was noted that in a retrospective clinical case of AK, there were reports of complete recovery in AK patients with the use of atropine in the eye (given as an adjuvant in AK) for which there was no explanation. In this context, the published research added an explanation to this occurrence by revealing

Evaluation of my contribution to the biology and drug target discovery in *Acanthamoeba* spp.

that successes with atropine were due to a possible antagonism of human-like mAChR in *Acanthamoeba* spp. [[Baig AM, 2014d [166]]. The published work provided the reason why successful outcomes were seen in AK with the use of atropine in retrospective cases [175].

5.2 The first evidence of the role of extracellular Ca²⁺ ion in the biology of *Acanthamoeba* trophozoites

Though *A. castellanii* has been known for its motility, phagocytosis, and other cellular events that use calcium for their execution, the role of the utilization of extracellular Ca²⁺ ion in the growth and viability of *A. castellanii* was not reported in the studies done in the past. The published work for the first time has shown that depletion of extracellular Ca²⁺ ion availability by chelation of this ion with EDTA, pirenixine [Baig AM, 2019c [156, 158], and that the Ca²⁺channel blockers [Baig AM, 2019d [146]] produce amoebicidal effects. *In vitro* models for Fura-2 AM staining of trophozoites and cysts after exposure to the above-mentioned drugs used in clinical practice were shown in the published papers for the very first time. This has a translational significance, as Ca²⁺channel blockers, in particular, can be repurposed in AK and GAE after human clinical trials (details below)

5.3 Potential of the re-purposing drugs tested in my assays in AK.

In the published work, the superiority of the drugs tested *in vitro* over biocides and natural products with unknown molecular targets [Baig AM, 2019 [156, 158]], used in AK has been highlighted. The drugs tested in the studies were published with the title “Re-purposing of Drugs” in the world-leading journal on ocular diseases [[Baig AM, 2019, [156, 158, 162]]. The later publications have debated the rationale of targeting the Ca²⁺ ion dependencies of *A. castellanii* to attain therapeutic gains in patients with AK.

5.4 Potential of the possible use of the experimented drugs in clinical trials and treatment of GAE

Like miltefosine, the drugs that were experimented with in my studies have possible molecular targets that are shared between humans and *Acanthamoeba* spp. [163, 173, 187], which includes targeting L-type VGGC as has been reported for *Leishmania donovani* [155]. The drugs experimented with and reported in published papers are safer than the list of drugs currently used in the treatment of GAE, of which the phenothiazine group has a wider margin of safety [159]. In the management of patients with GAE, we had proposed and published a neuroleptic-opioid combination of haloperidol-loperamide instead of fentanyl and droperidol for the induction of anesthesia in GAE to control seizures and pain as well as exert their amoebicidal effects [[Baig AM 2014,[165]]. Given the safety and known expected adverse effects [159, 181], we expect that drugs reported by this study will make it to the treatment of GAE after human clinical trials as drugs like procyclidine, prochlorperazine, apomorphine, and anticholinergic agents are already used in CNS diseases [Baig AM, 2013, [134]]. The drugs cross the blood-brain barrier (as they are given in diseases of the CNS) and have shown to be cysticidal previously [Baig AM, 2013, [134]], and recently [[Baig AM, 2020,[188]]. If repurposed, the use of the above drugs would reduce the chances of occurrence of GAE after organ transplantation [63, 79] and recurrences after drug treatment as detailed in chapter-1. Given aggressive routes like the intrathecal route, the efficacy of these drugs can be tested in clinical trials.

5.5 Possibility to extend the tested drugs in the treatment of infection caused by *Naegleria fowleri*.

The drugs that are already approved (Table-5) for clinical use and tested in *A. castellanii* assays (chapter-3) *in vitro* were also found to be significantly effective against trophozoites of *N. fowleri* [[Baig AM, 2014b [189]]. Popularly known by the term “Brain-eating amoeba”, *N. fowleri* claims the lives of swimmers and

Evaluation of my contribution to the biology and drug target discovery in *Acanthamoeba* spp.

water sports enthusiasts and those who perform ablution with water contaminated with *N. fowleri*. The disease is known as primary amoebic meningoencephalitis (PAM) with a mortality rate of nearly 99% [61, 62]. The currently used drugs have not improved the mortality rate of PAM [17, 36] and the drugs tested in our study *in vitro* have proven to be amoebicidal in trophozoites of *N. fowleri* as well and therefore can be tested in an animal model of PAM and repurposed for PAM in humans [[Baig AM, 2014b, Baig AM, 2016 [189, 190].

5.6 Rationale and experiments of our study projected to test the drugs in cancer cell lines

Acanthamoeba trophozoites are unicellular entities, which have tremendous replicative potential, the invasion into circulation, and dissemination to the brain and organ. Cancer cells also show similar attributes as their biological behavior. After reporting the human-like muscarinic receptors in *Acanthamoeba* spp, we hypothesized and published that similar receptor subtypes could be present in the cancer cell line of prostate cancer in particular which over-expresses mAChR1 over mAChR3 [[Baig AM, 2017b [191]]. In a later study, cytotoxic effects of dicyclomine (dicyclomine) and pirenzepine in LNCaP and PC3 prostate cancer cells were shown, as reported in our studies in *A. castellanii*.

5.7 Summary and Conclusion:

The reviewers of my published work have endorsed the rationale the use of the reported drugs being safer and having a greater target specificity than the biocides that are known for a wide range of actions on non-amoebal microbes [[Baig AM, 2019i [158]; [94] which can affect the normal flora of the human eye. The methodology and the bioinformatic approaches used in the identification of drug targets in the published work are being picked up by my peers, who by using similar methods in *A. castellanii* have published studies on drug targeting

Evaluation of my contribution to the biology and drug target discovery in *Acanthamoeba* spp.

enzymes in this protist pathogen [192]. The use of genomic and transcriptomic data to identify human-like drug targets in *A. castellanii* has been done exclusively reported in our studies that are expected to prove its translational significance in diseases like AK and GAE.

5.8 Publications and their impact:

After ensuring the reproducibility of the data of the research undertaken in the studies, publication in scientific journals was pursued and accomplished at the end of the respective project parts, as can be seen in the order in which the papers have surfaced between 2013-2019. Therefore, the dates of publication are illustrative of the time the results of the projects were undertaken and were produced. The relevant publications (a total of 10), which also represent the published work submitted for the degree of Ph.D., are attached in part-2 of this commentary. The impact of the presented published work is reflected by many citations by other researchers including leading scientists in this field. To date, the papers included in this thesis have been cited over 100 times as of June 4th, 2020, as shown by PubMed, Google Scholar, and ResearchGate. The research published has pioneered the use of bioinformatics computational tools for drug target discovery in *A. castellanii*, as reflected in the published papers that have surfaced. Also important is recognition of the work by the peers who in their published work have adopted the methodology of using the sequence similarities [192, 193], genome, and transcriptome, to elucidate target enzymes and proteins in *A. castellanii*. After the first published papers in 2016-17 that used bioinformatics computational tools in drug target discovery in *A. castellanii*, similar approaches by other scientists working on drug target discoveries in protozoa have surfaced [184, 185]. Though my publications are young, they are getting cited by my peers [194-203] in their work related to drug target discovery in *A. castellanii*. Scientists are picking up our approach, which has been seen to be extended to diverse protozoa like *Leishmania infantum* spp. [204] and *Naegleria fowleri* [111].

5.9 Future Directions:

It is expected that the published studies will prove to be translational in the repurposing of the drugs reported to have amoebicidal and cysticidal effects in *A. castellanii*. Plans are ongoing to design *in vivo* models of AK and GAE in animals to test the safety and efficacy of the drugs reported in this thesis. The ocular safety of the drugs reported in this commentary, in animal models of AK, is planned to be tested in the incoming months. Collaborations with groups working on ODAK-like clinical trials are ongoing, to take the research reported in this thesis to the next step. Fluorescent tagging of drug and molecular targets by using methods like fluorescence resonance energy transfer (FRET) is being planned as this thesis is being written. Downstream and upstream pathways affected by the drugs used and reported in this thesis are also under scrutiny to explain the mechanism involved in the dysregulation of Ca²⁺ homeostasis. For GAE most of the drugs reported in this study are already in use for CNS indications, therefore the drugs like promethazine, procyclidine, and prochlorperazine are planned to be tested in animal models of GAE shortly. Our group has recently extended collaborations with groups working on AK in Spain, Mexico, and the UK as well.

References:

References:

1. Fairlamb, A.H., et al., *Drug resistance in eukaryotic microorganisms*. Nature Microbiology, 2016. **1**(7): p. 1-15.
2. Jarroll, E.L. and K. Şener, *Potential drug targets in cyst-wall biosynthesis by intestinal protozoa*. Drug resistance updates, 2003. **6**(5): p. 239-246.
3. Jones, P. and A. George, *Multidrug resistance in parasites: ABC transporters, P-glycoproteins and molecular modelling*. International journal for parasitology, 2005. **35**(5): p. 555-566.
4. Vanaerschot, M., et al., *Drug resistance in vectorborne parasites: multiple actors and scenarios for an evolutionary arms race*. FEMS microbiology reviews, 2014. **38**(1): p. 41-55.
5. Mace, K.E., *Malaria surveillance—United States, 2016*. MMWR. Surveillance Summaries, 2019. **68**.
6. Organization, W.H., *Weekly Epidemiological Record, 1997, vol. 72, 14 [full issue]*. Weekly Epidemiological Record= Relevé épidémiologique hebdomadaire, 1997. **72**(14): p. 97-100.
7. Hotez, P.J., et al., *Rescuing the bottom billion through control of neglected tropical diseases*. The Lancet, 2009. **373**(9674): p. 1570-1575.
8. Chatelain, E. and J.-R. Ioset, *Drug discovery and development for neglected diseases: the DNDi model*. Drug design, development and therapy, 2011. **5**: p. 175.
9. Boniface, P.K. and F.I. Elizabeth, *Flavonoid-derived Privileged Scaffolds in anti-Trypanosoma brucei Drug Discovery*. Current Drug Targets, 2019. **20**(12): p. 1295-1314.
10. Frearson, J.A., et al., *Target assessment for antiparasitic drug discovery*. Trends in parasitology, 2007. **23**(12): p. 589-595.
11. Clarke, M., et al., *Genome of Acanthamoeba castellanii highlights extensive lateral gene transfer and early evolution of tyrosine kinase signaling*. Genome biology, 2013. **14**(2): p. 1-15.

References:

12. Fonseca, D.A., et al., *Orphan drugs: Major development challenges at the clinical stage*. Drug Discovery Today, 2019. **24**(3): p. 867-872.
13. Kumar Kakkar, A. and N. Dahiya, *The evolving drug development landscape: from blockbusters to niche busters in the orphan drug space*. Drug development research, 2014. **75**(4): p. 231-234.
14. Sharma, A., et al., *Orphan drug: Development trends and strategies*. Journal of Pharmacy and Bioallied Sciences, 2010. **2**(4): p. 290.
15. Delafont, V., et al., *Vermamoeba vermiformis: a free-living amoeba of interest*. Microbial ecology, 2018. **76**(4): p. 991-1001.
16. Khan, N.A., *Acanthamoeba: biology and increasing importance in human health*. FEMS microbiology reviews, 2006. **30**(4): p. 564-595.
17. Visvesvara, G.S., H. Moura, and F.L. Schuster, *Pathogenic and opportunistic free-living amoebae: Acanthamoeba spp., Balamuthia mandrillaris, Naegleria fowleri, and Sappinia diploidea*. FEMS Immunology & Medical Microbiology, 2007. **50**(1): p. 1-26.
18. Castellani, A., *An amoeba found in culture of yeast: preliminary note*. J Trop Med Hyg, 1930. **33**: p. 160.
19. Corsaro, D. and D. Venditti, *Phylogenetic evidence for a new genotype of Acanthamoeba (Amoebozoa, Acanthamoebida)*. Parasitology research, 2010. **107**(1): p. 233-238.
20. Douglas, M., *Notes on the classification of the amoeba found by Castellani in cultures of a yeast-like fungus*. J Trop Med London, 1930. **33**(33): p. 258-259.
21. Horn, M., et al., *Novel bacterial endosymbionts of Acanthamoeba spp. related to the Paramecium caudatum symbiont Caedibacter caryophilus*. Environmental Microbiology, 1999. **1**(4): p. 357-367.
22. Hewett, M.K., et al., *Identification of a new Acanthamoeba 18S rRNA gene sequence type, corresponding to the species Acanthamoeba jacobsi Sawyer, Nerad and Visvesvara, 1992 (Lobosea: Acanthamoebidae)*. Acta Protozoologica, 2003. **42**(4): p. 325-330.
23. Maghsood, A.H., et al., *Acanthamoeba genotype T4 from the UK and Iran and isolation of the T2 genotype from clinical isolates*. Journal of medical microbiology, 2005. **54**(8): p. 755-759.

References:

24. Cooper, G.M. and R. Hausman, *A molecular approach*. The Cell. 2nd ed. Sunderland, MA: Sinauer Associates, 2000.
25. Roger, A.J. and L.A. Hug, *The origin and diversification of eukaryotes: problems with molecular phylogenetics and molecular clock estimation*. Philosophical Transactions of the Royal Society B: Biological Sciences, 2006. **361**(1470): p. 1039-1054.
26. Bowers, B. and T.E. Olszewski, *Pinocytosis in Acanthamoeba castellanii: kinetics and morphology*. The Journal of cell biology, 1972. **53**(3): p. 681-694.
27. Goodall, R. and J. Thompson, *A scanning electron microscopic study of phagocytosis*. Experimental cell research, 1971. **64**(1): p. 1-8.
28. Volkonsky, M., *Hartmannella castellani Douglas et classification des Hartmannelles*. Arc. Zoolog. Exp. Gen., 1931. **72**: p. 317-319.
29. Culbertson, C., et al., *Experimental infection of mice and monkeys by Acanthamoeba*. The American journal of pathology, 1959. **35**(1): p. 185.
30. Ling, T.O.L., A.Z.A. Moh, and D. Yuru, *A simple mass culture of the amoeba Chaos carolinense: revisit*. Protistology, 2005. **4**(2).
31. Page, F.C., *A new key to freshwater and soil gymnamoebae: with instructions for culture*. 1988: Freshwater Biological Association.
32. Qvarnstrom, Y., T.A. Nerad, and G.S. Visvesvara, *Characterization of a new pathogenic Acanthamoeba species, A. byersi n. sp., isolated from a human with fatal amoebic encephalitis*. Journal of Eukaryotic Microbiology, 2013. **60**(6): p. 626-633.
33. Visvesvara, G., *Classification of Acanthamoeba*. Reviews of infectious diseases, 1991. **13**(Supplement_5): p. S369-S372.
34. da Rocha-Azevedo, B., H.B. Tanowitz, and F. Marciano-Cabral, *Diagnosis of infections caused by pathogenic free-living amoebae*. Interdisciplinary perspectives on infectious diseases, 2009. **2009**.
35. Diaz, J.H., *Increasing intracerebral infections caused by free-living amebae in the United States and Worldwide*. Journal of Neuroparasitology, 2010. **1**: p. 23-32.

References:

36. Visvesvara, G.S., *Free-living amoebae as opportunistic agents of human disease*. J Neuroparasitol, 2010. **1**(13): p. N100802.
37. Marciano-Cabral, F. and G. Cabral, *Acanthamoeba spp. as agents of disease in humans*. Clinical microbiology reviews, 2003. **16**(2): p. 273-307.
38. Siddiqui, R. and N.A. Khan, *Biology and pathogenesis of Acanthamoeba*. Parasites & vectors, 2012. **5**(1): p. 6.
39. Bowers, B. and E.D. Korn, *The fine structure of Acanthamoeba castellanii (Neff strain) II. Encystment*. The Journal of cell biology, 1969. **41**(3): p. 786-805.
40. Garajová, M., et al., *Cellulose fibrils formation and organisation of cytoskeleton during encystment are essential for Acanthamoeba cyst wall architecture*. Scientific reports, 2019. **9**(1): p. 1-21.
41. Moon, E.-K., et al., *Down-regulation of cellulose synthase inhibits the formation of endocysts in Acanthamoeba*. The Korean journal of parasitology, 2014. **52**(2): p. 131.
42. CHÁVEZ-MUNGUÍA, B., et al., *Ultrastructural study of encystation and excystation in Acanthamoeba castellanii*. Journal of eukaryotic microbiology, 2005. **52**(2): p. 153-158.
43. Bowers, B. and E.D. Korn, *The fine structure of Acanthamoeba castellanii: I. The Trophozoite*. The Journal of Cell Biology, 1968. **39**(1): p. 95-111.
44. Byers, T.J., et al., *Molecular aspects of the cell cycle and encystment of Acanthamoeba*. Reviews of infectious diseases, 1991. **13**(Supplement_5): p. S373-S384.
45. Clarholm, M., *Protozoan grazing of bacteria in soil—impact and importance*. Microbial Ecology, 1981. **7**(4): p. 343-350.
46. Korn, E.D. and R.A. Weisman, *Phagocytosis of Latex Beads by Acanthamoeba: II. Electron Microscopic Study of the Initial Events*. The Journal of cell biology, 1967. **34**(1): p. 219-227.
47. Brown, M.R. and J. Barker, *Unexplored reservoirs of pathogenic bacteria: protozoa and biofilms*. Trends in microbiology, 1999. **7**(1): p. 46-50.
48. Bowers, B. and T.E. Olszewski, *Acanthamoeba discriminates internally between digestible and indigestible particles*. The Journal of cell biology, 1983. **97**(2): p. 317-322.

References:

49. Oates, P.J. and O. Touster, *In vitro fusion of Acanthamoeba phagolysosomes. I. Demonstration and quantitation of vacuole fusion in Acanthamoeba homogenates*. The Journal of cell biology, 1976. **68**(2): p. 319-338.
50. Drozanski, W., *Fatal bacterial infection in soil amoebae*. Acta microbiologica Polonica (1952), 1956. **5**(3-4): p. 315-317.
51. Mölled, K.-D., E.N. Schmid, and R. Michel, *Intracellular Bacteria of Acanthamoebae Resembling Legionella spp. Turned Out to be Cytophaga sp.* Zentralblatt für Bakteriologie, 1999. **289**(4): p. 389-397.
52. Guimaraes, A.J., et al., *Acanthamoeba spp. as a universal host for pathogenic microorganisms: One bridge from environment to host virulence*. Microbiological research, 2016. **193**: p. 30-38.
53. Samba-Louaka, A., et al., *Environmental Mycobacterium avium subsp. paratuberculosis hosted by free-living amoebae*. Frontiers in cellular and infection microbiology, 2018. **8**: p. 28.
54. Nyamai, D.W. and Ö.T. Bishop, *Aminoacyl tRNA synthetases as malarial drug targets: a comparative bioinformatics study*. Malaria journal, 2019. **18**(1): p. 34.
55. Carnt, N., et al., *Acanthamoeba keratitis: confirmation of the UK outbreak and a prospective case-control study identifying contributing risk factors*. British Journal of Ophthalmology, 2018. **102**(12): p. 1621-1628.
56. Dart, J.K., V.P. Saw, and S. Kilvington, *Acanthamoeba keratitis: diagnosis and treatment update 2009*. American journal of ophthalmology, 2009. **148**(4): p. 487-499. e2.
57. Di Cave, D., et al., *Acanthamoeba T4 and T15 genotypes associated with keratitis infections in Italy*. European journal of clinical microbiology & infectious diseases, 2009. **28**(6): p. 607-612.
58. Robaei, D., et al., *Therapeutic and optical keratoplasty in the management of Acanthamoeba keratitis: risk factors, outcomes, and summary of the literature*. Ophthalmology, 2015. **122**(1): p. 17-24.
59. Orosz, E., et al., *Clinical course of Acanthamoeba keratitis by genotypes T4 and T8 in Hungary*. Acta microbiologica et immunologica Hungarica, 2019. **66**(3): p. 289-300.

References:

60. Scruggs, B.A., et al., *Notes from the Field: Acanthamoeba Keratitis Cases—Iowa, 2002–2017*. Morbidity and Mortality Weekly Report, 2019. **68**(19): p. 448.
61. Sütçü, M., et al., *Granulomatous amebic encephalitis caused by Acanthamoeba in an immunocompetent child*. The Turkish Journal of Pediatrics, 2018. **60**(3): p. 340-343.
62. Thamtam, V.K., et al., *Fatal granulomatous amoebic encephalitis caused by Acanthamoeba in a newly diagnosed patient with systemic lupus erythematosus*. Neurology India, 2016. **64**(1): p. 101.
63. Brondfield, M.N., et al., *Disseminated A canthamoeba infection in a heart transplant recipient treated successfully with a miltefosine-containing regimen: Case report and review of the literature*. Transplant Infectious Disease, 2017. **19**(2): p. e12661.
64. Megha, K., R. Sehgal, and S. Khurana, *Genotyping of Acanthamoeba spp. isolated from patients with granulomatous amoebic encephalitis*. The Indian journal of medical research, 2018. **148**(4): p. 456.
65. Dickson, J.M., et al., *Acanthamoeba rhinosinusitis*. Journal of Otolaryngology-Head and Neck Surgery, 2009. **38**(3): p. E87.
66. Juan, A., et al., *Successful treatment of sinusitis by Acanthamoeba in a pediatric patient after allogeneic stem cell transplantation*. The Pediatric infectious disease journal, 2016. **35**(12): p. 1350-1351.
67. Baig, A., *HANDBOOK OF FOODBORNE DISEASES*, in *Food Microbiology series*. Taylor and Francis Group: CRC Press.
68. Yoder, J.S., et al., *Acanthamoeba keratitis: the persistence of cases following a multistate outbreak*. Ophthalmic epidemiology, 2012. **19**(4): p. 221-225.
69. Panjwani, N., *Pathogenesis of Acanthamoeba keratitis*. The ocular surface, 2010. **8**(2): p. 70-79.
70. Witschel, H., R. Sundmacher, and H. Seitz, *Amebic keratitis: clinico-histopathologic case report*. Klinische Monatsblätter für Augenheilkunde, 1984. **185**(1): p. 46.
71. Samples, J.R., et al., *Acanthamoeba keratitis possibly acquired from a hot tub*. Archives of ophthalmology, 1984. **102**(5): p. 707-710.

References:

72. Baig, A.M., *Pathogenesis of amoebic encephalitis: are the amoebae being credited to an 'inside job' done by the host immune response?* Acta tropica, 2015. **148**: p. 72-76.
73. Baig, A.M. and N.A. Khan, *A proposed cascade of vascular events leading to granulomatous amoebic encephalitis.* Microbial pathogenesis, 2015. **88**: p. 48-51.
74. Lorenzo-Morales, J., et al., *Acanthamoeba keratitis: an emerging disease gathering importance worldwide?* Trends in parasitology, 2013. **29**(4): p. 181-187.
75. Borin, S., et al., *Rapid diagnosis of Acanthamoeba keratitis using non-nutrient agar with a lawn of E. coli.* Journal of ophthalmic inflammation and infection, 2013. **3**(1): p. 1-2.
76. Galarza, C., et al., *Cutaneous acanthamebiasis infection in immunocompetent and immunocompromised patients.* International journal of dermatology, 2009. **48**(12): p. 1324-1329.
77. Deol, I., et al., *Encephalitis due to a free-living amoeba (Balamuthia mandrillaris): case report with literature review.* Surgical neurology, 2000. **53**(6): p. 611-616.
78. Doan, N., et al., *Granulomatous amebic encephalitis following hematopoietic stem cell transplantation.* Surgical neurology international, 2015. **6**(Suppl 18): p. S459.
79. FRIEDLAND, L.R., et al., *Disseminated Acanthamoeba infection in a child with symptomatic human immunodeficiency virus infection.* The Pediatric infectious disease journal, 1992. **11**(5): p. 404-407.
80. Geith, S., et al., *Lethal outcome of granulomatous acanthamoebic encephalitis in a man who was human immunodeficiency virus-positive: a case report.* Journal of medical case reports, 2018. **12**(1): p. 201.
81. Nachege, J.B., et al., *Case Report: Successful Treatment of Acanthamoeba Rhinosinusitis in a Patient with AIDS.* AIDS Patient Care & STDs, 2005. **19**(10): p. 621-625.
82. Brinen, L.S., et al., *A target within the target: probing cruzain's PI' site to define structural determinants for the Chagas' disease protease.* Structure, 2000. **8**(8): p. 831-840.
83. Sabnis, Y., et al., *Homology modeling of falcipain-2: validation, de novo ligand design and synthesis of novel inhibitors.* Journal of Biomolecular Structure and Dynamics, 2002. **19**(5): p. 765-774.

References:

84. Fraser, M.N., et al., *Characteristics of an Acanthamoeba keratitis outbreak in British Columbia between 2003 and 2007*. *Ophthalmology*, 2012. **119**(6): p. 1120-1125.
85. Joslin, C.E., et al., *Epidemiological characteristics of a Chicago-area Acanthamoeba keratitis outbreak*. *American journal of ophthalmology*, 2006. **142**(2): p. 212-217. e2.
86. Page, M.A. and W.D. Mathers, *Acanthamoeba keratitis: a 12-year experience covering a wide spectrum of presentations, diagnoses, and outcomes*. *Journal of ophthalmology*, 2013. **2013**.
87. Parmar, D.N., et al., *Tandem scanning confocal corneal microscopy in the diagnosis of suspected Acanthamoeba keratitis*. *Ophthalmology*, 2006. **113**(4): p. 538-547.
88. Iljin, K., et al., *High-throughput cell-based screening of 4910 known drugs and drug-like small molecules identifies disulfiram as an inhibitor of prostate cancer cell growth*. *Clinical Cancer Research*, 2009. **15**(19): p. 6070-6078.
89. Cousin, M.A., et al., *Larval zebrafish model for FDA-approved drug repositioning for tobacco dependence treatment*. *PLoS One*, 2014. **9**(3): p. e90467.
90. Lloyd, D., *Encystment in Acanthamoeba castellanii: a review*. *Experimental parasitology*, 2014. **145**: p. S20-S27.
91. Schlander, M., et al. *8th European Conference on Rare Diseases & Orphan Products (ECRD 2016)*. in *Orphanet Journal of Rare Diseases*. 2016. BioMed Central.
92. Xu, M., et al., *Identification of small-molecule inhibitors of Zika virus infection and induced neural cell death via a drug repurposing screen*. *Nature medicine*, 2016. **22**(10): p. 1101-1107.
93. *Food and Drug Administration, Office of Orphan Products Development*. [cited 2018 October 19.]; (301) 796-8660:[Available from: <http://www.fda.gov/ForIndustry/DevelopingProductsforRareDiseasesConditions/default.htm>].
94. *Orphanet*. [cited 2019 May]; Available from: [https://www.orpha.net/consor/cgibin/Disease_Search.php?lng=EN&data_id=10903 & Disease_Disease_Search_diseaseGroup=Acanthamoeba keratitis&Disease_Disease_Search_diseaseType=Pat&Disease\(s\)/group%20of%20diseas](https://www.orpha.net/consor/cgibin/Disease_Search.php?lng=EN&data_id=10903&Disease_Disease_Search_diseaseGroup=Acanthamoeba_keratitis&Disease_Disease_Search_diseaseType=Pat&Disease(s)/group%20of%20diseas)

References:

- es=Acanthamoeba -keratitis&title=Acanthamoeba
%20keratitis&search=Disease_Search_Simple.
95. *Orphan drug status approval for Acanthamoeba Keratitis received by Profounda for Miltefosine.* [cited 2018 October 19.]; Available from: [://www.profounda.com/single-post/2016/12/31/Orphan-drug-status-approval-for-Acanthamoeba -Keratitis-received-by-Profounda-for-Miltefosine](http://www.profounda.com/single-post/2016/12/31/Orphan-drug-status-approval-for-Acanthamoeba-Keratitis-received-by-Profounda-for-Miltefosine).
 96. Schnuch, A., et al., *The biocide polyhexamethylene biguanide remains an uncommon contact allergen: Recent multicentre surveillance data.* *Contact Dermatitis*, 2007. **56**(4): p. 235-239.
 97. Scannell, J.W., et al., *Diagnosing the decline in pharmaceutical R&D efficiency.* *Nature reviews Drug discovery*, 2012. **11**(3): p. 191.
 98. Schuster, F. and N. Mandel, *Phenothiazine compounds inhibit in vitro growth of pathogenic free-living amoebae.* *Antimicrobial agents and chemotherapy*, 1984. **25**(1): p. 109-112.
 99. Gaulton, A., et al., *The ChEMBL database in 2017.* *Nucleic acids research*, 2017. **45**(D1): p. D945-D954.
 100. Gaulton, A., et al., *The ChEMBL bioactivity database: an update.* *NatSD*, 2013. **2**: p. 150032.
 101. Wishart, D.S., et al., *HMDB 3.0—the human metabolome database in 2013.* *Nucleic acids research*, 2012. **41**(D1): p. D801-D807.
 102. Sateriale, A., et al., *Drug repurposing: mining protozoan proteomes for targets of known bioactive compounds.* *Journal of the American Medical Informatics Association*, 2014. **21**(2): p. 238-244.
 103. Guney, E., et al., *Network-based in silico drug efficacy screening.* *Nature communications*, 2016. **7**(1): p. 1-13.
 104. Chavali, A.K., et al., *Systems analysis of metabolism in the pathogenic trypanosomatid Leishmania major.* *Molecular systems biology*, 2008. **4**(1): p. 177.
 105. Barratt, M.J. and D.E. Frail, *Drug repositioning: Bringing new life to shelved assets and existing drugs.* 2012: John Wiley & Sons.

References:

106. Chong, C.R., et al., *A clinical drug library screen identifies astemizole as an antimalarial agent*. Nature chemical biology, 2006. **2**(8): p. 415-416.
107. Debnath, A., M. Ndao, and S.L. Reed, *Reprofiled drug targets ancient protozoans: drug discovery for parasitic diarrheal diseases*. Gut microbes, 2013. **4**(1): p. 66-71.
108. Berman, H., Henrick, K., Nakamura, H. and Markley, J.L., Nucleic Acids Res., 2007. **35**: p. 301-303.
109. de Azevedo Junior, W.F., et al., *Bioinformatics tools for screening of antiparasitic drugs*. Current drug targets, 2009. **10**(3): p. 232-239.
110. Doerig, C., L. Meijer, and J.C. Mottram, *Protein kinases as drug targets in parasitic protozoa*. Trends in parasitology, 2002. **18**(8): p. 366-371.
111. Milanes, J.E., et al., *Enzymatic and structural characterization of the Naegleria fowleri glucokinase*. Antimicrobial agents and chemotherapy, 2019. **63**(5).
112. Lee, M.-R., et al., *The identification of antigenic proteins: 14-3-3 protein and propionyl-CoA carboxylase in Clonorchis sinensis*. Molecular and biochemical parasitology, 2012. **182**(1-2): p. 1-6.
113. Fairlamb, A.H., *Metabolic pathway analysis in trypanosomes and malaria parasites*. Philosophical Transactions of the Royal Society of London. Series B: Biological Sciences, 2002. **357**(1417): p. 101-107.
114. Bennuru, S., et al., *Mining filarial genomes for diagnostic and therapeutic targets*. Trends in parasitology, 2018. **34**(1): p. 80-90.
115. Jana, S. and J. Paliwal, *Novel molecular targets for antimalarial chemotherapy*. International journal of antimicrobial agents, 2007. **30**(1): p. 4-10.
116. Rout, S., N.P. Patra, and R.K. Mahapatra, *An in silico strategy for identification of novel drug targets against Plasmodium falciparum*. Parasitology research, 2017. **116**(9): p. 2539-2559.
117. Gupta, I., et al., *Ubiquitin Proteasome pathway proteins as potential drug targets in parasite Trypanosoma cruzi*. Scientific reports, 2018. **8**(1): p. 1-12.

References:

118. Takeda, J.-i., et al., *H-DBAS: human-transcriptome database for alternative splicing: update 2010*. *Nucleic acids research*, 2010. **38**(suppl_1): p. D86-D90.
119. Weigelt, J., *Structural genomics—impact on biomedicine and drug discovery*. *Experimental cell research*, 2010. **316**(8): p. 1332-1338.
120. *Computational Biology Market Size Worth \$13.6 Billion By 2026*. [cited 2019 June 1.]; Available from: <https://www.grandviewresearch.com/press-release/global-computational-biology-market>.
121. Leung, E.L., et al., *Network-based drug discovery by integrating systems biology and computational technologies*. *Briefings in bioinformatics*, 2013. **14**(4): p. 491-505.
122. Ewing, T.J., et al., *DOCK 4.0: search strategies for automated molecular docking of flexible molecule databases*. *Journal of computer-aided molecular design*, 2001. **15**(5): p. 411-428.
123. Goodsell, D.S., G.M. Morris, and A.J. Olson, *Automated docking of flexible ligands: applications of AutoDock*. *Journal of molecular recognition*, 1996. **9**(1): p. 1-5.
124. Morris, G.M., et al., *Automated docking using a Lamarckian genetic algorithm and an empirical binding free energy function*. *Journal of computational chemistry*, 1998. **19**(14): p. 1639-1662.
125. Joy, S., et al., *Detailed comparison of the protein-ligand docking efficiencies of GOLD, a commercial package and ArgusLab, a licensable freeware*. *In silico biology*, 2006. **6**(6): p. 601-605.
126. Verdonk, M.L., et al., *Improved protein–ligand docking using GOLD*. *Proteins: Structure, Function, and Bioinformatics*, 2003. **52**(4): p. 609-623.
127. Kramer, B., M. Rarey, and T. Lengauer, *Evaluation of the FLEXX incremental construction algorithm for protein–ligand docking*. *Proteins: Structure, Function, and Bioinformatics*, 1999. **37**(2): p. 228-241.
128. Rarey, M., et al., *A fast flexible docking method using an incremental construction algorithm*. *Journal of molecular biology*, 1996. **261**(3): p. 470-489.
129. Chen, R., L. Li, and Z. Weng, *ZDOCK: an initial-stage protein-docking algorithm*. *Proteins: Structure, Function, and Bioinformatics*, 2003. **52**(1): p. 80-87.

References:

130. Pierce, B., W. Tong, and Z. Weng, *M-ZDOCK: a grid-based approach for C_n symmetric multimer docking*. *Bioinformatics*, 2005. **21**(8): p. 1472-1478.
131. Sauton, N., et al., *MS-DOCK: accurate multiple conformation generator and rigid docking protocol for multi-step virtual ligand screening*. *BMC bioinformatics*, 2008. **9**(1): p. 1-12.
132. Jain, A.N., *Surflex: fully automatic flexible molecular docking using a molecular similarity-based search engine*. *Journal of medicinal chemistry*, 2003. **46**(4): p. 499-511.
133. Liu, M. and S. Wang, *MCDOCK: a Monte Carlo simulation approach to the molecular docking problem*. *Journal of computer-aided molecular design*, 1999. **13**(5): p. 435-451.
134. **Baig, A.M.**, J. Iqbal, and N.A. Khan, *In vitro efficacies of clinically available drugs against growth and viability of an Acanthamoeba castellanii keratitis isolate belonging to the T4 genotype*. *Antimicrobial agents and chemotherapy*, 2013. **57**(8): p. 3561-3567.
135. **Baig AM**, Kulsoom, H., et al., *Combined drug therapy in the management of granulomatous amoebic encephalitis due to Acanthamoeba spp., and Balamuthia mandrillaris*. *Experimental parasitology*, 2014. **145**: p. S115-S120.
136. Hartung, T., et al., *ECVAM good cell culture practice task force report 1*. *Alternatives to Laboratory Animals*, 2002. **30**(4): p. 407-414.
137. Meng, X.-Y., et al., *Molecular docking: a powerful approach for structure-based drug discovery*. *Current computer-aided drug design*, 2011. **7**(2): p. 146-157.
138. Agarwala, R., et al., *Database resources of the national center for biotechnology information*. *Nucleic Acids Research*, 2018. **46**(D 1): p. D8-D13.
139. Madden, T., *The BLAST sequence analysis tool*, in *The NCBI Handbook [Internet]. 2nd edition*. 2013, National Center for Biotechnology Information (US).
140. Marti-Renom, M.A., M. Madhusudhan, and A. Sali, *Alignment of protein sequences by their profiles*. *Protein Science*, 2004. **13**(4): p. 1071-1087.
141. **Baig AM.**, et al., *Antibiotic Effects of Loperamide: Homology of Human Targets of Loperamide with Targets in Acanthamoeba spp.* *Recent Patents on Anti-Infective Drug Discovery*, 2017. **12**(1): p. 44-60.

References:

142. **Baig, A.M.**, et al., *Bioinformatic Insights on Target Receptors of Amiodarone in Human and Acanthamoeba castellanii*. Infectious Disorders Drug Targets, 2017. **17**(3): p. 160-177.
143. Pundir, S., M.J. Martin, and C. O'Donovan, *UniProt protein knowledgebase*, in *Protein Bioinformatics*. 2017, Springer. p. 41-55.
144. Luscombe, N.M., D. Greenbaum, and M. Gerstein, *What is bioinformatics? A proposed definition and overview of the field*. Methods of information in medicine, 2001. **40**(04): p. 346-358.
145. Cook, C.E., et al., *The European Bioinformatics Institute in 2018: tools, infrastructure and training*. Nucleic acids research, 2019. **47**(D1): p. D15-D22.
146. **Baig, A.M.**, et al., *Evidence of human-like Ca²⁺ channels and effects of Ca²⁺ channel blockers in Acanthamoeba castellanii*. Chemical biology & drug design, 2019. **93**(3): p. 351-363.
147. **Baig, A.M.**, et al., *Evolution of pH buffers and water homeostasis in eukaryotes: homology between humans and Acanthamoeba proteins*. Future microbiology, 2018. **13**(2): p. 195-207.
148. Biasini, M., et al., *SWISS-MODEL: modelling protein tertiary and quaternary structure using evolutionary information*. Nucleic acids research, 2014. **42**(W1): p. W252-W258.
149. **Baig, A.M.** and H. Ahmad, *Evidence of a M1-muscarinic GPCR homolog in unicellular eukaryotes: featuring Acanthamoeba spp bioinformatics 3D-modelling and experimentations*. Journal of Receptors and Signal Transduction, 2017. **37**(3): p. 267-275.
150. Sliwoski, G., et al., *Computational methods in drug discovery*. Pharmacological reviews, 2014. **66**(1): p. 334-395.
151. Schneidman-Duhovny, D., et al., *PatchDock and SymmDock: servers for rigid and symmetric docking*. Nucleic acids research, 2005. **33**(suppl_2): p. W363-W367.
152. Shatsky, M., et al., *BioInfo3D: a suite of tools for structural bioinformatics*. Nucleic acids research, 2004. **32**(suppl_2): p. W503-W507.
153. Brylinski, M. and J. Skolnick, *FINDSITE LHM: a threading-based approach to ligand homology modeling*. PLoS Comput Biol, 2009. **5**(6): p. e1000405.

References:

154. Glaser, F., et al., *A method for localizing ligand binding pockets in protein structures*. PROTEINS: Structure, Function, and Bioinformatics, 2006. **62**(2): p. 479-488.
155. Pinto-Martinez, A.K., et al., *Mechanism of action of miltefosine on Leishmania donovani involves the impairment of acidocalcisome function and the activation of the sphingosine-dependent plasma membrane Ca²⁺ channel*. Antimicrobial agents and chemotherapy, 2018. **62**(1).
156. Baig, A.M., *Drug targeting in Acanthamoeba keratitis: rational of using drugs that are already approved for ocular use in non-keratitis indications*. Eye, 2019. **33**(3): p. 509-518.
157. Baig, A.M., et al., *Neuroleptic Drug Targets a Brain-Eating Amoeba: Effects of Promethazine on Neurotropic Acanthamoeba castellanii*. ACS chemical neuroscience, 2019. **10**(6): p. 2868-2876.
158. Baig, A.M., et al., *Repurposing drugs: Ca²⁺ ion dependency that can be exploited to treat keratitis caused by Acanthamoeba castellanii*. Eye, 2019. **33**(11): p. 1823-1825.
159. Laurence L. Brunton, B.A.C., Björn C. Knollmann., *Goodman & Gilman's The Pharmacological basis of Therapeutics*. 12th ed. 2011, Copyright © 2011 by The McGraw-Hill Companies, Inc: NYC.
160. **Baig, A.M.**, et al., *Traced on the Timeline: Discovery of Acetylcholine and the Components of the Human Cholinergic System in a Primitive Unicellular Eukaryote Acanthamoeba spp*. ACS chemical neuroscience, 2017. **9**(3): p. 494-504.
161. **Baig, A.M.**, et al., *Forte of bioinformatics computational tools in identification of targets of digitalis in unicellular eukaryotes: featuring Acanthamoeba castellanii*. EC Microbiol, 2016. **6**: p. 831-844.
162. Baig, A.M., *Torn from the headlines: role of public awareness and bench-to-bedside research in prevention and treatment of Acanthamoeba keratitis*. Eye, 2019. **33**(5): p. 698-701.
163. Polat, Z.A., et al., *Miltefosine and polyhexamethylene biguanide: a new drug combination for the treatment of A canthamoeba keratitis*. Clinical & experimental ophthalmology, 2014. **42**(2): p. 151-158.
164. **Baig, A.M.**, S. Lalani, and N.A. Khan, *Apoptosis in Acanthamoeba castellanii belonging to the T4 genotype*. Journal of basic microbiology, 2017. **57**(7): p. 574-579.

References:

165. Baig, A.M. and N.A. Khan, *Anesthesia with antiamebic effects: can anesthesia choice affect the clinical outcome of granulomatous amoebic encephalitis due to Acanthamoeba spp.?* Journal of neurosurgical anesthesiology, 2014. **26**(4): p. 409-410.
166. Baig, A.M., H. Zuberi, and N.A. Khan, *Recommendations for the management of Acanthamoeba keratitis.* Journal of Medical Microbiology, 2014. **63**(5): p. 770-771.
167. Sexton, A.E., et al., *Post-Genomic Approaches to Understanding Malaria Parasite Biology: Linking Genes to Biological Functions.* ACS infectious diseases, 2019. **5**(8): p. 1269-1278.
168. Mattana, A., et al., *In vitro evaluation of the effectiveness of the macrolide rokitamycin and chlorpromazine against Acanthamoeba castellanii.* Antimicrobial agents and chemotherapy, 2004. **48**(12): p. 4520-4527.
169. Schuster, F.L. and G.S. Visvesvara, *Efficacy of novel antimicrobials against clinical isolates of opportunistic amebas.* Journal of Eukaryotic Microbiology, 1998. **45**(6): p. 612-618.
170. Chu, D.-M., et al., *Amebicidal activity of plant extracts from Southeast Asia on Acanthamoeba spp.* Parasitology research, 1998. **84**(9): p. 746-752.
171. Derda, M., et al., *Artemisia annua L. as a plant with potential use in the treatment of acanthamoebiasis.* Parasitology Research, 2016. **115**(4): p. 1635-1639.
172. Croft, S., L. Vivas, and S. Brooker, *Recent advances in research and control of malaria, leishmaniasis, trypanosomiasis and schistosomiasis.* EMHJ-Eastern Mediterranean Health Journal, 9 (4), 518-533, 2003, 2003.
173. Walochnik, J., et al., *Anti-Acanthamoeba efficacy and toxicity of miltefosine in an organotypic skin equivalent.* Journal of antimicrobial chemotherapy, 2009. **64**(3): p. 539-545.
174. Deng, Y., et al., *Artemether exhibits amoebicidal activity against Acanthamoeba castellanii through inhibition of the serine biosynthesis pathway.* Antimicrobial agents and chemotherapy, 2015. **59**(8): p. 4680-4688.
175. Agahan, A., R. Lim, and M.J. Valenton, *Successful treatment of Acanthamoeba keratitis without anti-amoebic agents.* Annals of the Academy of Medicine, Singapore, 2009. **38**(2): p. 175.

References:

176. Martín-Navarro, C.M., et al., *Amoebicidal activity of caffeine and maslinic acid by the induction of programmed cell death in Acanthamoeba*. Antimicrobial agents and chemotherapy, 2017. **61**(6).
177. Awan, A.R., A. Manfredo, and J.A. Pleiss, *Lariat sequencing in a unicellular yeast identifies regulated alternative splicing of exons that are evolutionarily conserved with humans*. Proceedings of the National Academy of Sciences, 2013. **110**(31): p. 12762-12767.
178. Berman, H.M., et al., *The protein data bank*. Nucleic acids research, 2000. **28**(1): p. 235-242.
179. Emmert, D.B., et al., *The European bioinformatics institute (EBI) databases*. Nucleic Acids Research, 1994. **22**(17): p. 3445-3449.
180. Miyazaki, S., et al., *DNA data bank of Japan (DDBJ) in XML*. Nucleic Acids Research, 2003. **31**(1): p. 13-16.
181. Aurrecochea, C., et al., *AmoebaDB and MicrosporidiaDB: functional genomic resources for Amoebozoa and Microsporidia species*. Nucleic acids research, 2010. **39**(suppl_1): p. D612-D619.
182. Baig, A.M., *Innovative Methodology in the Discovery of Novel Drug Targets in the Free-Living Amoebae*. Current drug targets, 2019. **20**(1): p. 60-69.
183. Veiga-Santos, P., et al., *Effects of amiodarone and posaconazole on the growth and ultrastructure of Trypanosoma cruzi*. International journal of antimicrobial agents, 2012. **40**(1): p. 61-71.
184. Shabardina, V., et al., *Environmental adaptation of Acanthamoeba castellanii and Entamoeba histolytica at genome level as seen by comparative genomic analysis*. International journal of biological sciences, 2018. **14**(3): p. 306.
185. Wu, D., et al., *Molecular and biochemical characterization of key enzymes in the cysteine and serine metabolic pathways of Acanthamoeba castellanii*. Parasites & vectors, 2018. **11**(1): p. 1-10.
186. Zhou, W., et al., *Enzymatic chokepoints and synergistic drug targets in the sterol biosynthesis pathway of Naegleria fowleri*. PLoS pathogens, 2018. **14**(9): p. e1007245.

References:

187. Elsheikha, H.M., R. Siddiqui, and N.A. Khan, *Drug Discovery against Acanthamoeba Infections: Present Knowledge and Unmet Needs*. Pathogens, 2020. **9**(5): p. 405.
188. Baig, A.M., et al., '*Targeting the feast of a sleeping beast*': Nutrient and mineral dependencies of encysted *Acanthamoeba castellanii*. Chemical Biology & Drug Design, 2020.
189. Baig, A., H. Kulsoom, and N.A. Khan, *Primary amoebic meningoencephalitis: amoebicidal effects of clinically approved drugs against Naegleria fowleri*. Journal of medical microbiology, 2014.
190. Baig, A.M., *Primary amoebic meningoencephalitis: neurochemotaxis and neurotropic preferences of Naegleria fowleri*. 2016, ACS Publications.
191. Mannan Baig, A., et al., *Differential receptor dependencies: expression and significance of muscarinic M1 receptors in the biology of prostate cancer*. Anti-cancer drugs, 2017. **28**(1): p. 75-87.
192. Thomson, S., et al., *Characterisation of sterol biosynthesis and validation of 14 α -demethylase as a drug target in Acanthamoeba*. Scientific Reports, 2017. **7**(1): p. 1-9.
193. Wang, Y.-J., W.-C. Lin, and M.-S. He, *The Acanthamoeba SBDS, a cytoskeleton-associated gene, is highly expressed during phagocytosis and encystation*. Journal of Microbiology, Immunology and Infection, 2019.
194. Gabriel, S., et al., *Development of nanoparticle-assisted PCR assay in the rapid detection of brain-eating amoebae*. Parasitology research, 2018. **117**(6): p. 1801-1811.
195. Heredero-Bermejo, I., et al., *Evaluation of the activity of new cationic carbosilane dendrimers on trophozoites and cysts of Acanthamoeba polyphaga*. Parasitology research, 2015. **114**(2): p. 473-486.
196. Lau, H.L., et al., *Granulomatous amoebic encephalitis caused by Acanthamoeba in a patient with AIDS: a challenging diagnosis*. Acta Clinica Belgica, 2019: p. 1-5.
197. Leopold, A.V., D.M. Shcherbakova, and V.V. Verkhusha, *Fluorescent biosensors for neurotransmission and neuromodulation: engineering and applications*. Frontiers in cellular neuroscience, 2019. **13**.

References:

198. Lukies, M.W., et al., *Amoebic encephalitis: case report and literature review of neuroimaging findings*. BJR| case reports, 2016: p. 20150499.
199. Parija, S.C., K. Dinoop, and H. Venugopal, *Management of granulomatous amebic encephalitis: Laboratory diagnosis and treatment*. Tropical Parasitology, 2015. **5**(1): p. 23.
200. Rosales, M., et al., *In vitro activity of squaramides and acyclic polyamine derivatives against trophozoites and cysts of Acanthamoeba castellanii*. Journal of Biosciences and Medicines, 2018. **6**(08): p. 1-14.
201. Saoudi, S., et al., *Anti-Acanthamoeba activity of Tunisian Thymus capitatus essential oil and organic extracts*. Experimental parasitology, 2017. **183**: p. 231-235.
202. Saylor, D., K. Thakur, and A. Venkatesan, *Acute encephalitis in the immunocompromised individual*. Current opinion in infectious diseases, 2015. **28**(4): p. 330-336.
203. Sifaoui, I., et al., *Optimized combinations of statins and azoles against Acanthamoeba trophozoites and cysts in vitro*. Asian Pacific Journal of Tropical Medicine, 2019. **12**(6): p. 283.
204. Chávez-Fumagalli, M.A., et al., *A computational approach using bioinformatics to screening drug targets for Leishmania infantum species*. Evidence-Based Complementary and Alternative Medicine, 2018. **2018**.

Part 2: Published Work

Due to copyright restrictions the full works cannot be included. However the work may be accessed through the sites detailed below:

Baig AM, Iqbal J, Khan NA. 'In vitro efficacies of clinically available drugs against growth and viability of an *Acanthamoeba castellanii* keratitis isolate belonging to the T4 genotype'. *Antimicrobial Agents and Chemotherapy*. 2013 Aug;57(8):3561-7. doi: 10.1128/AAC.00299-13. Epub 2013 May 13. PMID: 23669391; PMCID: PMC3719691. <https://www.ncbi.nlm.nih.gov/pmc/articles/PMC3719691/>

Kulsoom H, Baig AM, Siddiqui R, Khan NA. 'Combined drug therapy in the management of granulomatous amoebic encephalitis due to *Acanthamoeba* spp., and *Balamuthia mandrillaris*'. *Experimental Parasitology*. 2014 Nov;145 Suppl:S115-20. doi: 10.1016/j.exppara.2014.03.025. Epub 2014 Apr 12. PMID: 24726699. <https://pubmed.ncbi.nlm.nih.gov/24726699/>

Baig AM, Rana Z, Waliani N, Karim S, Rajabali M. 'Evidence of human-like Ca^{2+} channels and effects of Ca^{2+} channel blockers in *Acanthamoeba castellanii*'. *Chemical Biology and Drug Design*. 2019 Mar;93(3):351-363. doi: 10.1111/cbdd.13421. Epub 2019 Jan 29. PMID: 30362253. <https://pubmed.ncbi.nlm.nih.gov/30362253/>

Baig AM, Rana Z, Mannan M, Tariq S, Ahmad HR. 'Antibiotic Effects of Loperamide: Homology of Human Targets of Loperamide with Targets in *Acanthamoeba* spp'. *Recent Patents on Anti-infective Drug Discovery*. 2017;12(1):44-60. doi: 10.2174/1574891X12666170425170544. PMID: 28506204. <https://pubmed.ncbi.nlm.nih.gov/28506204/>

Baig AM, Rana Z, Tariq SS, Ahmad HR. 'Bioinformatic Insights on Target Receptors of Amiodarone in Human and *Acanthamoeba castellanii*'. *Infectious Disorders- Drug Targets*. 2017;17(3):160-177. doi: 10.2174/1871526517666170622075154. PMID: 28637420. <https://pubmed.ncbi.nlm.nih.gov/28637420/>

Baig AM, Zohaib R, Tariq S, Ahmad HR. 'Evolution of pH buffers and water homeostasis in eukaryotes: homology between humans and *Acanthamoeba* proteins'. *Future Microbiology*. 2018 Feb;13:195-207. doi: 10.2217/fmb-2017-0116. Epub 2018 Jan 11. PMID: 29322818. <https://pubmed.ncbi.nlm.nih.gov/29322818/>

Baig AM, Ahmad HR, 'Evidence of a M_1 -muscarinic GPCR homolog in unicellular eukaryotes: featuring *Acanthamoeba* spp bioinformatics 3D-modelling and experimentations.' *Journal of Receptors and Signal Transduction Research*. 2017

Jun;37(3):267-275. doi: 10.1080/10799893.2016.1217884. Epub 2016 Sep 7. PMID: 27601178. <https://pubmed.ncbi.nlm.nih.gov/27601178/>

Abdul Mannan Baig, Zohaib Rana, Sumayya Tariq, Salima Lalani, and H. R. Ahmad, 'Traced on the Timeline: Discovery of Acetylcholine and the Components of the Human Cholinergic System in a Primitive Unicellular Eukaryote *Acanthamoeba* spp.' *ACS Chemical Neuroscience* 2018 9 (3), 494-504, DOI: 10.1021/acscchemneuro.7b00254
<https://pubs.acs.org/doi/abs/10.1021/acscchemneuro.7b00254>

Abdul Mannan Baig., et al. 'Forte of Bioinformatic Computational Tools in Identification of Targets of Digitalis in Unicellular Eukaryotes: Featuring *Acanthamoeba Castellanii*'. *EC Microbiology* 4.6 (2016): 831-844.
<https://www.echronicon.com/ecmi/pdf/ECMI-04-0000121.pdf>

Baig AM, Lalani S, Khan NA. 'Apoptosis in *Acanthamoeba castellanii* belonging to the T4 genotype'. *Journal of Basic Microbiology*. 2017 Jul;57(7):574-579. doi: 10.1002/jobm.201700025. Epub 2017 May 3. PMID: 28466971.
<https://pubmed.ncbi.nlm.nih.gov/28466971/>